Clusters of Primodial Black Holes

Dawn GW Cosmology, Benasque, 9th May 25

Juan García-Bellido
IFT-UAM/CSIC

Outline

- Fundamental Physics and PBH:
  - Critical Higgs Inflation
  - Quantum Diffusion and PNG tails
- PBH cluster dynamics:
  - Binary parameter distributions
  - Spin induction in dense clusters
- Observational Evidences:
  - Gravitational Waves (GWTC-3)

PHYSICAL REVIEW D VOLUME 54, NUMBER 10 15 NOVEMBER 1996

Density perturbations and black hole formation in hybrid inflation

Juan García-Bellido
Astronomy Centre, University of Sussex, Falmer, Brighton BN1 9QH, United Kingdom

Andrei Linde
Physics Department, Stanford University, Stanford, California 94305-4060

David Wands
School of Mathematical Studies, University of Portsmouth, Portsmouth PO1 2EG, United Kingdom
and Astronomy Centre, University of Sussex, Falmer, Brighton BN1 9QH, United Kingdom

. The resulting density inhomogeneities lead to a copious production of black holes.

quantum fluctuations at the time corresponding to the phase transition between the two inflationary stages can

for certain values of parameters these black holes may constitute the dark matter in the Universe.

these models can be made extremely small, but in general it could be sufficiently large to have important cosmological and astrophysical implications. In particular, for certain values of parameters these black holes may constitute the dark matter in the Universe. It is also possible to have hybrid models with two stages of inflation where the black hole production is not suppressed, but where the typical masses of the black holes are very small. Such models lead to a completely different thermal history of the Universe, where postinflationary reheating occurs via black hole evaporation. [S0556-2821(96)00522-X]

PACS number(s): 98.80.Cq

Steven Weinberg

"*our problem is not that we take our theories too seriously, but that we don't take them seriously enough*"

PHYSICAL REVIEW D **92**, 023524 (2015)

Massive primordial black holes from hybrid inflation as dark matter and the seeds of galaxies

Sébastien Clesse[1,*] and Juan García-Bellido[2,†]

[1]*Namur Center of Complex Systems (naXys), Department of Mathematics, University of Namur, Rempart de la Vierge 8, 5000 Namur, Belgium*

[2]*Instituto de Física Teórica UAM-CSIC, Universidad Autonóma de Madrid, Cantoblanco, 28049 Madrid, Spain*

(Received 9 March 2015; published 16 July 2015)

In this paper we present a new scenario where massive primordial black holes (PBHs) are produced from the collapse of large curvature perturbations generated during a mild-waterfall phase of hybrid inflation. We determine the values of the inflaton potential parameters leading to a PBH mass spectrum peaking on planetarylike masses at matter-radiation equality and producing abundances comparable to those of dark matter today, while the matter power spectrum on scales probed by cosmic microwave background (CMB) anisotropies agrees with Planck data. These PBHs could have acquired large stellar masses today, via merging, and the model passes both the constraints from CMB distortions and microlensing. This scenario is supported by Chandra observations of numerous BH candidates in the central region of Andromeda. Moreover, the tail of the PBH mass distribution could be responsible for the seeds of supermassive black holes at the center of galaxies, as well as for ultraluminous x-ray sources. We find that our effective hybrid

These PBHs could have acquired large stellar masses today, via merging, the model passes both the constraints from CMB distortions and microlensing.

the tail of the PBH mass distribution could be responsible for the seeds of supermassive black holes at the center of galaxies, as well as for ultraluminous x-ray sources.

PHYSICAL REVIEW D **92**, 023524 (2015)

Moreover, PBH binaries should emit gravitational waves that could be detected by future gravitational wave experiments such as LIGO, DECIGO and eLISA [70,71].

Binaries of PBHs forming a fraction of dark matter should emit gravitational waves; this results in a background of gravitational waves that could be observed by LIGO, DECIGO and eLISA [70–72].

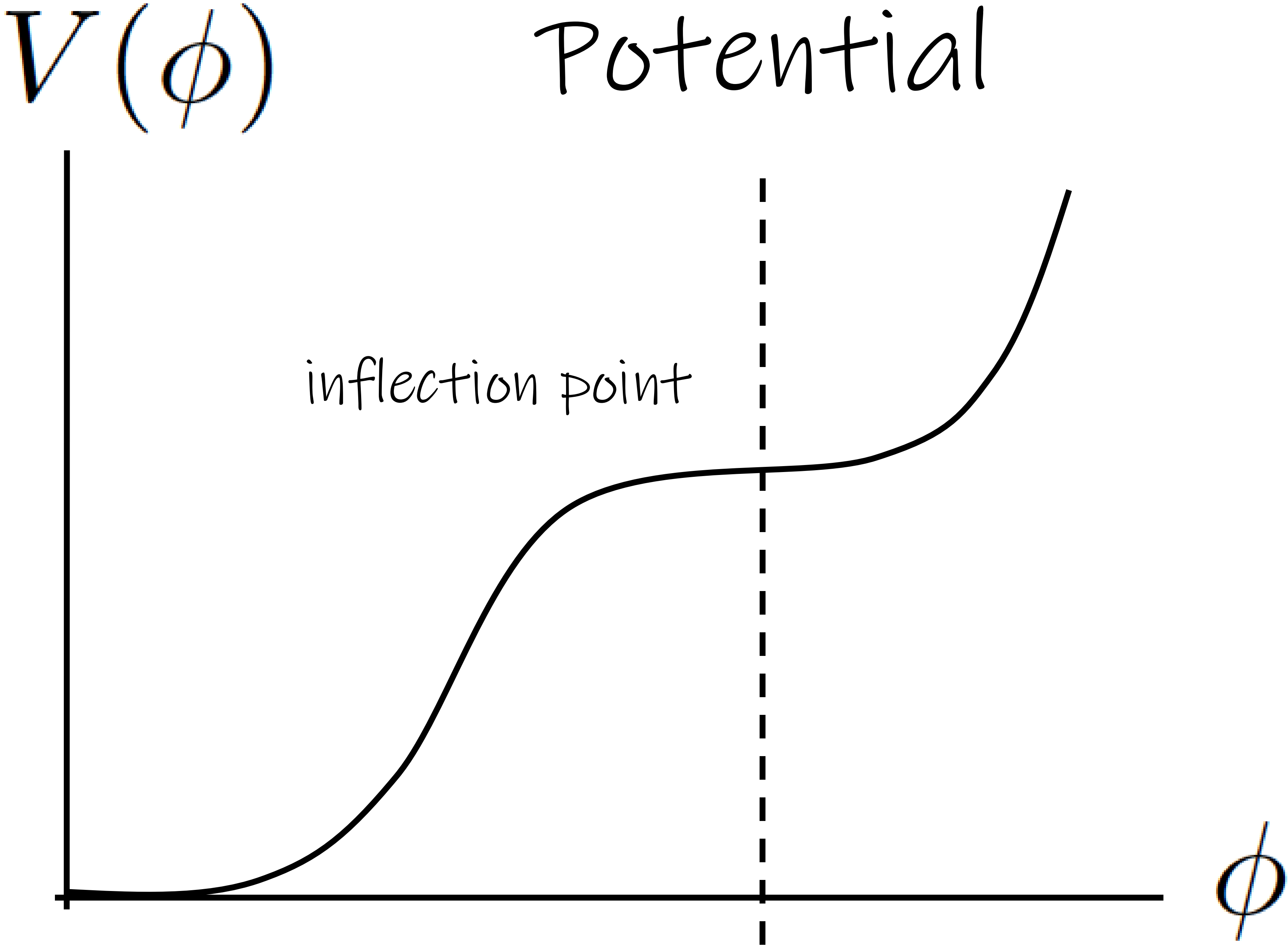
$V(\phi)$
Potential
inflection point
ϕ

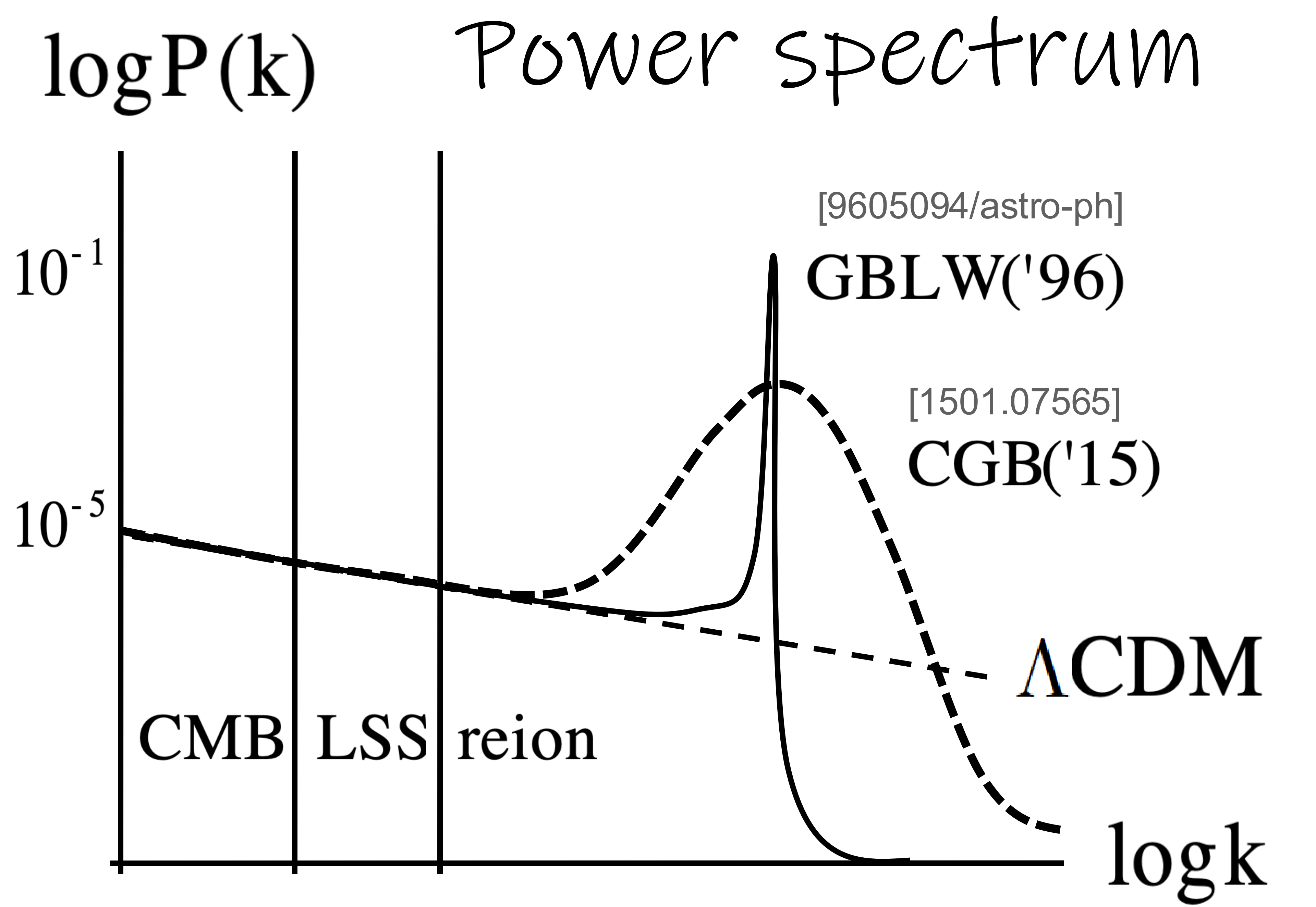

Power spectrum
logP(k)
[9605094/astro-ph]
10^{-1}
GBLW('96)
[1501.07565]
CGB('15)
10^{-5}
ΛCDM
CMB
LSS
reion
logk

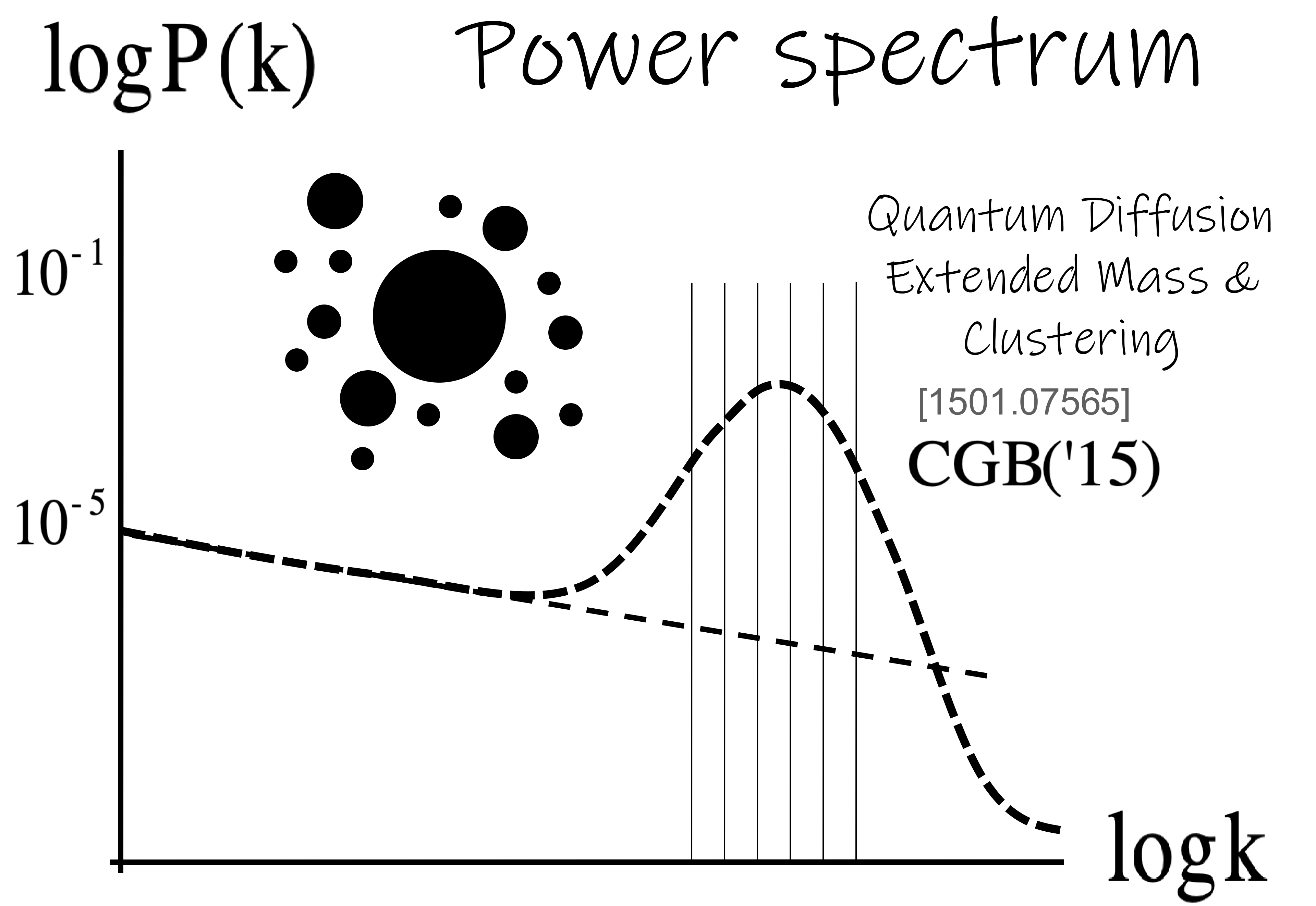
logP(k)
Power spectrum
Quantum Diffusion
Extended Mass &
Clustering
[1501.07565]
CGB('15)
10^{-1}
10^{-5}
logk

Single Field Inflation

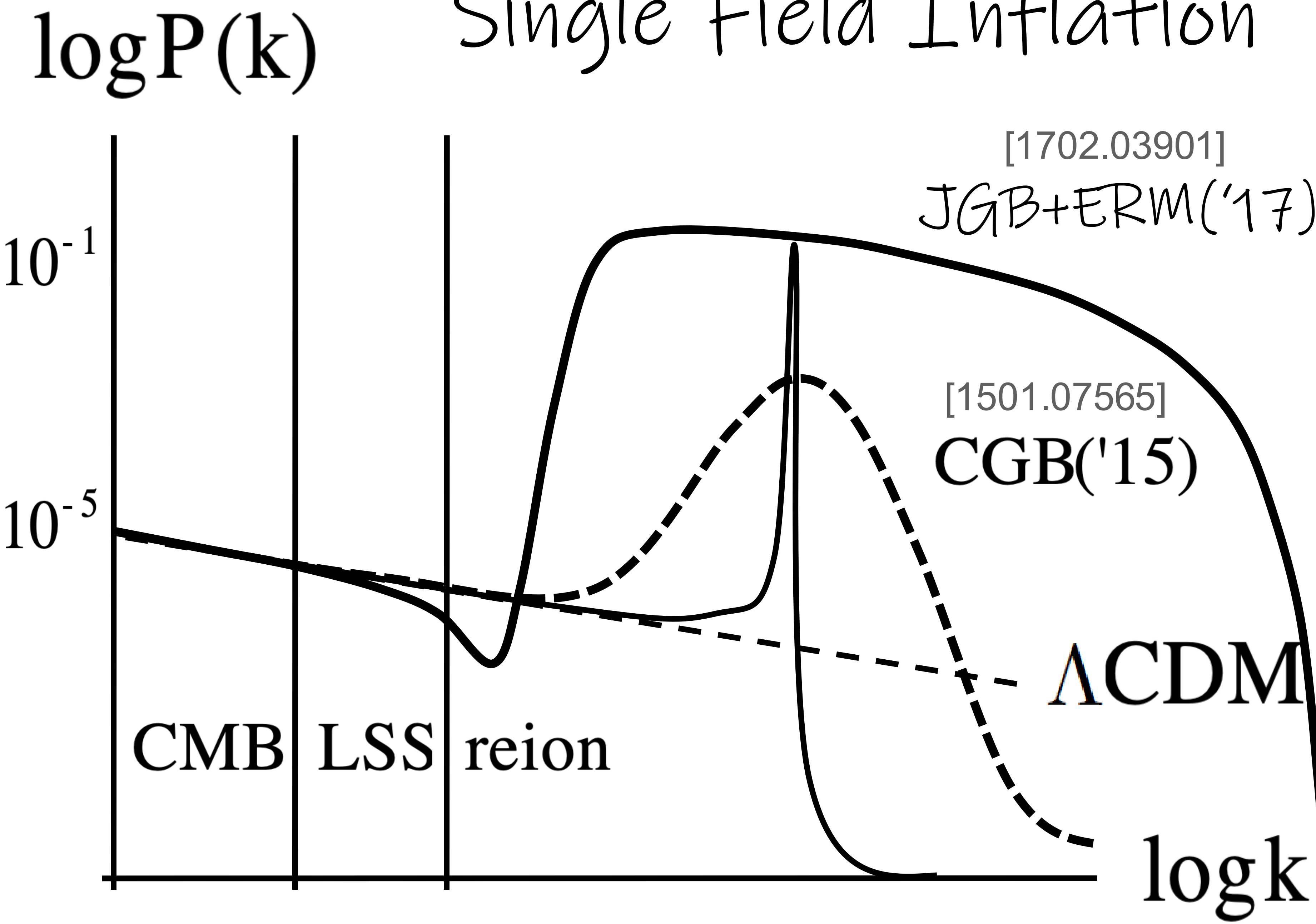

Standard Model Lagrangian

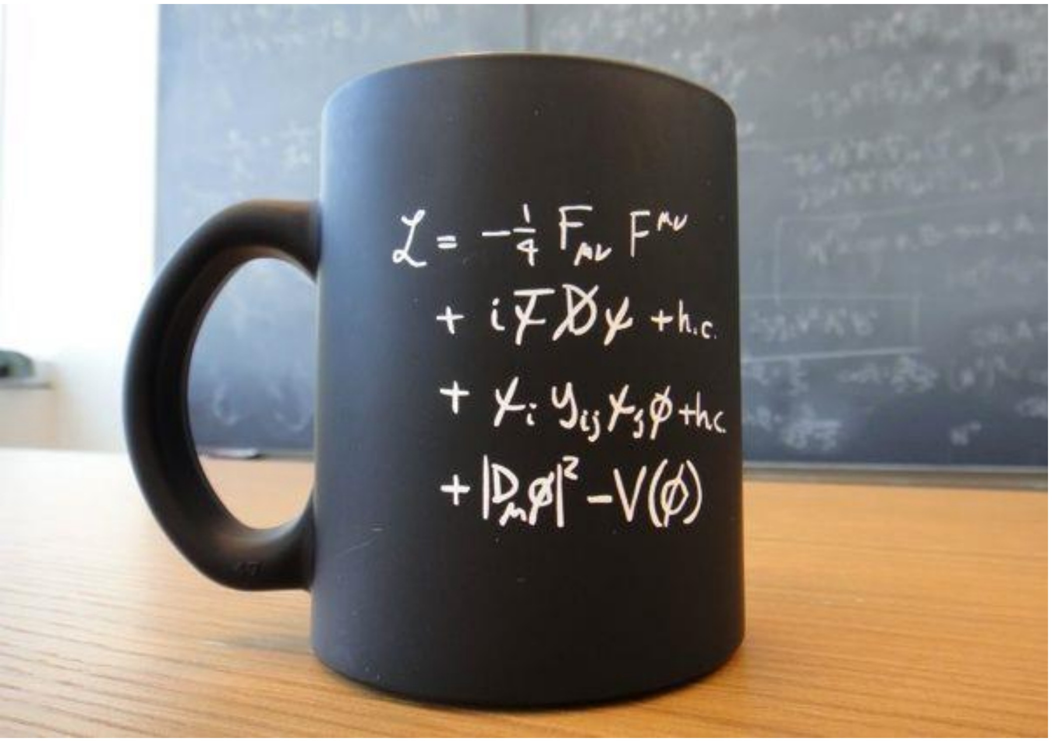

$$
\begin{aligned}
\mathcal{L} = & -\frac{1}{4} F_{\mu\nu} F^{\mu\nu} \\
& + i \bar{\Psi} \not{D} \Psi + h.c. \\
& + \bar{\Psi}_i y_{ij} \Psi_j \phi + h.c. \\
& + |D_\mu \phi|^2 - V(\phi) \\
& + \xi |\phi|^2 R
\end{aligned}
$$

$$R = 12H^2 + 6\dot{H} \rightarrow R_0 = 9.2\, H_0^2 \rightarrow m_H = \sqrt{\xi R_0} = 2 \times 10^{-32}\ \mathrm{eV}$$

EW vacuum metastability

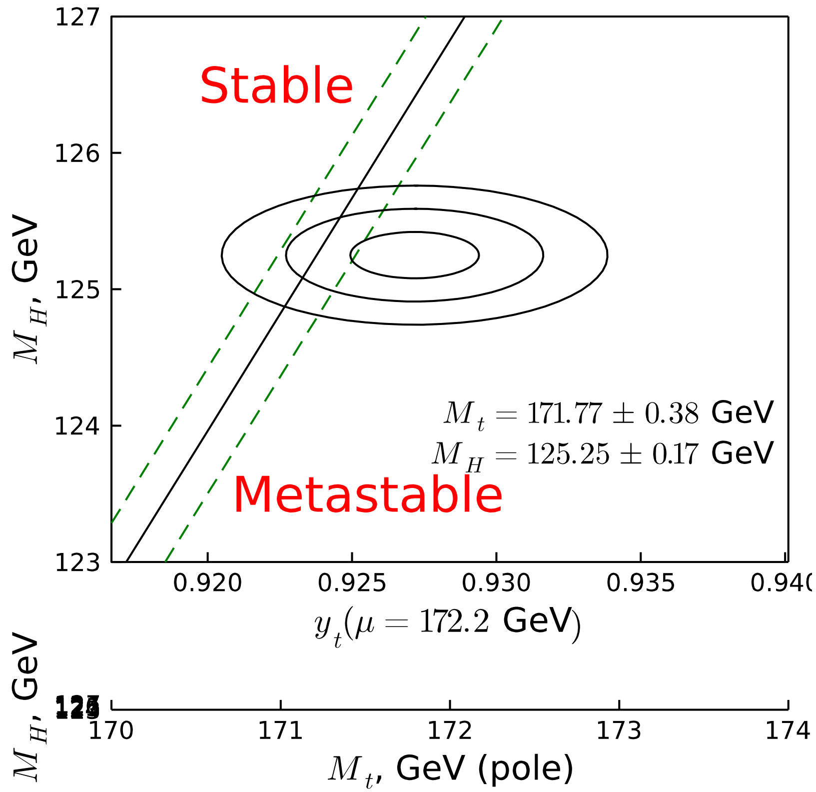

$$m_t^{pole} = 170.5 \pm 0.8\,\text{GeV}$$

$$\alpha_S(m_Z) = 0.1135^{+0.0021}_{-0.0017}$$

LHC-CMS Collab. (2020)

https://arxiv.org/abs/1904.05237

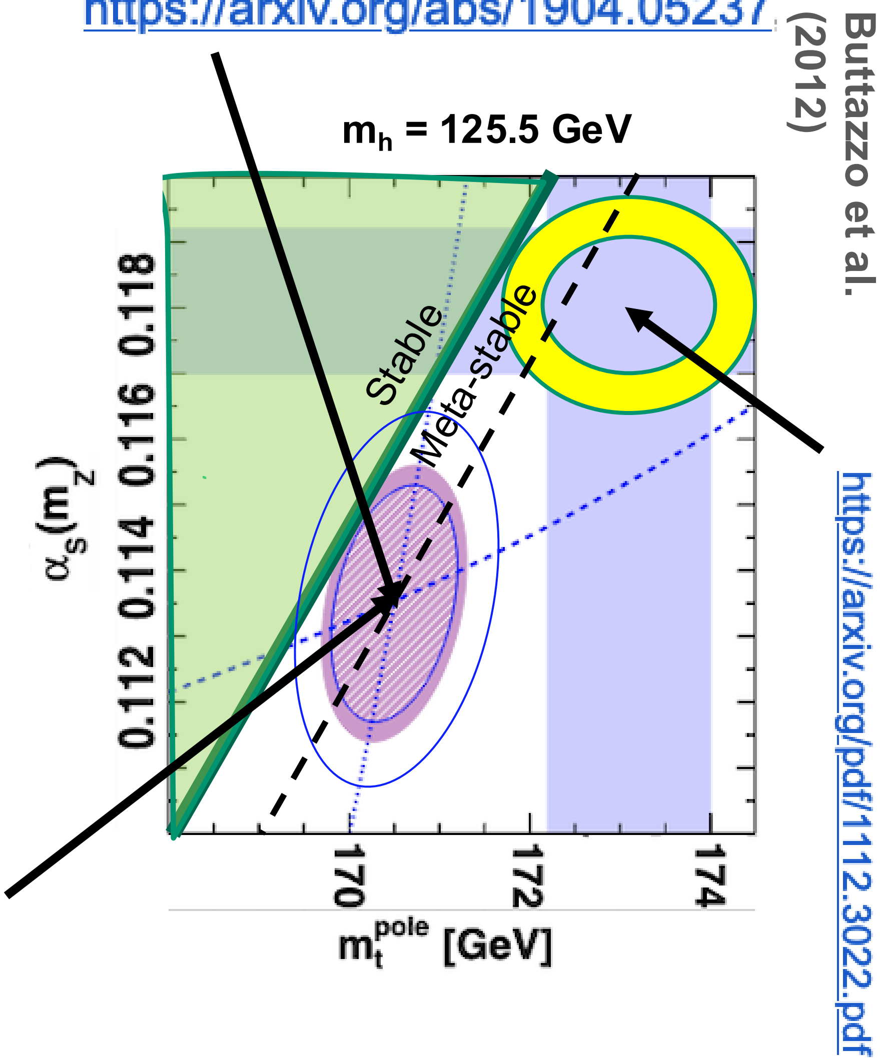

Renormalization of Higgs couplings

Ezquiaga, JGB, Ruiz [1705.04861]

$$\lambda(\phi) = \lambda_0 + b_\lambda \ln^2(\phi/\mu) ,$$
$$\xi(\phi) = \xi_0 + b_\xi \ln(\phi/\mu) ,$$

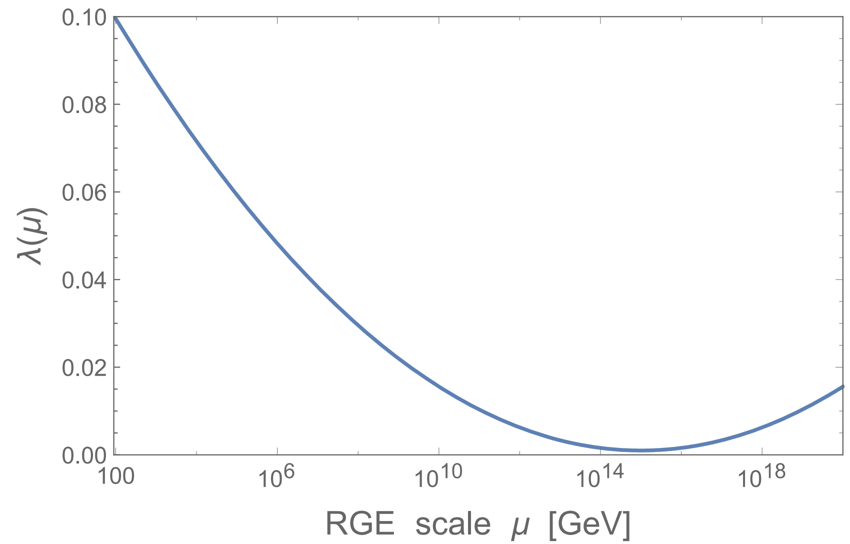

Buttazzo et al (2014)

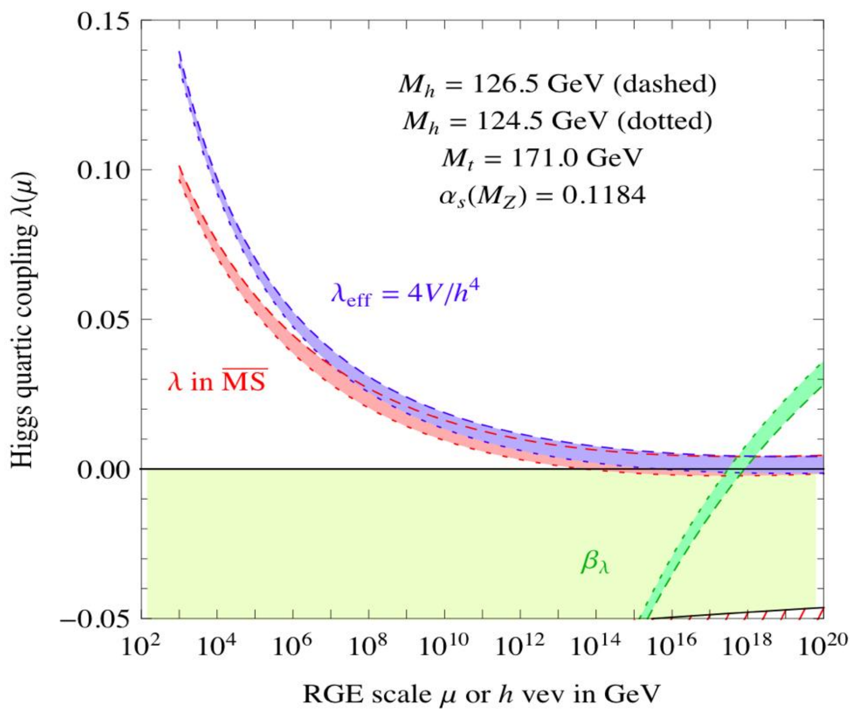

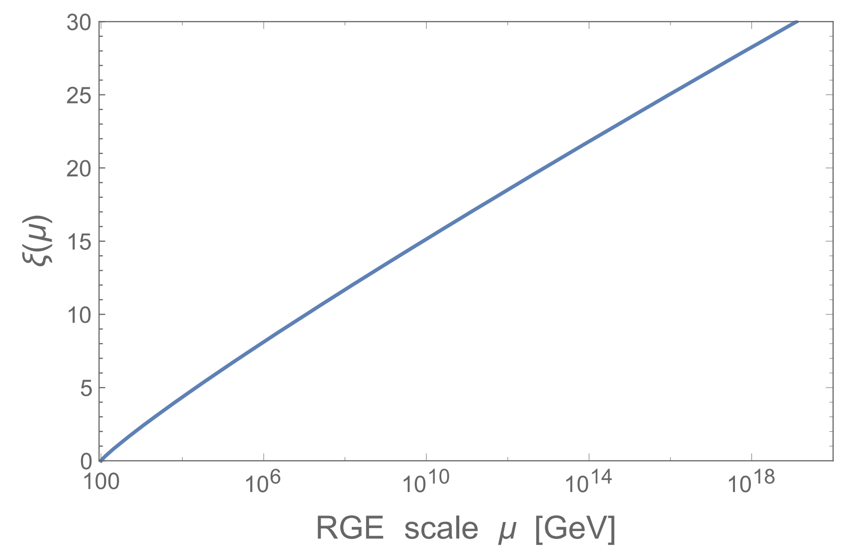

Critical Higgs Inflation

Ezquiaga, JGB, Ruiz Morales [1705.04861]

$$S=\int d^4x\sqrt{g}\left[\left(\frac{1}{2\kappa^2}+\frac{\xi(\phi)}{2}\phi^2\right)R-\frac{1}{2}(\partial\phi)^2-\frac{1}{4}\lambda(\phi)\phi^4\right]$$

$$g_{\mu\nu}\to h_{\mu\nu}=(1+\xi\phi^2)g_{\mu\nu}$$

$$\begin{aligned}\lambda(\phi) &= \lambda_0+b_\lambda\ln^2(\phi/\mu)\ ,\\ \xi(\phi) &= \xi_0+b_\xi\ln(\phi/\mu)\ ,\end{aligned}$$

$$\frac{d\varphi}{d\phi}=\frac{\sqrt{1+\xi(\phi)\,\phi^2+6\,\phi^2\,(\xi(\phi)+\phi\,\xi'(\phi)/2)^2}}{1+\xi(\phi)\,\phi^2}$$

$$V(x)=\frac{V_0\,(1+a\,\ln^2x)\,x^4}{(1+c\,(1+b\,\ln x)\,x^2)^2}\qquad x=\phi/\mu$$

$$V_0=\lambda_0\mu^4/4,\ a=b_\lambda/\lambda_0,\ b=b_\xi/\xi_0\ \text{and}\ c=\xi_0\,\kappa^2\mu^2$$

JGB, Ruiz Morales [1702.03901]

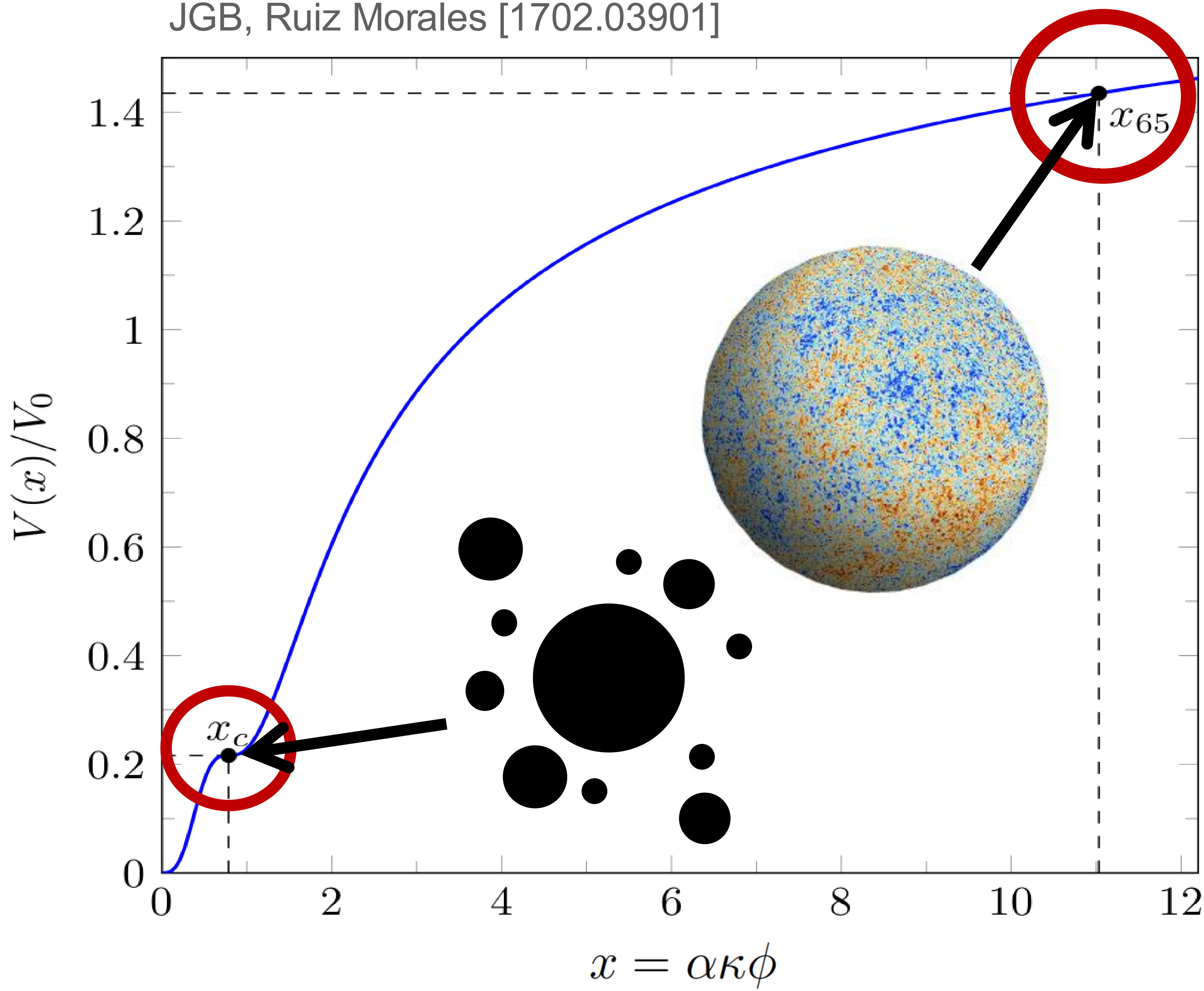

Inflation

JGB [1702.08275]

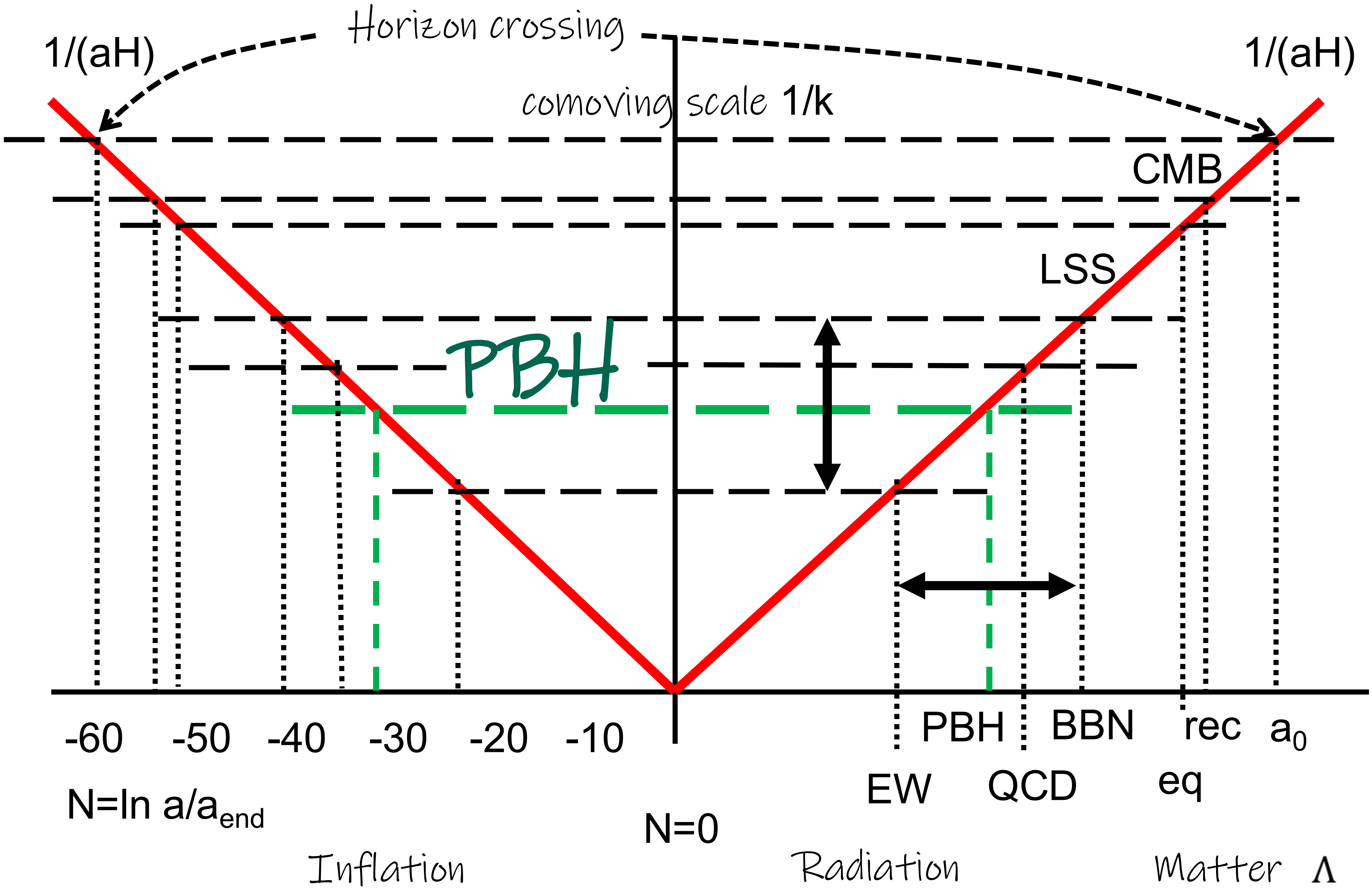

Primordial Power Spectrum

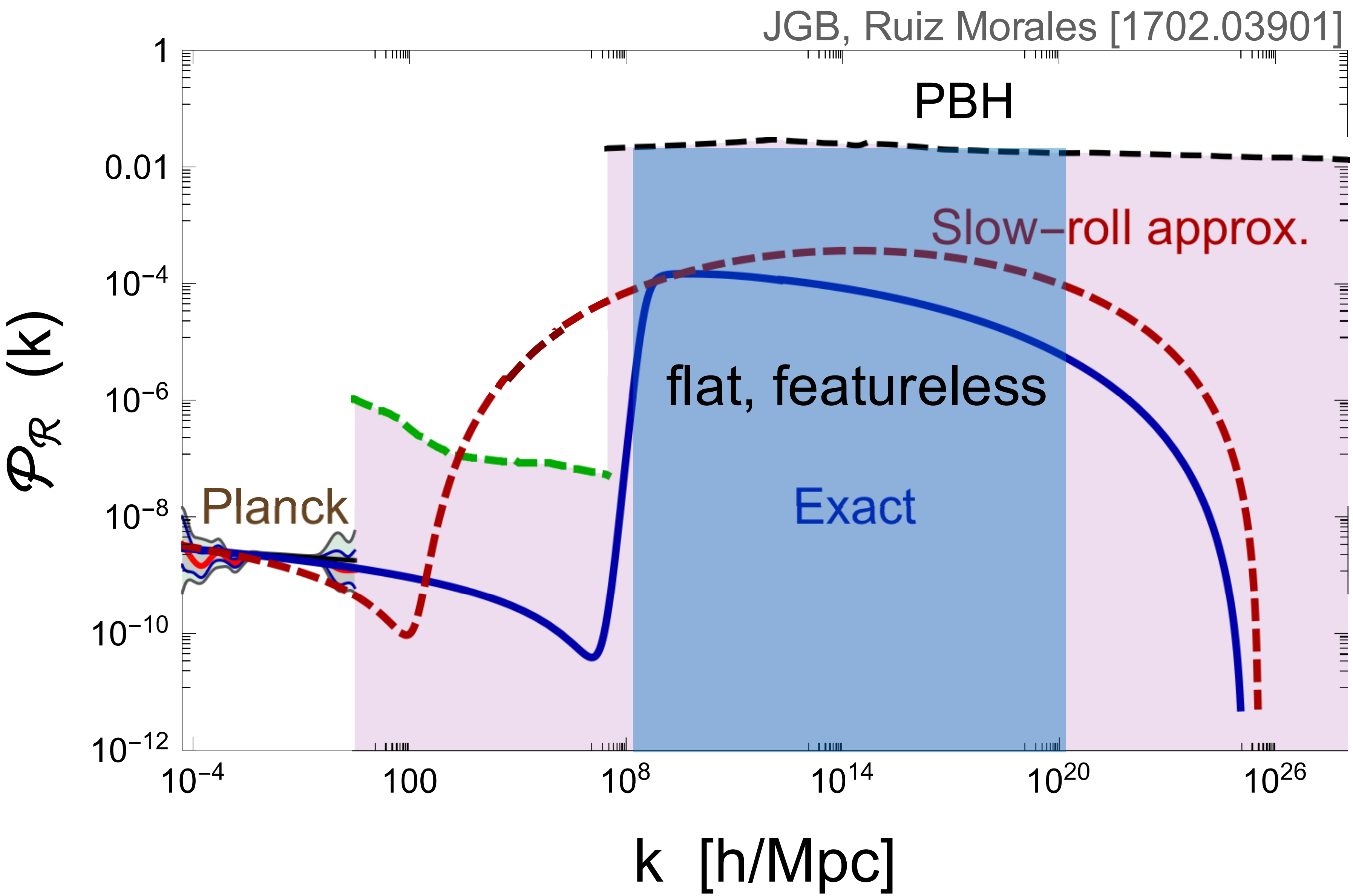

Extended Mass Function of PBH

JGB, Clesse [1501.07565]

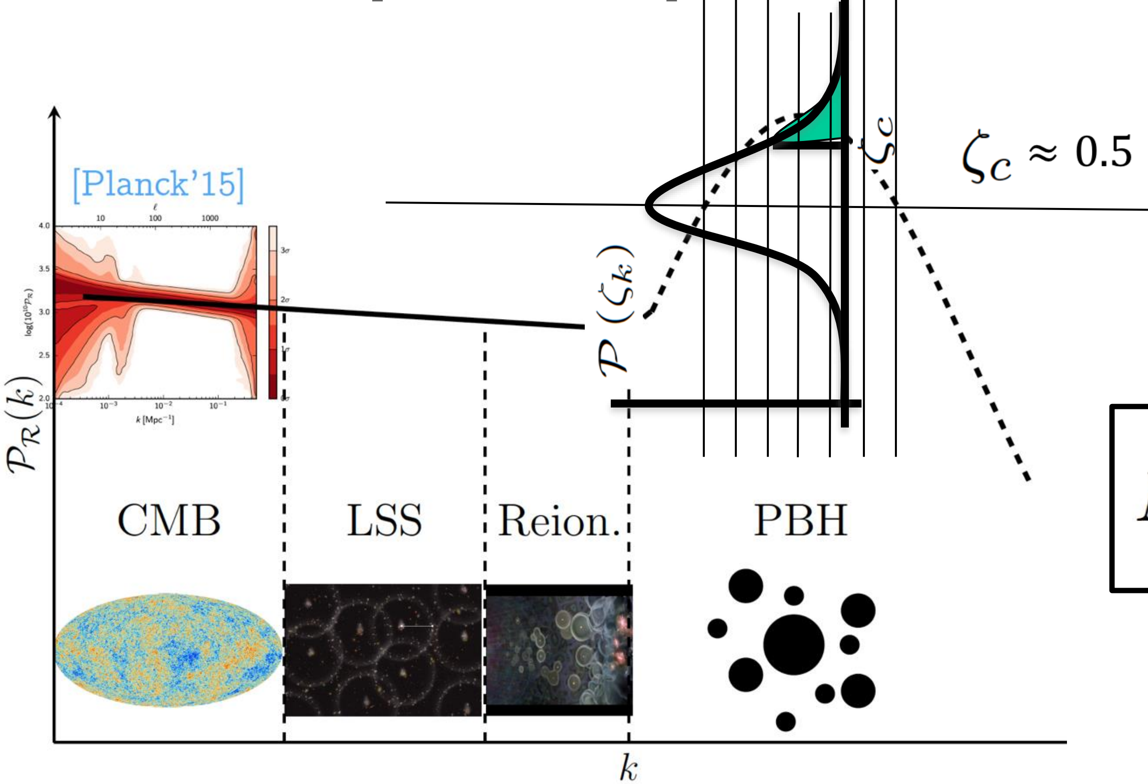

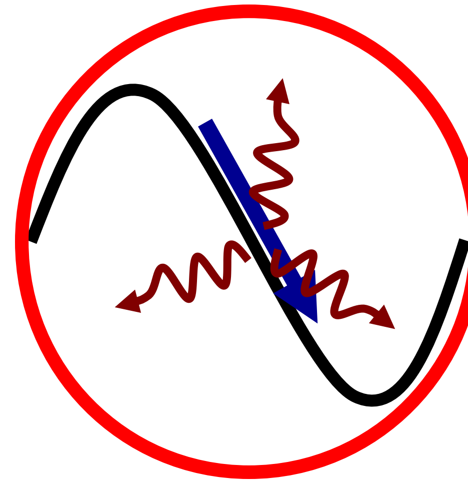

$$M_{\rm PBH} \simeq 30\, M_\odot\, e^{2(N-36)}$$

$$\beta^{\rm form}(M_k) = \int_{\zeta_c}^{\infty} \mathcal{P}(\zeta_k)\, d\zeta_k$$

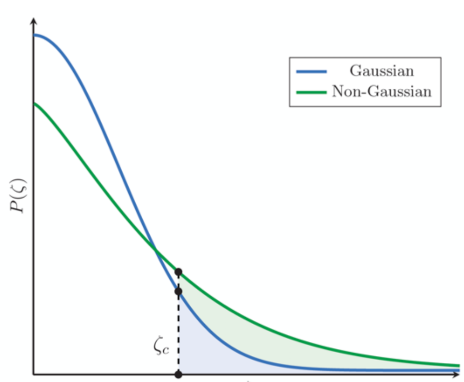

$$\beta(N) = \begin{cases} \mathrm{Erfc}\left(\dfrac{\zeta_c}{\sqrt{2P_\zeta(N)}}\right), & \text{Gaussian statistics}, \\ \mathrm{Erfc}\left(\sqrt{\dfrac{1}{2} + \dfrac{\zeta_c}{\sqrt{2P_\zeta(N)}}}\right), & \chi^2 \ \text{statistics} \end{cases}$$

Thermal history of the universe

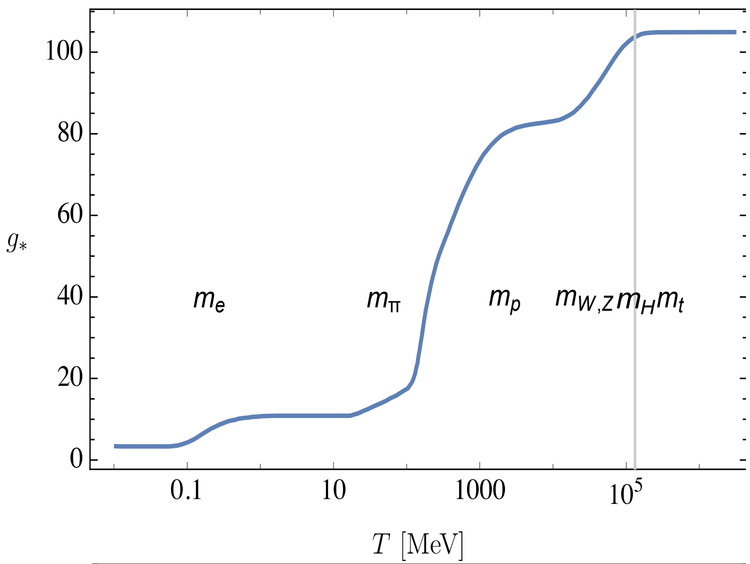

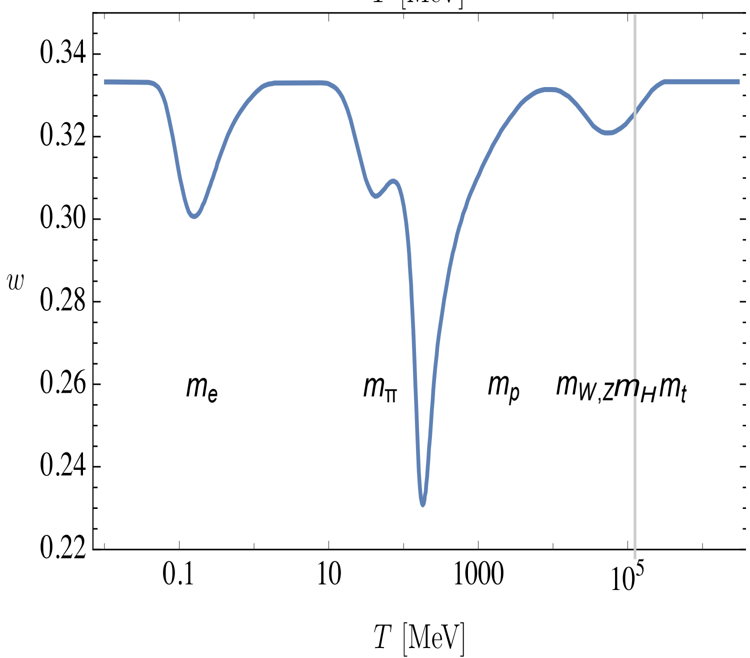

Carr, Clesse, JGB, Kühnel [1906.08217]

PBH mass spectrum

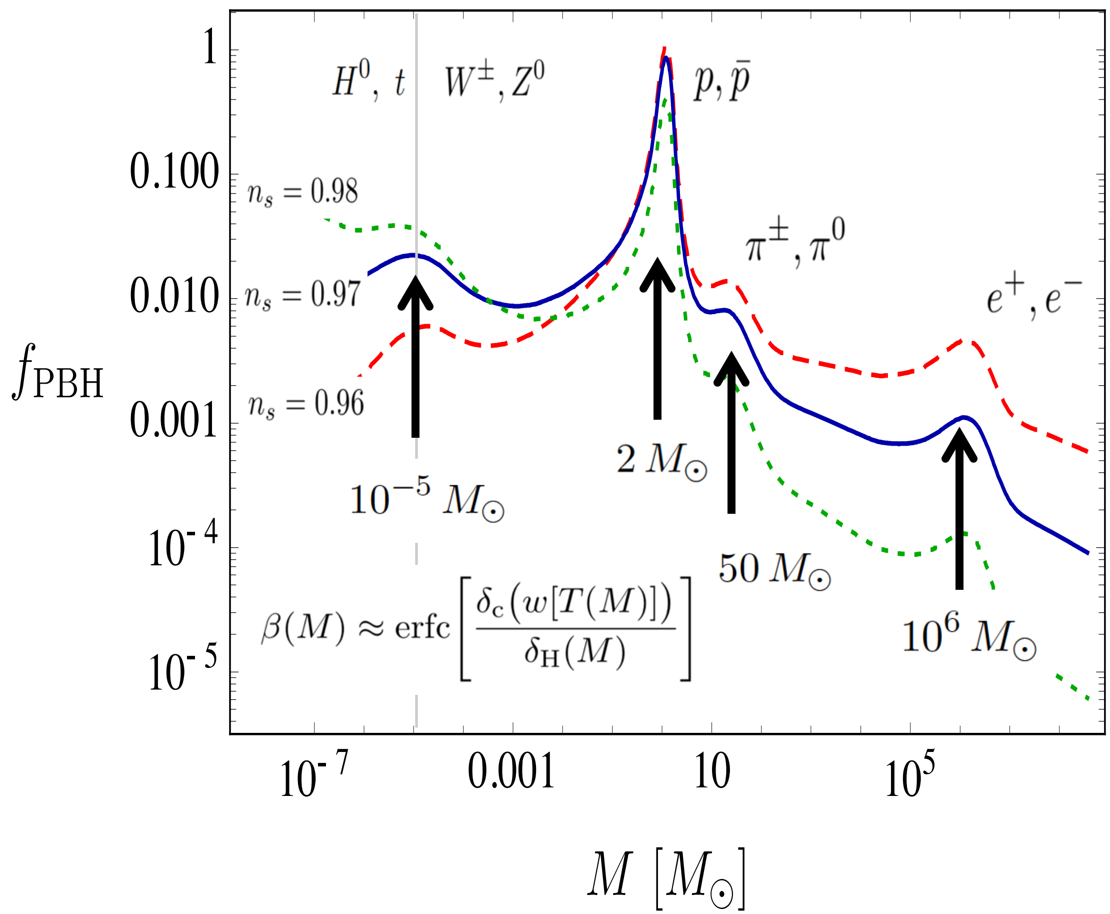

What about clusters of PBH?

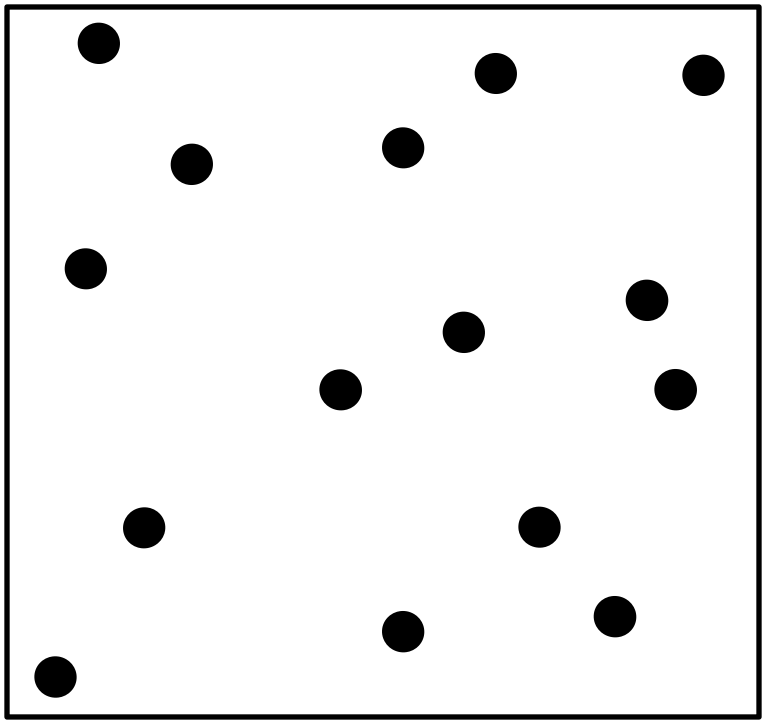

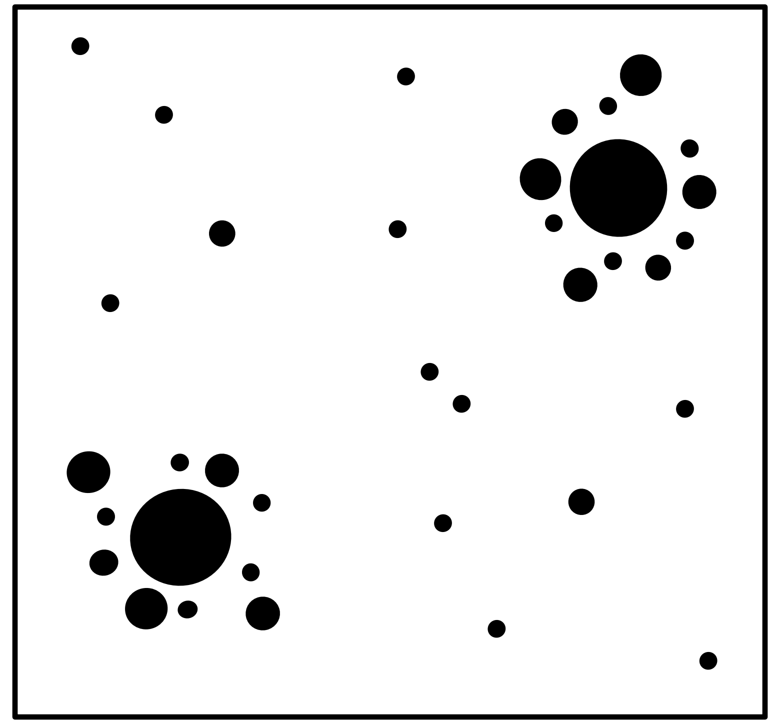

- Monochromatic (m)
- Uniformly distributed
- Gaussian statistics

- Broad range of masses
- PBH in dense clusters
- Non-Gaussian tails

JGB [1702.08275]

Stochastic δN - formalism

Coarse-grained curvature perturbation

$$\mathrm{d}s^2 = -\mathrm{d}t^2 + a^2(t)e^{2\zeta(t,\mathbf{x})}\delta_{ij}\mathrm{d}x^i\mathrm{d}x^j \qquad \zeta_{\rm cg}(\mathbf{x}) = \delta N_{\rm cg}(\mathbf{x}) = \mathcal{N}(\mathbf{x}) - \langle\mathcal{N}\rangle$$

$$\frac{1}{M_{\rm pl}^2}\frac{\mathrm{d}}{\mathrm{d}\mathcal{N}}P_{\mathbf{\Phi}}(\mathcal{N}) = \left(-\sum_i \frac{v_{\phi_i}}{v}\frac{\partial}{\partial\phi_i} + v\sum_i\frac{\partial^2}{\partial\phi_i^2}\right)\cdot P_{\mathbf{\Phi}}(\mathcal{N})$$

Fokker-Planck Diffusion Eq.

Determined by the poles of the characteristic function

$$P_\phi(\mathcal{N}) = \frac{1}{2\pi}\int_{-\infty}^{\infty} e^{-it\mathcal{N}}\chi_{\mathcal{N}}(t,\phi)dt = \sum_n a_n(\phi)\, e^{-\Lambda_n\mathcal{N}}$$

$$\chi_{\mathcal{N}}(t,\phi) = \sum_n \frac{a_n(\phi)}{\Lambda_n - it} + \text{regular func}$$

Ezquiaga, JGB, Vennin [1912.05399]

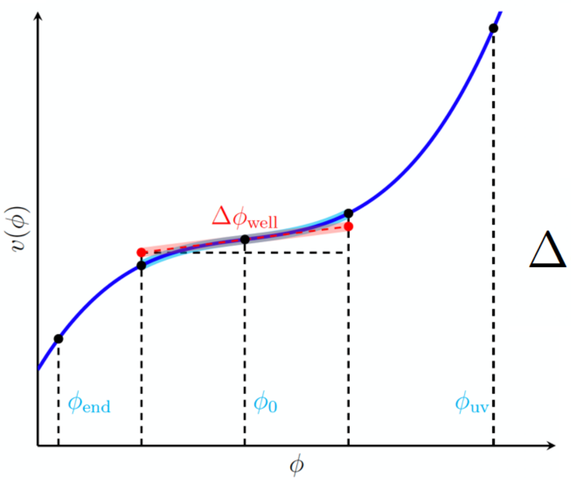

$$\alpha \gg (v_0^2\beta)^{1/3}$$

$$\Delta\phi_{\rm well} \simeq 2M_{\rm pl}\sqrt{\frac{\alpha}{3\beta}}$$

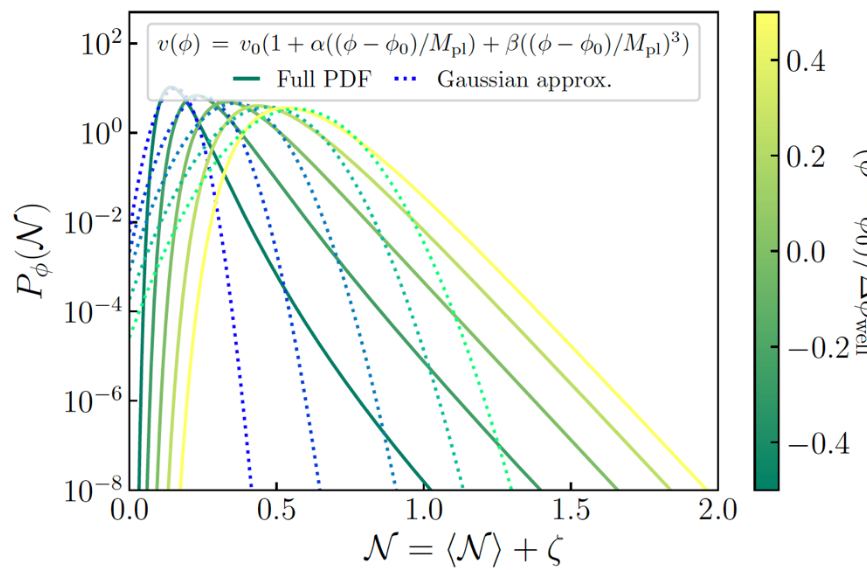

Quantum Diffusion @ CMB & LSS

Ezquiaga, JGB, Vennin [2207.06317]

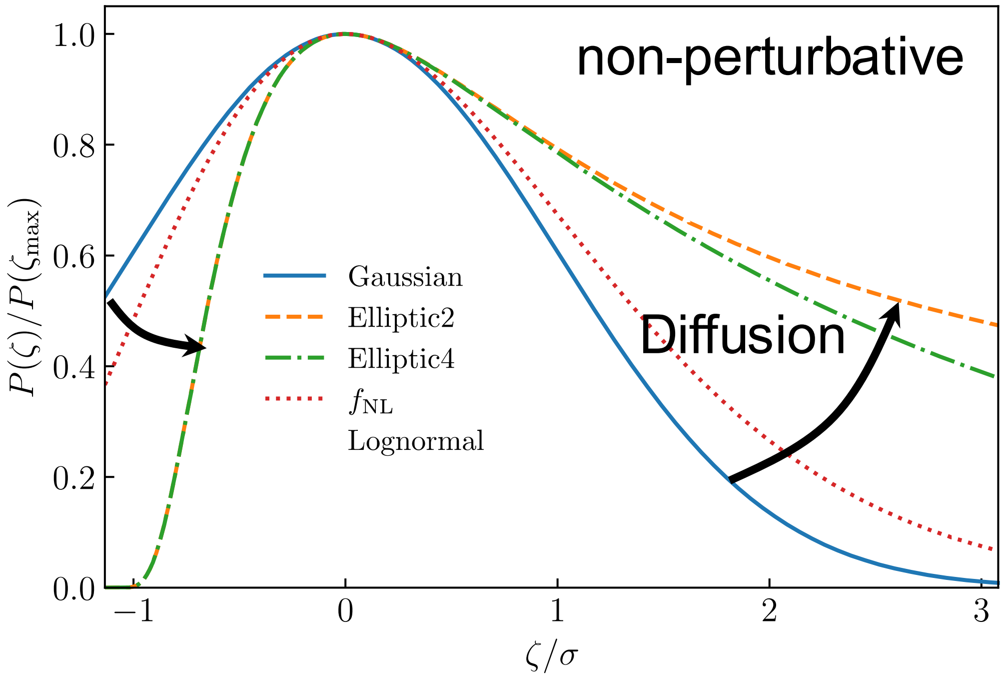

Elliptic Functions

$$P_2(\zeta_k) = -\frac{\pi}{2\mu^2}\vartheta_2'\left(\frac{\pi\alpha_k}{2}, e^{-\frac{\pi^2}{\mu^2}\mathcal{N}_k}\right)$$

$$P_4(\zeta_k) = \frac{\pi}{2\mu^2\alpha_k}\vartheta_4'\left(\frac{\pi\alpha_k}{2}, e^{-\frac{\pi^2}{\mu^2}\mathcal{N}_k}\right)$$

$f_{\rm NL}$ – expansion (not enough)

$$\zeta(x) = \zeta_{\rm G}(x) + \frac{3}{5} f_{\rm NL}\left[\zeta_{\rm G}^2(x) - \sigma_{\rm G}^2(x)\right]$$

$$P_{\rm NL}(\zeta) = \frac{1}{\sqrt{2\pi\sigma_{\rm G}^2\Delta}}\left[e^{-\frac{25(\sqrt{\Delta}-1)^2}{72 f_{\rm NL}^2\sigma_{\rm G}^2}} + e^{-\frac{25(\sqrt{\Delta}+1)^2}{72 f_{\rm NL}^2\sigma_{\rm G}^2}}\right]$$

where $\quad \Delta(\zeta) = 1 + \frac{12}{5} f_{\rm NL}\zeta + \frac{36}{25} f_{\rm NL}^2\sigma_{\rm G}^2.$

Lognormal distributions

$$\mathrm{LN}(x,\,\rho,\,\sigma) = \frac{1}{\rho\,\sigma\sqrt{2\pi}}\,\exp\left[-\frac{\ln(x/\rho)^2}{2\sigma^2} - \frac{\sigma^2}{2}\right]$$

$$\mathrm{G}(x,\,\rho,\,\sigma_{\rm G}) = \frac{1}{\sigma_{\rm G}\sqrt{2\pi}}\,\exp\left[-\frac{(x-\rho)^2}{2\sigma_{\rm G}^2}\right]$$

Quantum Diffusion @ CMB & LSS

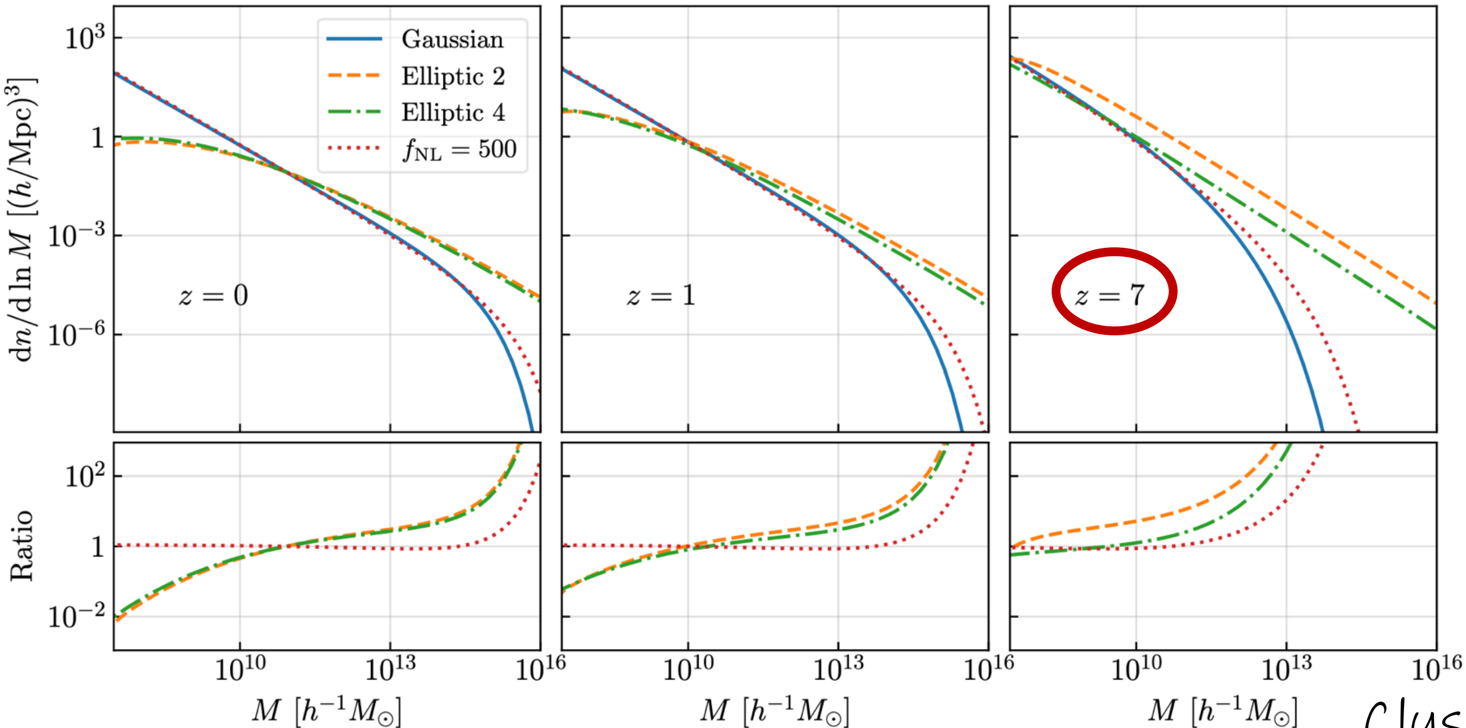

Halo Mass Function

Cluster Abundance

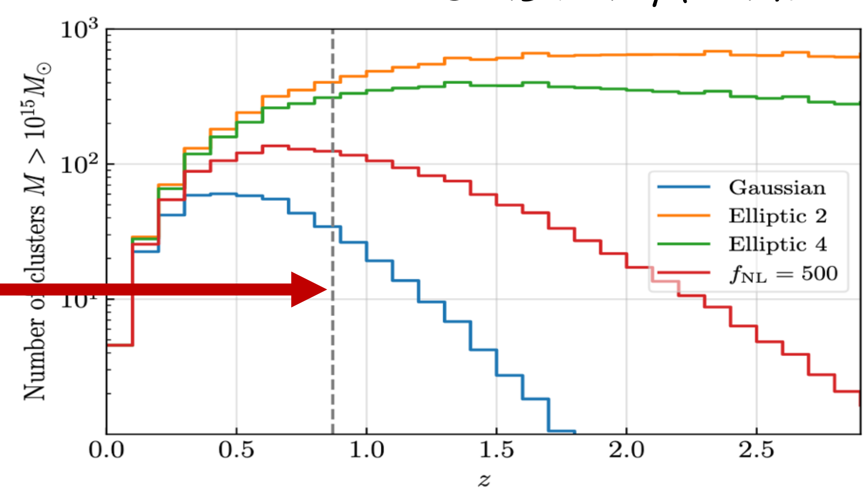

Ezquiaga, JGB, Vennin [2207.06317]

El Gordo

$$M \sim 3 \cdot 10^{15} M_\odot \text{ at } z = 0.87$$

PBH could explain the SMBH in the center of galaxies seen by JWST at z ~ 13-16

JGB, Clesse [1501.07565]
Ezquiaga, JGB, Vennin [2207.06317]

PBH clusters explain the cumply Nature of “Little Red Dots”

Tanaka et al. [2410.00104]

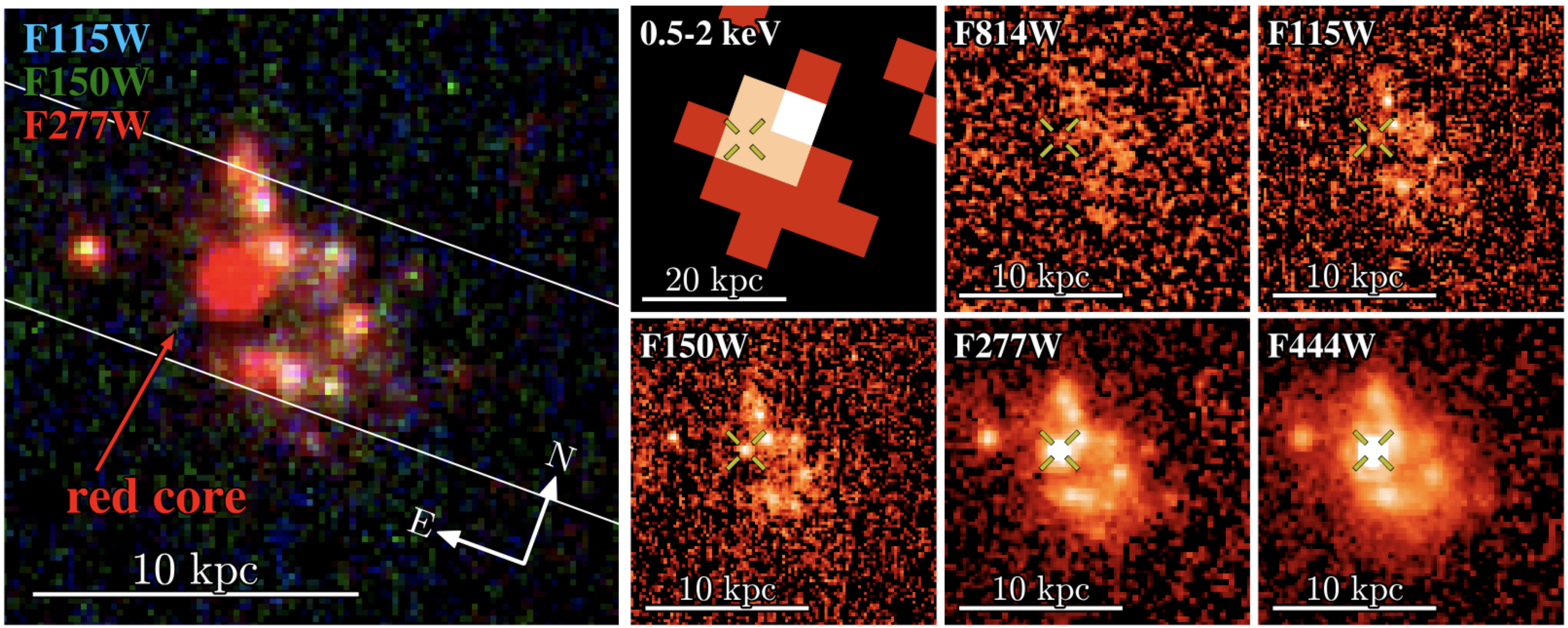

Fig. 1. Three-color (JWST/NIRCam F277W, F150W, and F115W for RGB) image and separate filter images of CID-931. The slit position of Keck-II/DEIMOS observation is shown by the white lines. Note that the Chandra 0.5-2 keV image has a different cutout size ($6'' \times 6''$) due to a much lower pixel scale ($0.''984/\mathrm{pixel}$) than the HST and JWST images ($3'' \times 3''$ cutout with the pixel scale of $0.''03/\mathrm{pixel}$). Yellow bars in right panels indicate the position of the red core.

Clusters from Quantum Diffusion

2-pt distribution function

Animali, Vennin [2402.08642]

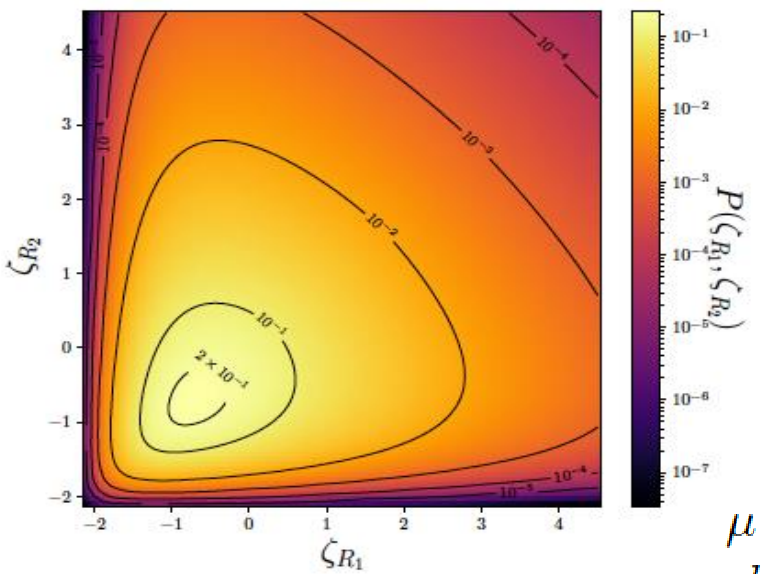

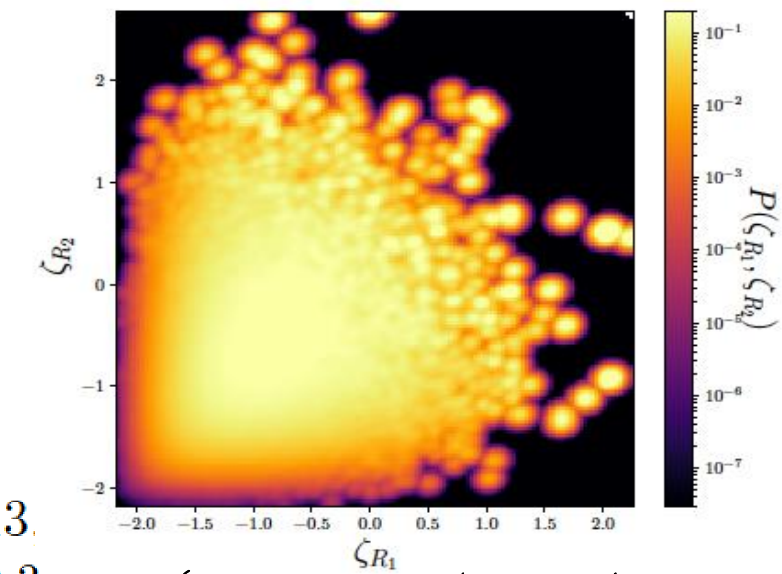

$\mu = 13$

$d = 0.3$

Tilted-well potential

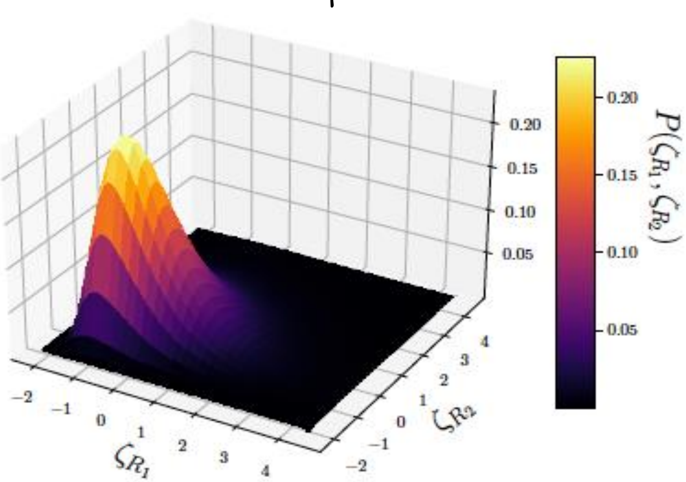

10^6 numerical simulations

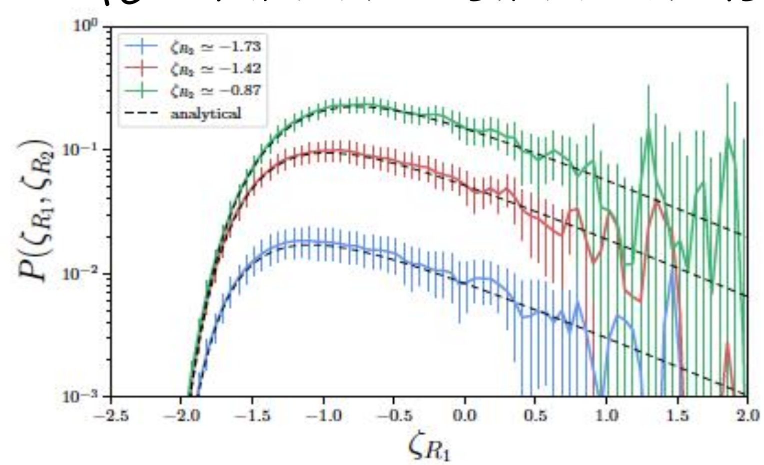

PBH and Stochastic Inflation

A. Linde (1994)

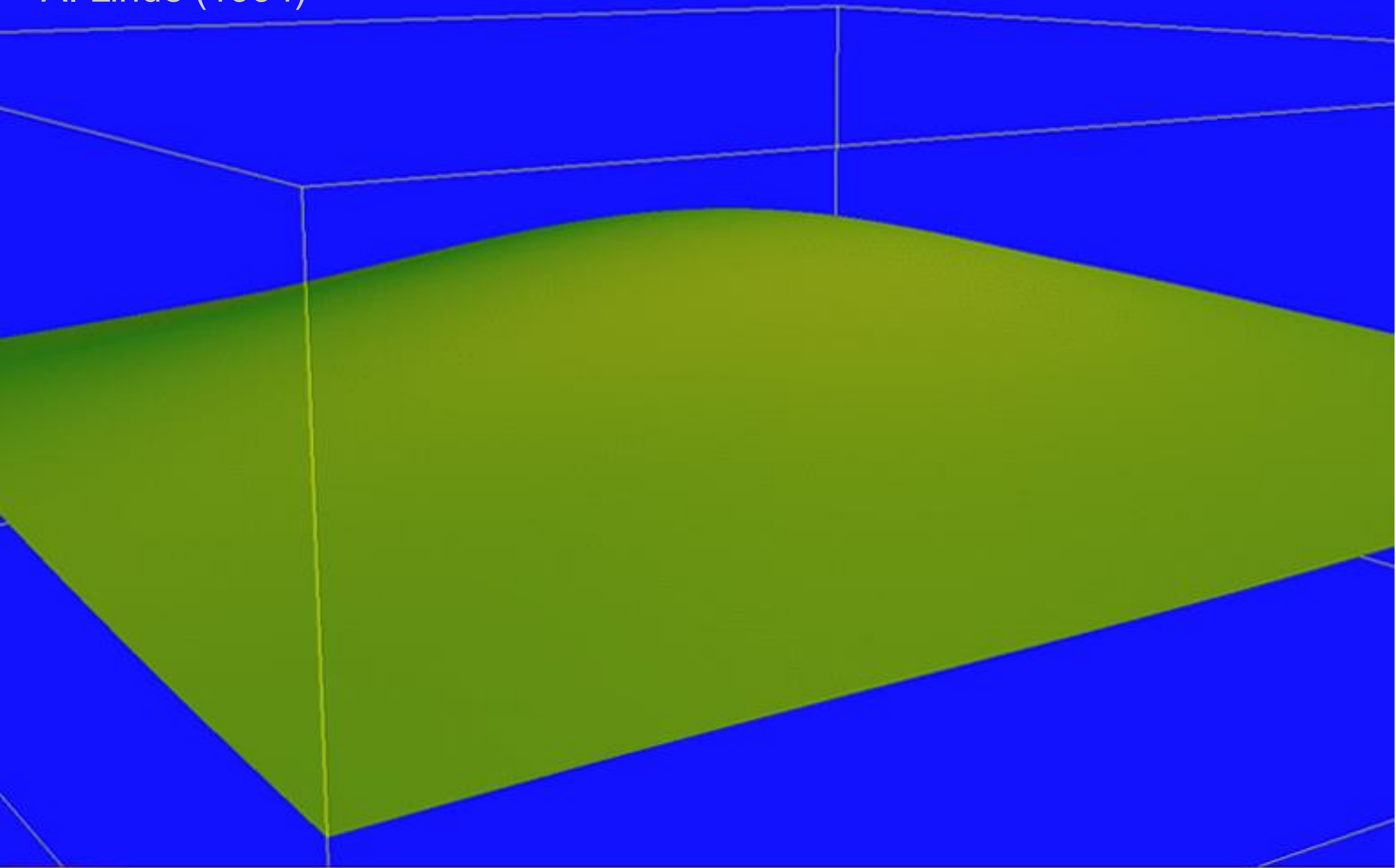

Spatial Distribution PBH

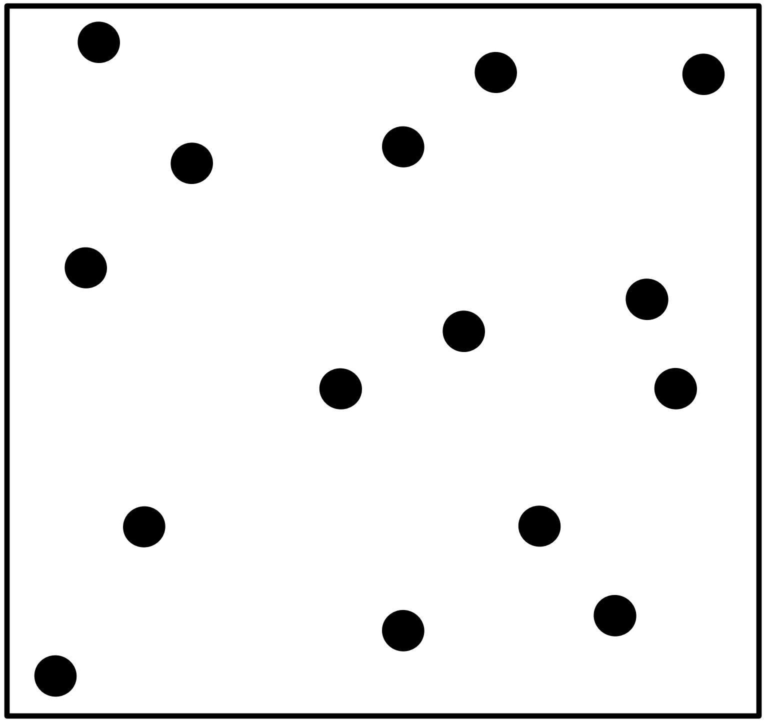

- Monochromatic
- Uniformly distributed

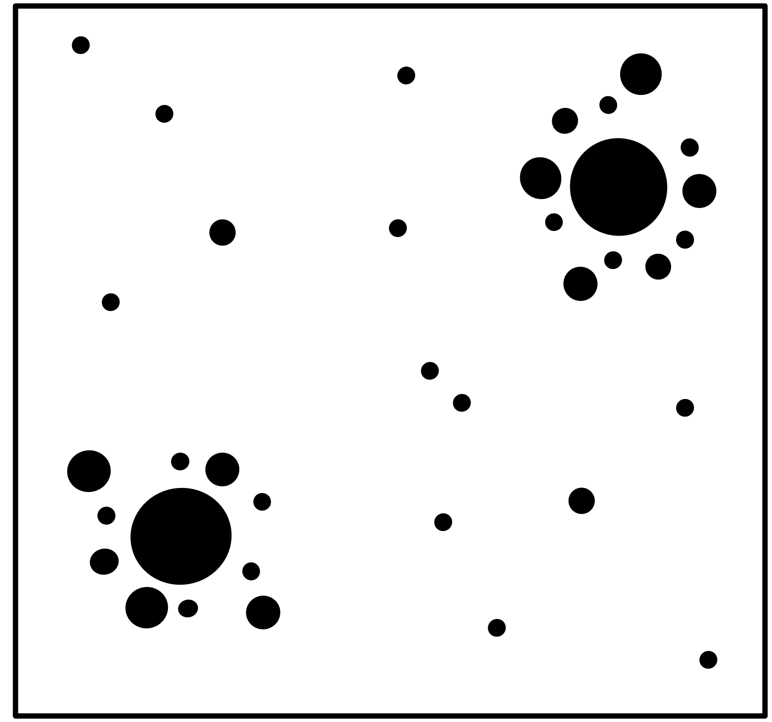

- Broad range of masses
- PBH in dense clusters

JGB [1702.08275]

Cluster Dynamics

- Initial conditions
- Binary parameter distributions
- Hierarchical mergers (w/ kicks)
- Merger rates
- Spin induction

Cluster Dynamics

J.F. Nuño Siles, JGB [2405.06391]

Lognormal mass distribution

$$N \sim \mathcal{O}(10^3 - 20 \cdot 10^3)$$

$$M_{\text{tot}} \sim \mathcal{O}(10^3 - 10^5) M_\odot$$

Maxwellian velocity distribution

Plummer density profile

$\{M\&A, \sigma_{0.5}, \sigma_1, \sigma_{1.5}\}$

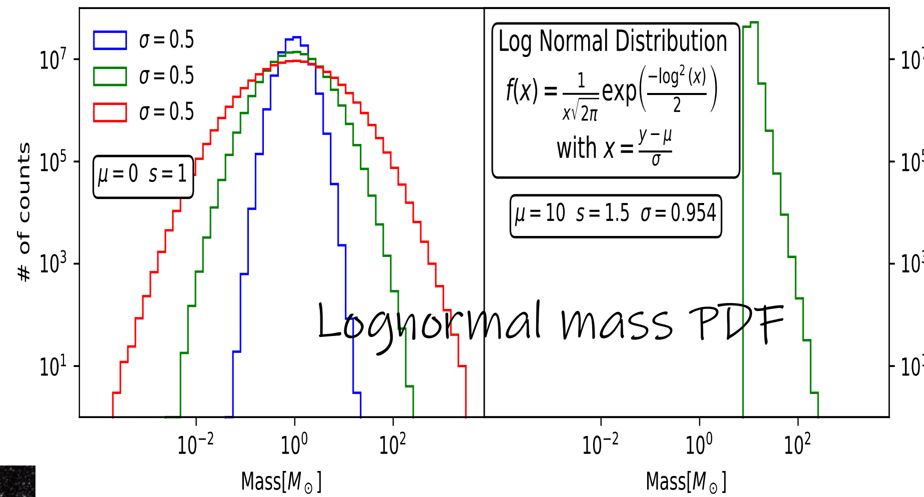

Galactic potential MW
(point-mass galaxy)
M=4.36953E+10 $M_\odot$
with circular orbit at R=34 kpc

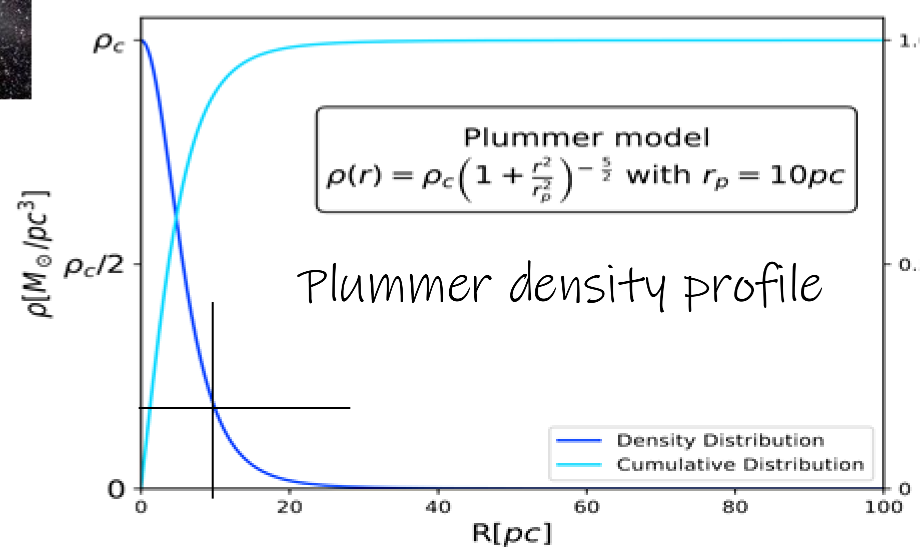

No primordial binaries

Zero natal spin

Code used: Nbody6++GPU

Multiple simulations

J.F. Nuño Siles, JGB [2405.06391]

ID M&A	$M_{total}[M_\odot]$ $t=0$	$M_{max}[M_\odot]$ $t=0$	$M_{max}[M_\odot]$ $t=T_U$	$R_{HM}[pc]$ $t=0$	$R_{HM}[pc]$ $t=T_U$	ID $\sigma_{0.5}$	$M_{total}[M_\odot]$ $t=0$	$M_{max}[M_\odot]$ $t=0$	$M_{max}[M_\odot]$ $t=T_U$	$R_{HM}[pc]$ $t=0$	$R_{HM}[pc]$ $t=T_U$
1295	16140	46.54	46.54	2.20	27.04	1520	1389	5.03	5.03	9.72	12.25
2570	32166	66.10	97.80	2.38	27.17	3345	3007	4.50	5.08	3.23	15.55
4046	50088	63.64	91.98	4.27	26.74	5480	5009	6.67	6.67	0.77	16.21
5199	64280	69.98	74.80	2.20	28.39	7678	7008	5.69	7.52	1.92	15.15
8077	100116	78.27	78.27	12.53	29.50	9937	9001	5.48	5.48	1.25	15.85
8922	110196	76.15	81.52	13.31	32.01	12201	11001	5.00	7.77	2.90	15.29
10372	128337	104.26	104.26	6.20	27.54	14366	13005	5.42	8.22	2.65	16.04
10535	130198	68.50	74.35	9.72	28.20	16428	14912	7.72	7.72	0.48	16.04
16159	200392	57.75	113.59	4.44	27.24	18776	17007	5.40	6.51	2.29	15.00
20738	256346	134.10	145.70	1.37	26.65	20866	18918	5.31	7.36	3.91	15.35

ID σ_1	$M_{total}[M_\odot]$ $t=0$	$M_{max}[M_\odot]$ $t=0$	$M_{max}[M_\odot]$ $t=T_U$	$R_{HM}[pc]$ $t=0$	$R_{HM}[pc]$ $t=T_U$	ID $\sigma_{1.5}$	$M_{total}[M_\odot]$ $t=0$	$M_{max}[M_\odot]$ $t=0$	$M_{max}[M_\odot]$ $t=T_U$	$R_{HM}[pc]$ $t=0$	$R_{HM}[pc]$ $t=T_U$
1505	2003	32.07	32.07	1.93	27.07	1220	3020	63.67	63.67	3.37	58.92
3090	4004	18.56	18.56	7.52	22.21	3423	8010	105.74	105.74	7.15	41.00
5288	7007	34.14	34.14	7.60	21.97	5258	13014	541.18	541.18	1.95	40.15
7507	10001	25.82	34.29	3.95	24.77	8025	20021	157.23	157.23	0.41	41.62
10663	14000	46.77	46.77	6.64	26.96	10011	24187	179.83	280.36	1.45	60.33
12834	17004	32.81	58.06	4.41	23.91	12409	30007	114.51	114.51	0.07	55.98
15136	20000	58.31	58.31	0.47	25.47	14691	38027	731.69	1004.13	1.40	37.81
17554	23008	45.68	64.90	0.82	25.62	17182	43013	554.27	554.27	5.59	46.36
20590	27008	51.60	76.41	4.70	26.64	20261	49021	657.47	784.02	3.52	41.41

Cluster Dynamics

Clusters expand with time while core radius stays almost constant

JFN+JGB [2405.06391]

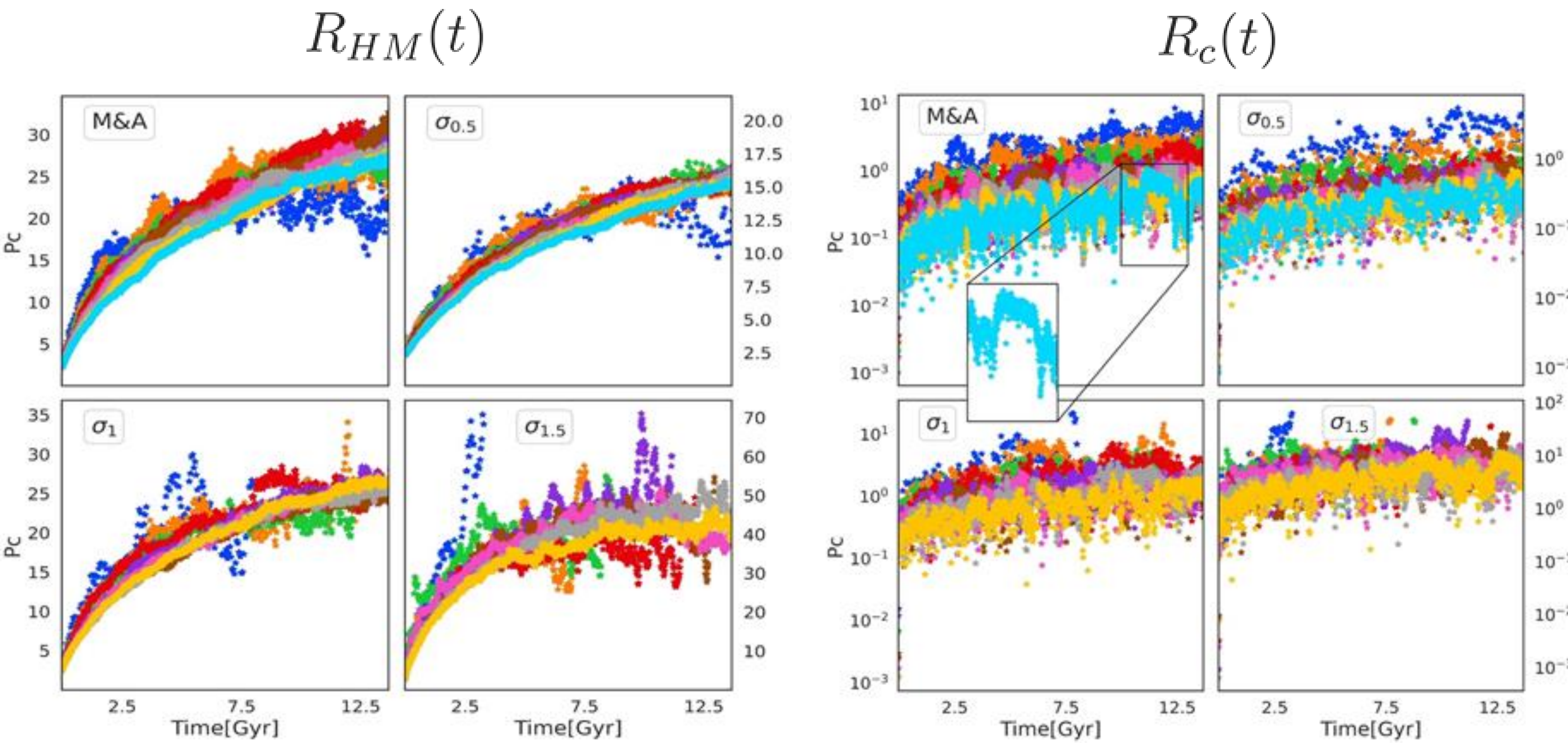

Cluster Dynamics

J.F. Nuño Siles, JGB [2405.06391]

All the clusters are metastable or directly unstable, that is, they dissolved in a time comparable with the age of the Universe or will do so in the future

Some types of clusters are more stable than others, depending on the mass ratio distribution of the pairwise interactions.

More stable $\xrightarrow{\{M\&A, \sigma_{0.5}, \sigma_1, \sigma_{1.5}\}}$ Less stable

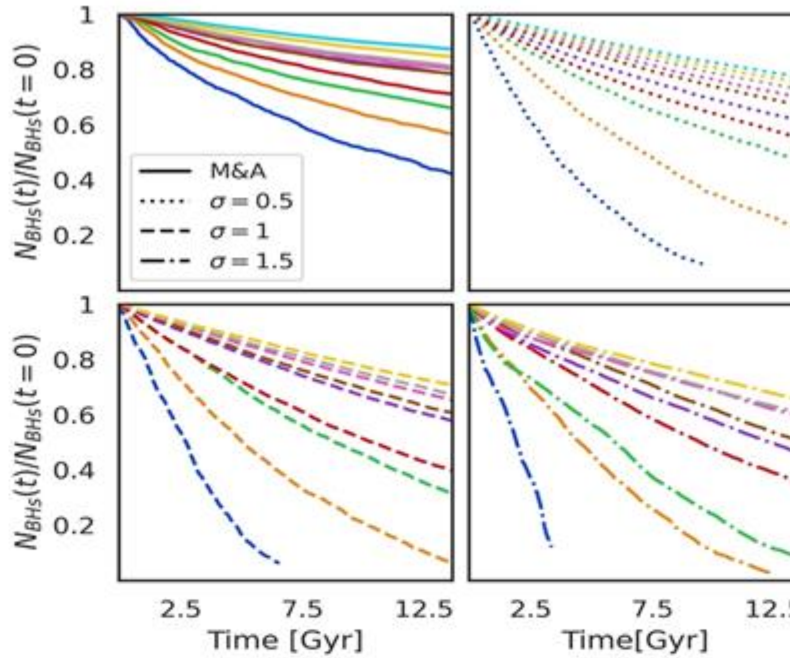

BHs remaining in clusters within 13.6 Gyr

Cluster Dynamics

Trashorras, JGB, Nesseris [2006.15018]

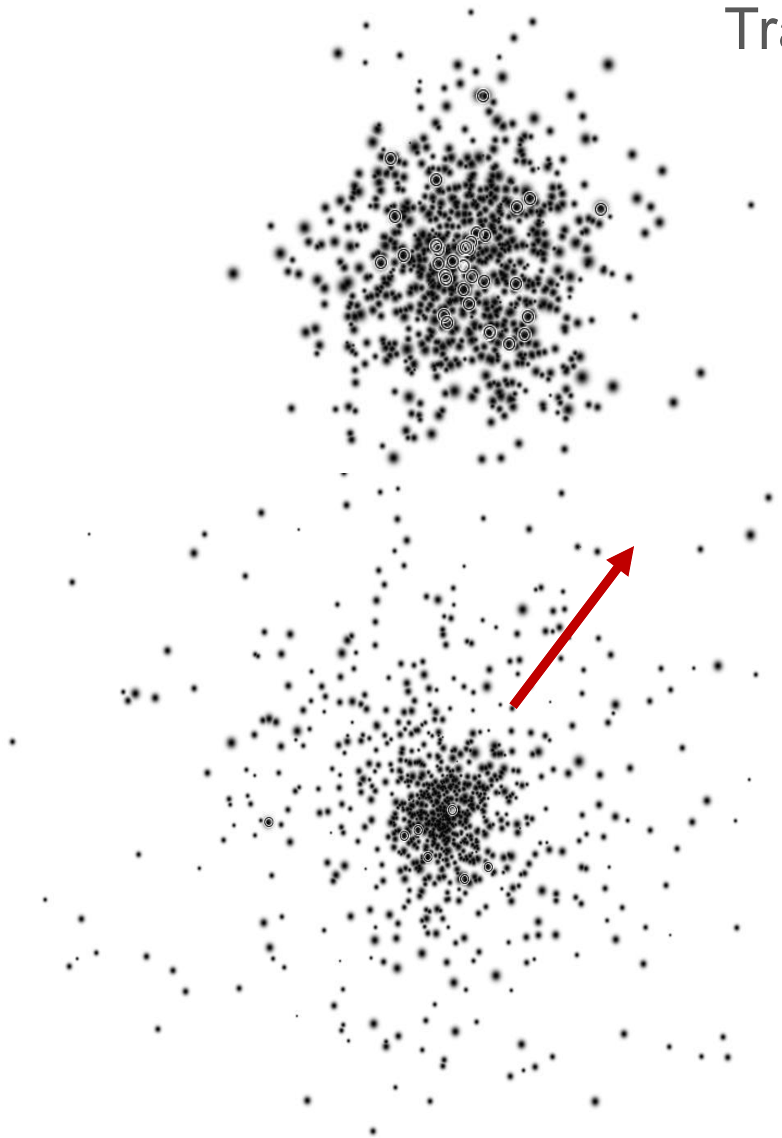

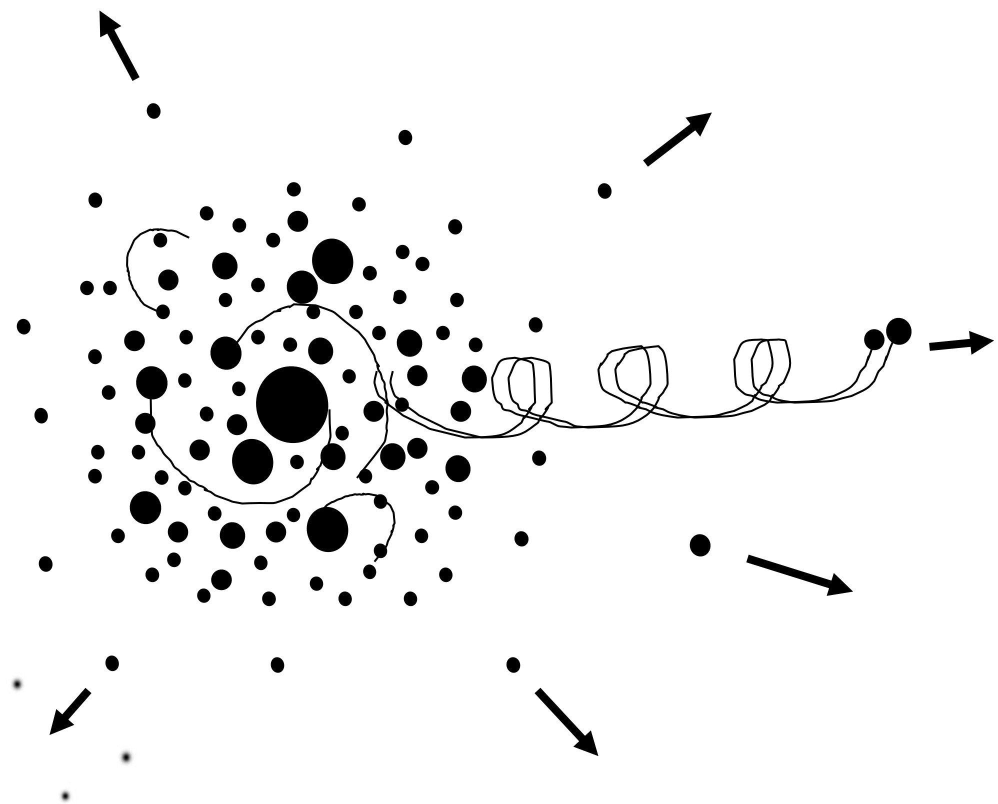

Distribution of escapers

JFN+JGB [2405.06391]

Mass

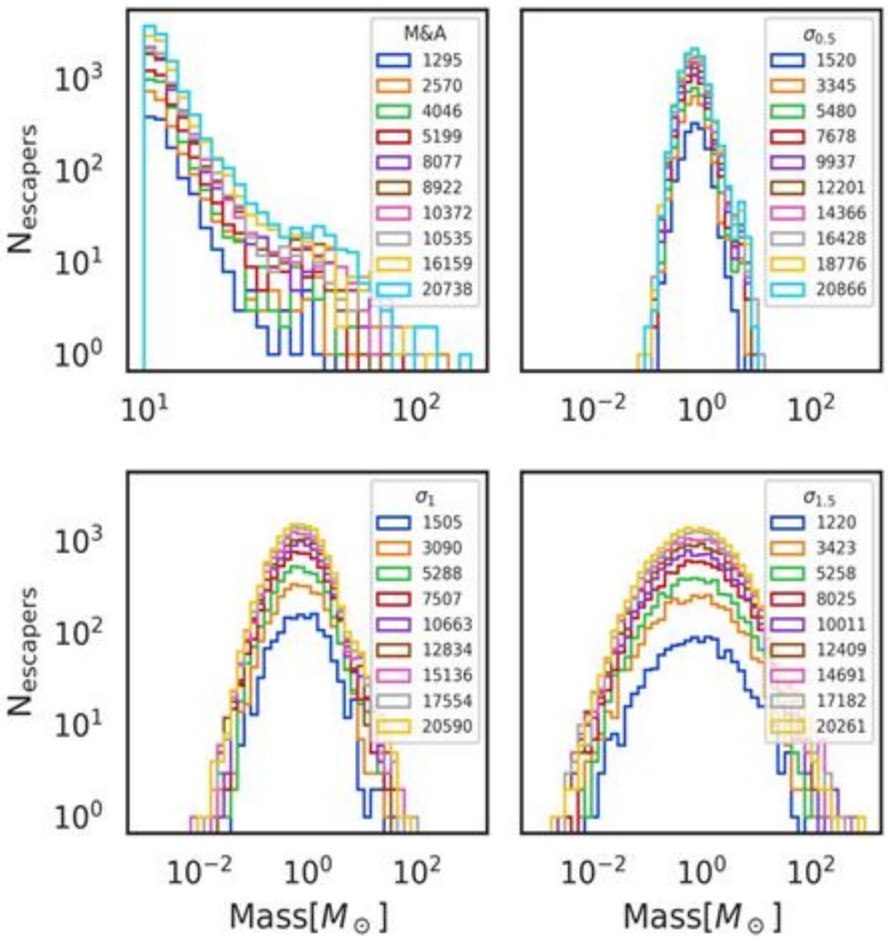

Escape velocity

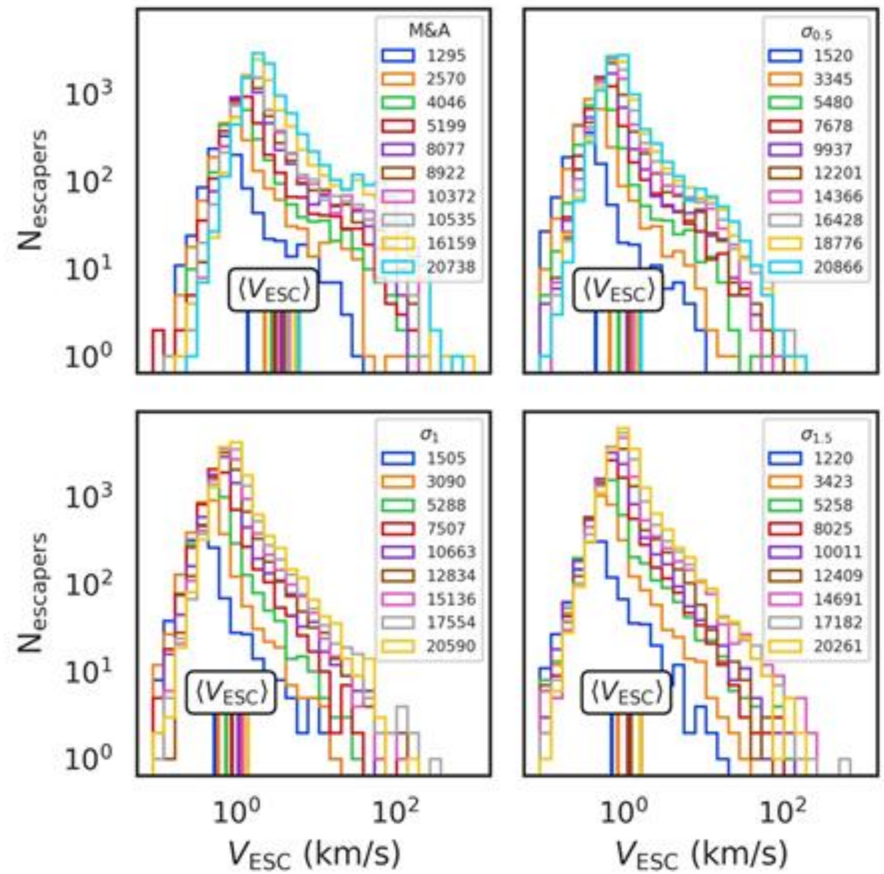

Binary escapers

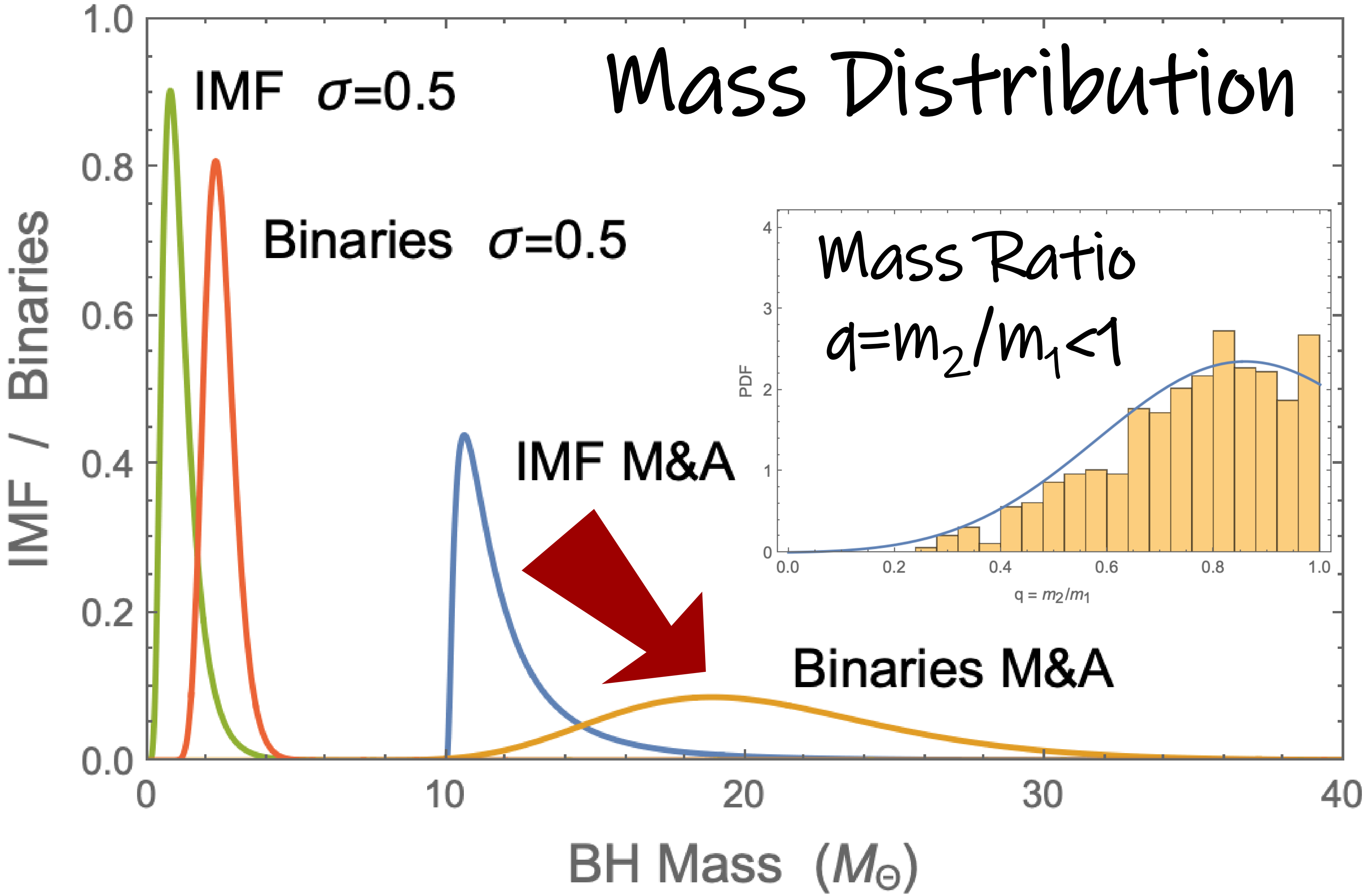

Binary escapers

- The larger the initial N, the harder the binary needs to be to escape.
- Mainly highly eccentric (at birth) binaries coalesce in a Hubble time.
- Most binaries would not have merged by now. Only {58,7,0,0} of the {504,371,153,60} binary escapers are off-cluster mergers within the age of the universe.
- Binary escapers merger rate lognormal in time

JFN+JGB [2405.06391]

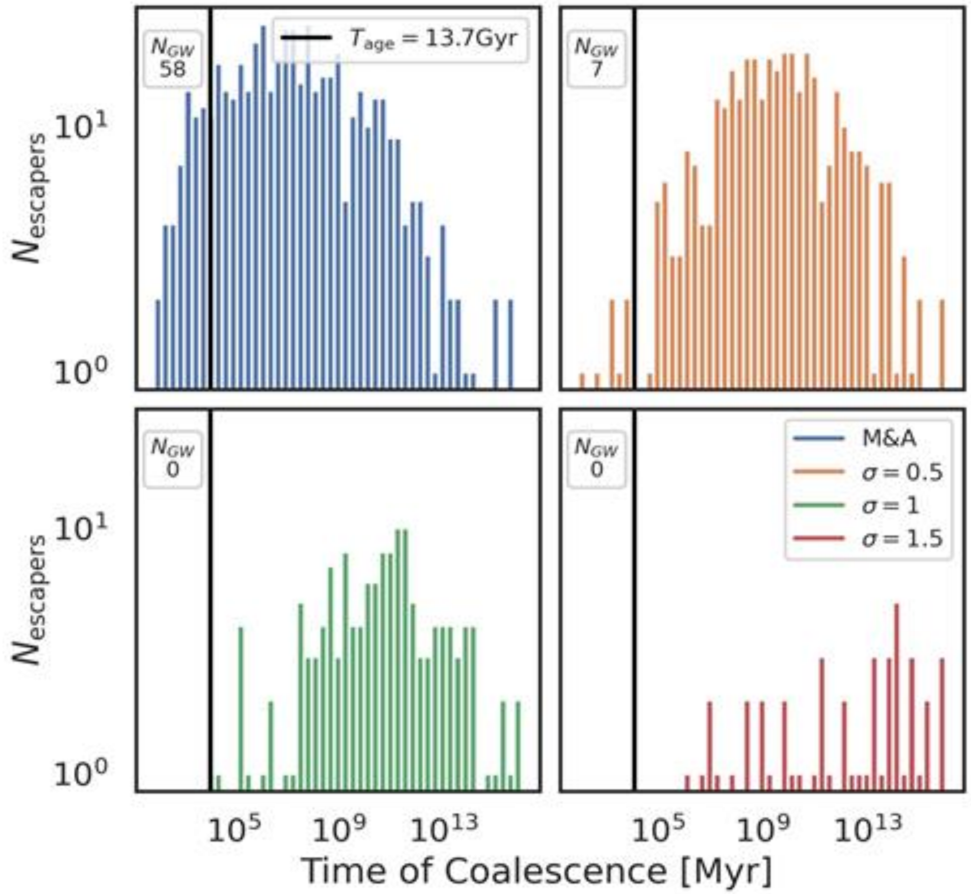

Distribution of merger times for binary escapers using the quasi-circular orbit approximation

Binary escapers

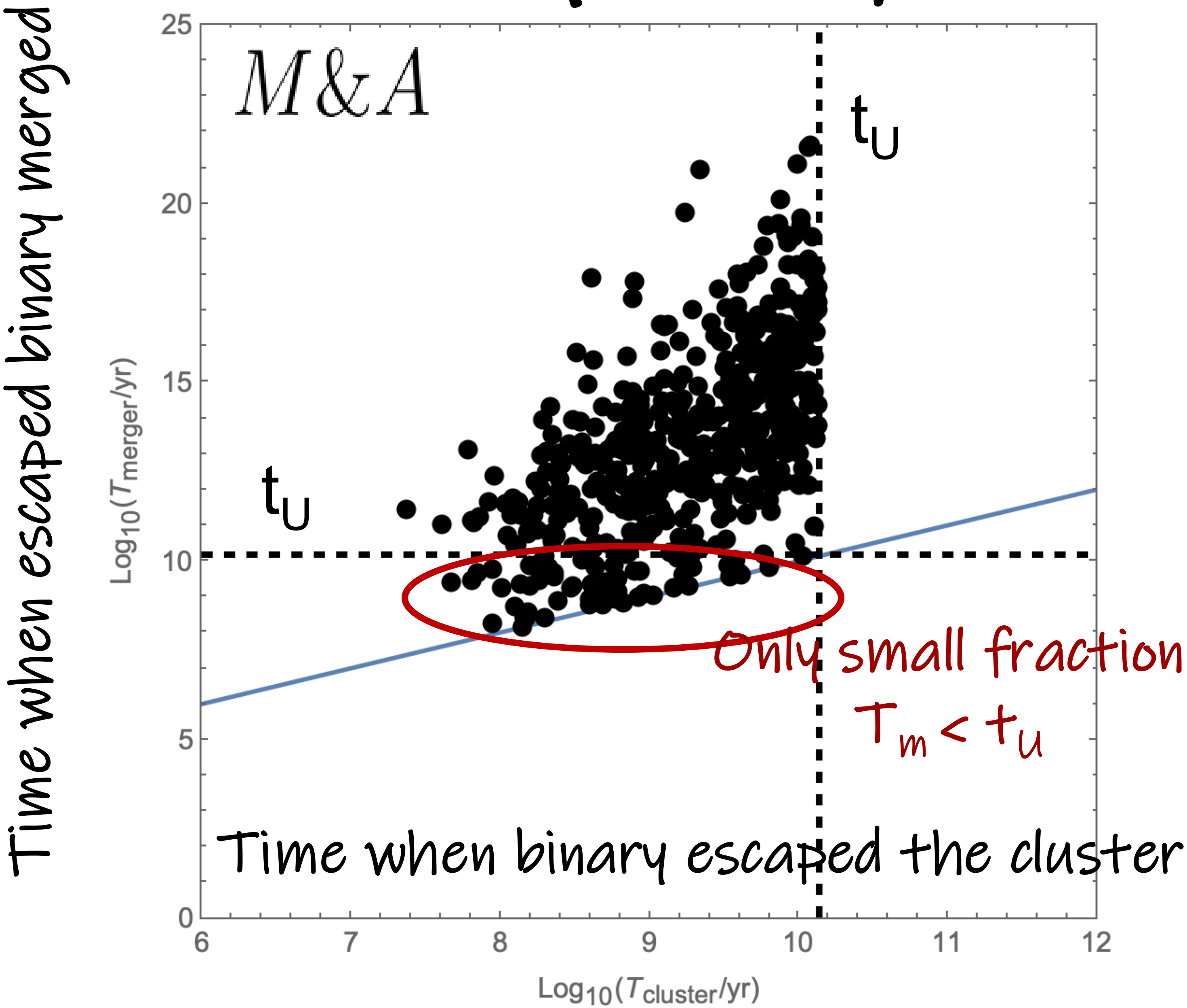

Binary escapers

$M\&A$

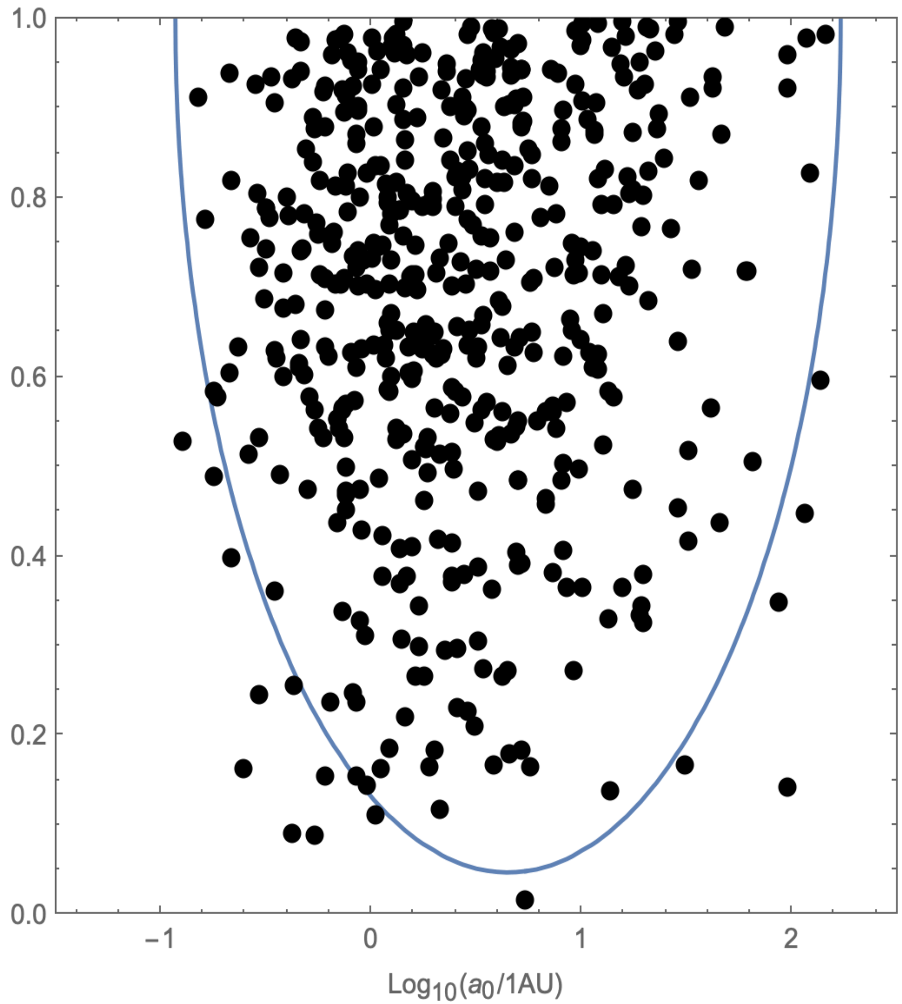

eccentricities

semimajor axis [AU]

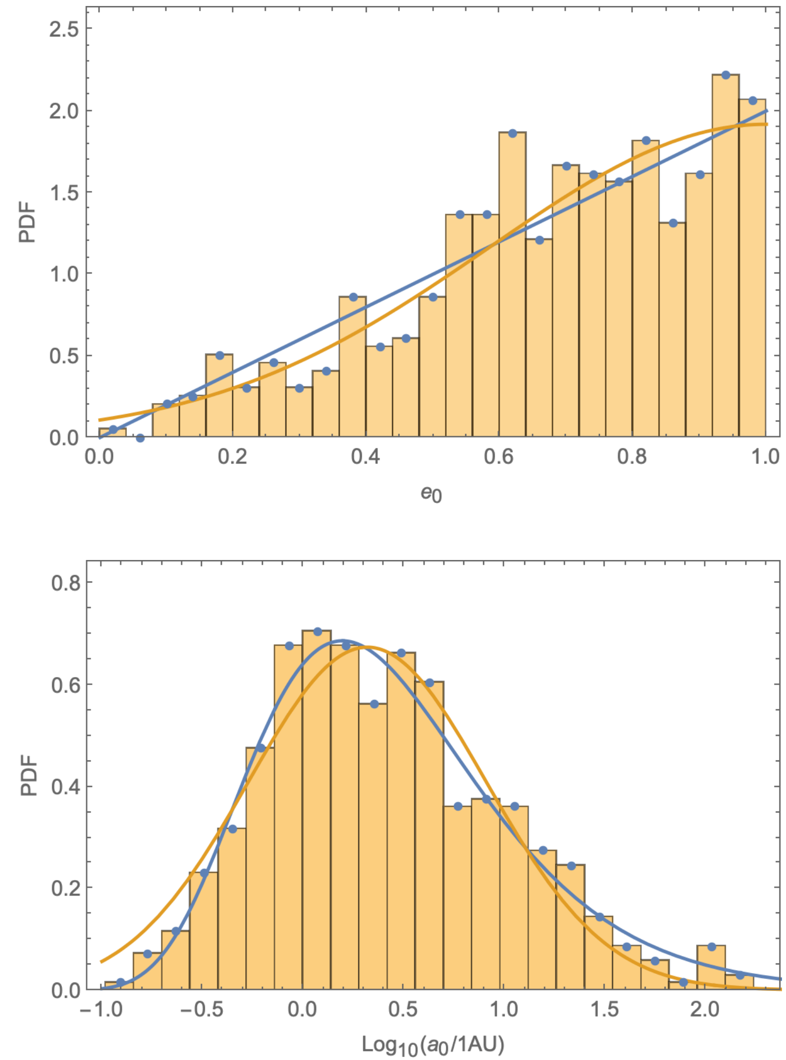

Binary escapers

Numbers increase with initial density but ratio decreases

The larger the initial N, the smaller the semimajor axis of the binaries, that is, the harder the binary.

Mainly highly eccentric binaries coalesce in a Hubble time

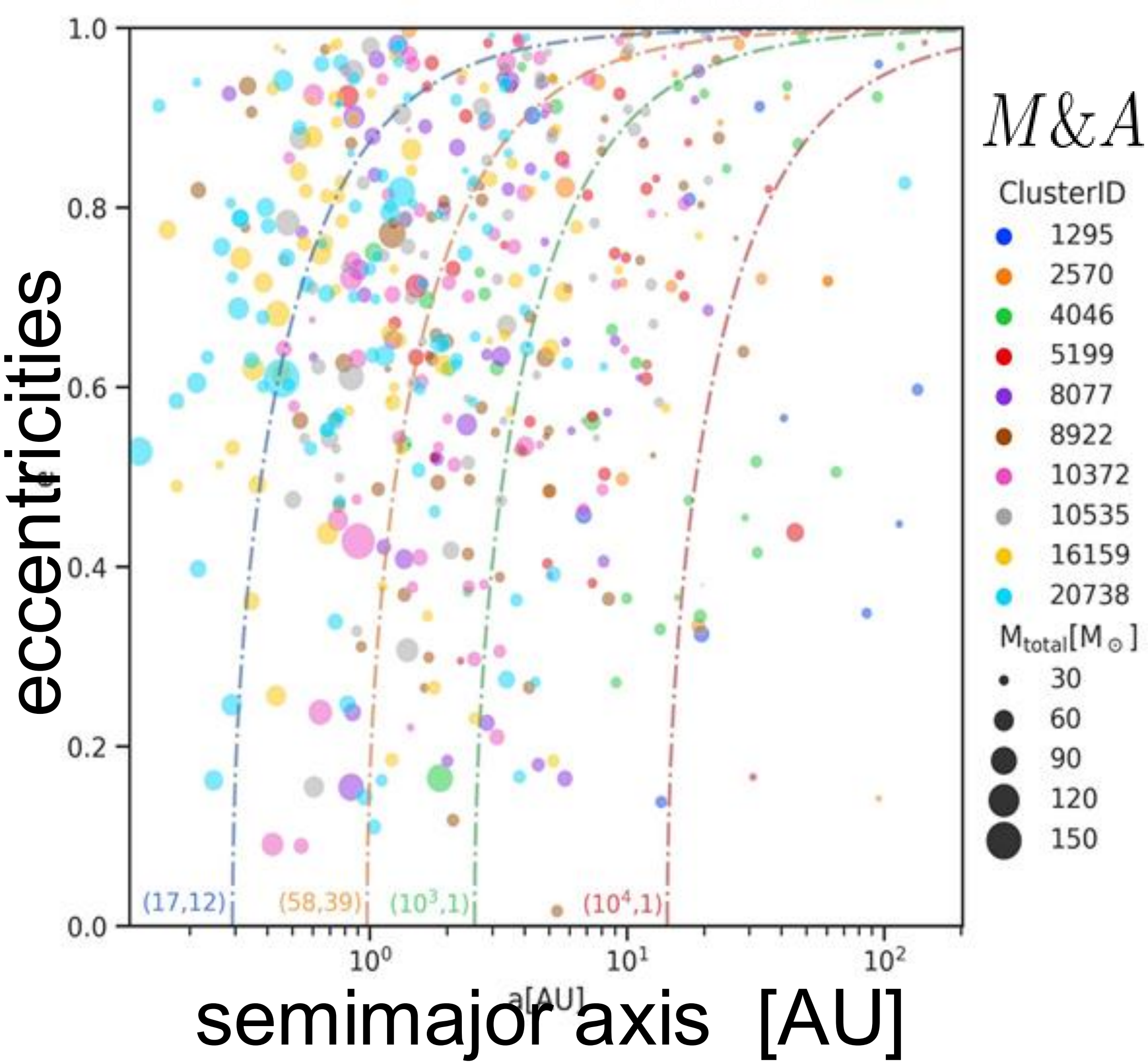

Distribution of eccentricities and semimajor axes of the binary escapers.

BBH merger rates

In-cluster merger rate
for $\sigma_{0.5}$ peaks at z~8
for $M\&A$ peaks at z~2

Escapers merger rate
$\sigma_{0.5}$ peaks at 10^3 t_u
$M\&A$ peaks at 10^5 t_u

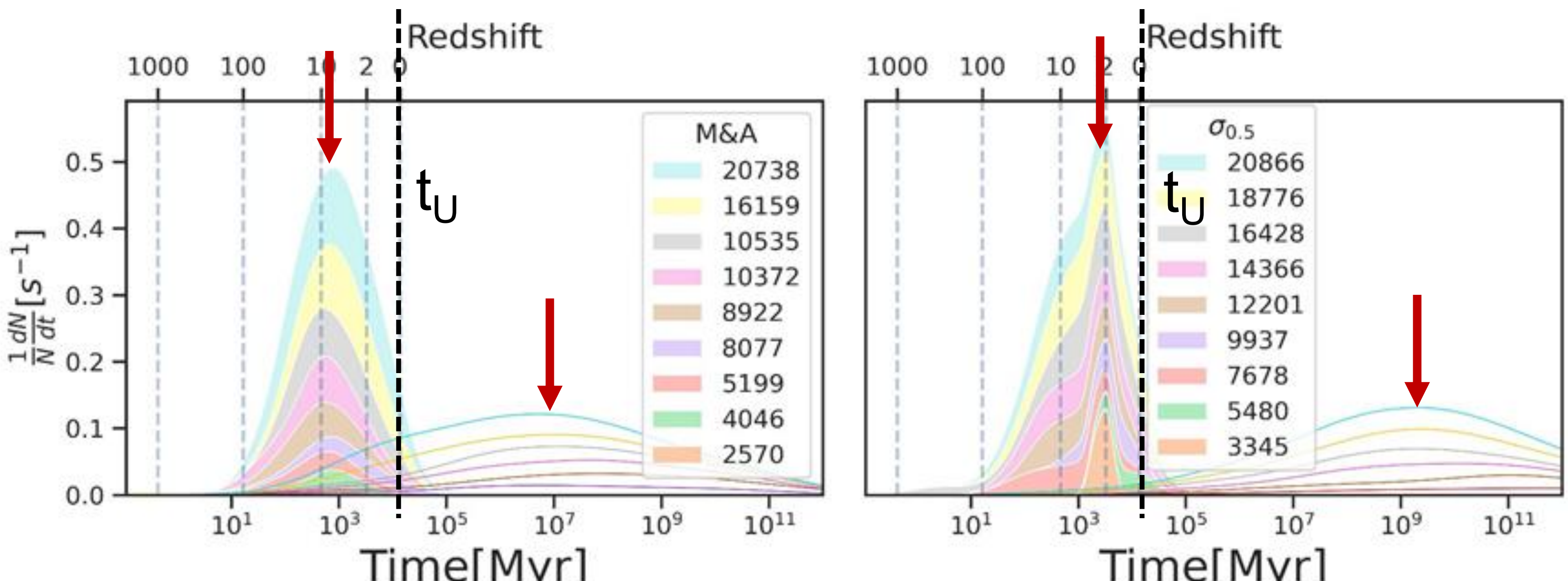

In-cluster and binary escapers merger rate

BBH merger masses

$M\&A$

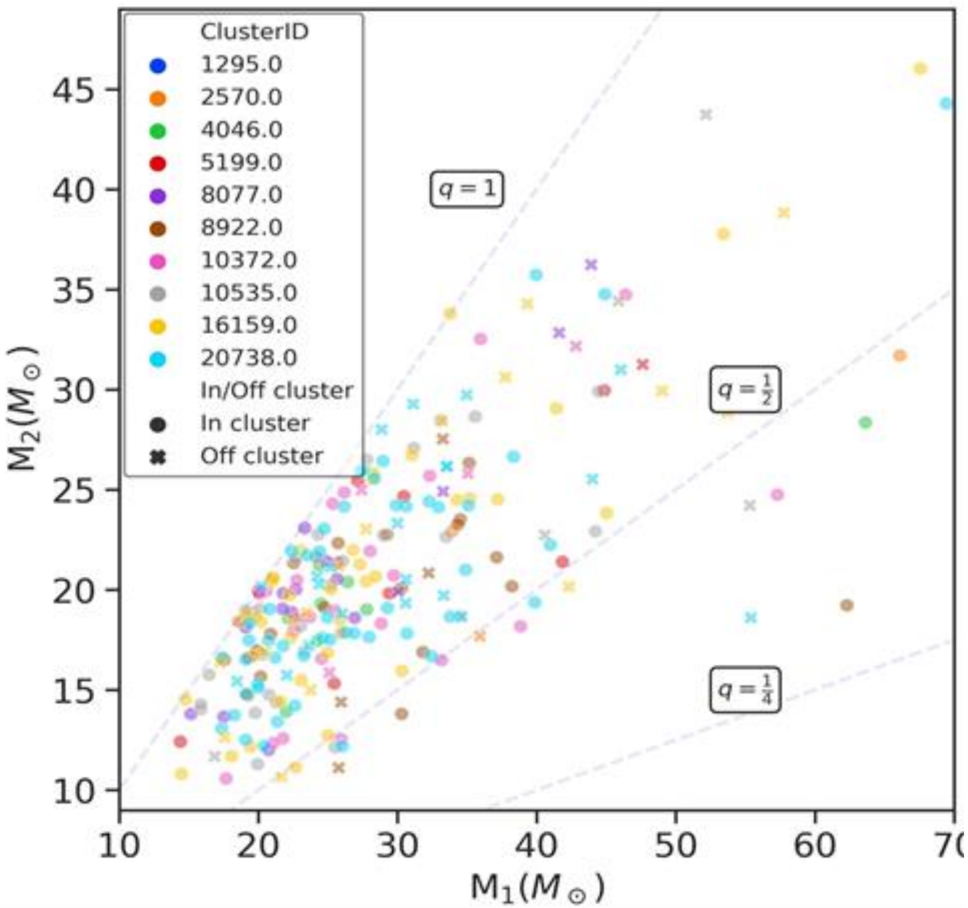

$\sigma_{0.5}$

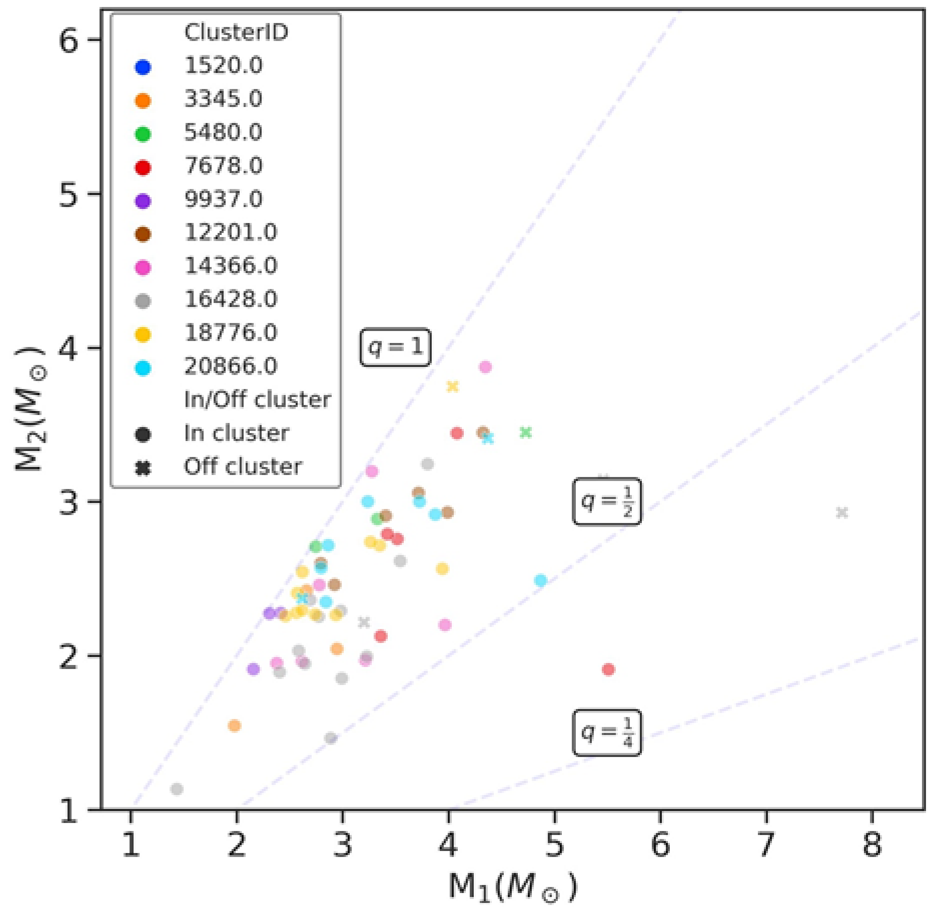

Distribution of the masses (m_1, m_2) of the BBHs mergers

BBH merger kicks

Best environment to study and understand implications as collisions are numerous

BH kicks as implemented in **Nbody6++GPU** based on Campanelli et al.

Probability of hierarchical mergers drastically reduced

$M\&A$

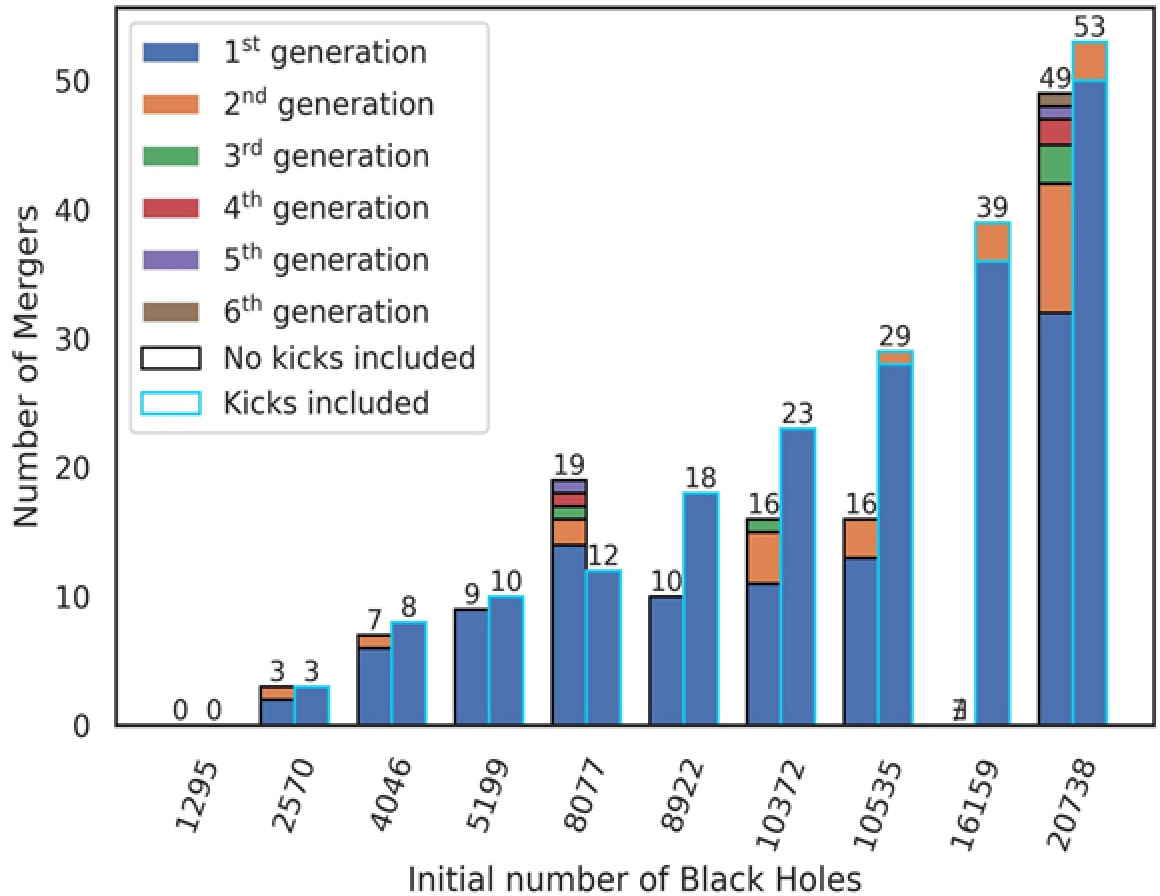

Histogram of the number of in-cluster mergers for the $M\&A$ type with and without considering BH kicks

BBH merger eccent.'s

GW searches assume quasi-circular approx. How good is this hypothesis?

Residual eccentricity less than 10^{-4} at f=10Hz

Uncorrelated with redshift

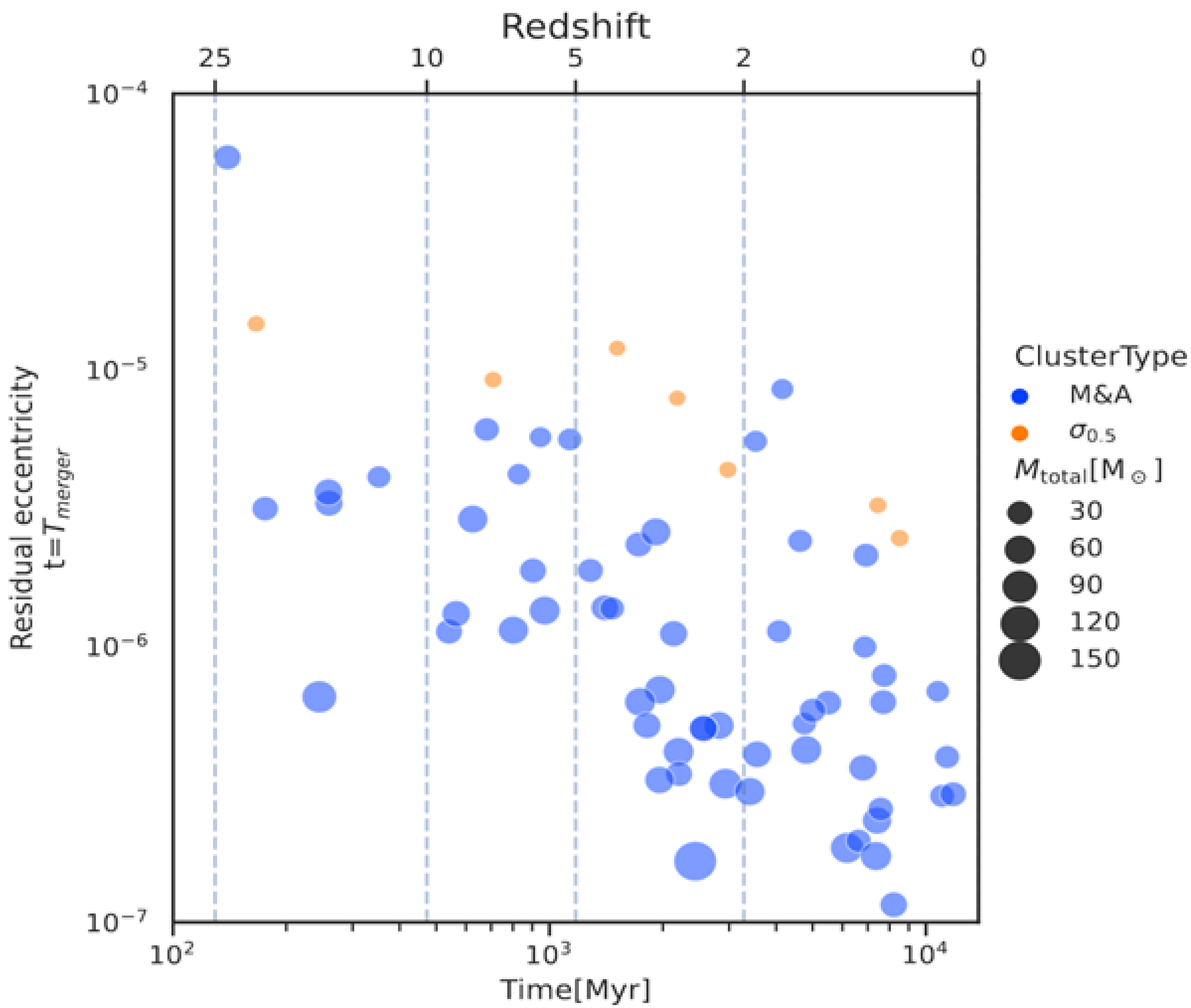

Residual eccentricity of the off-cluster mergers

Inspirals vs scatterings

Jaraba, JGB [2106.01436]

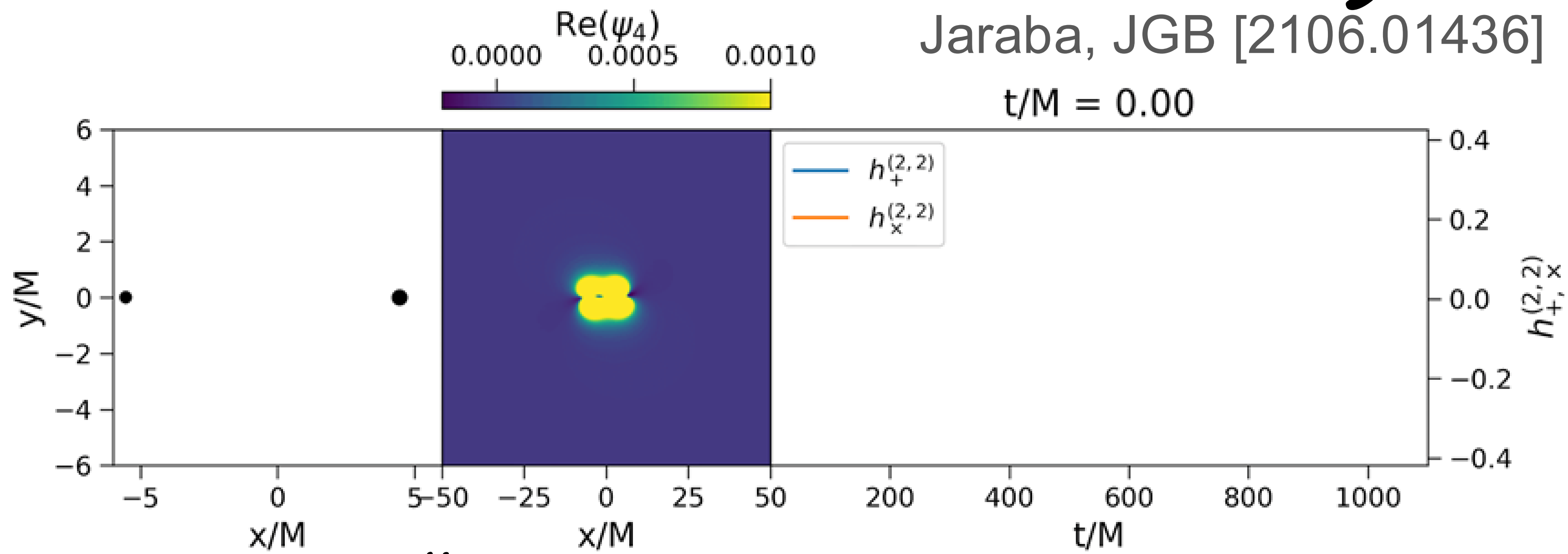

Einstein Toolkit

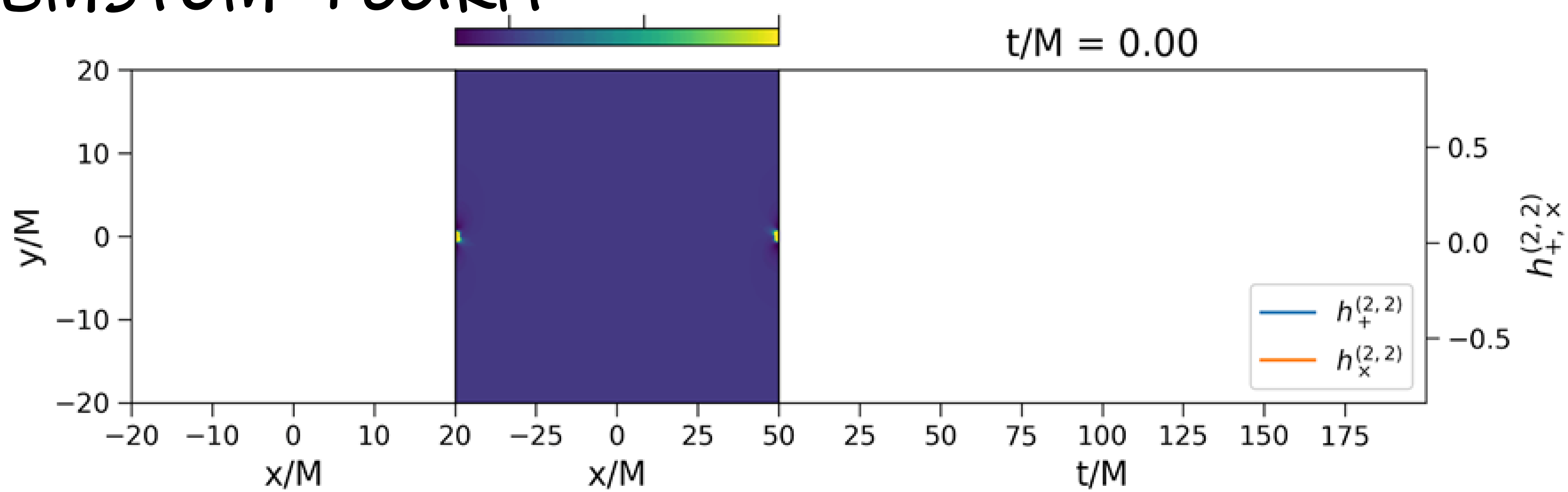

Inspirals vs scatterings

CBC (GW150914)

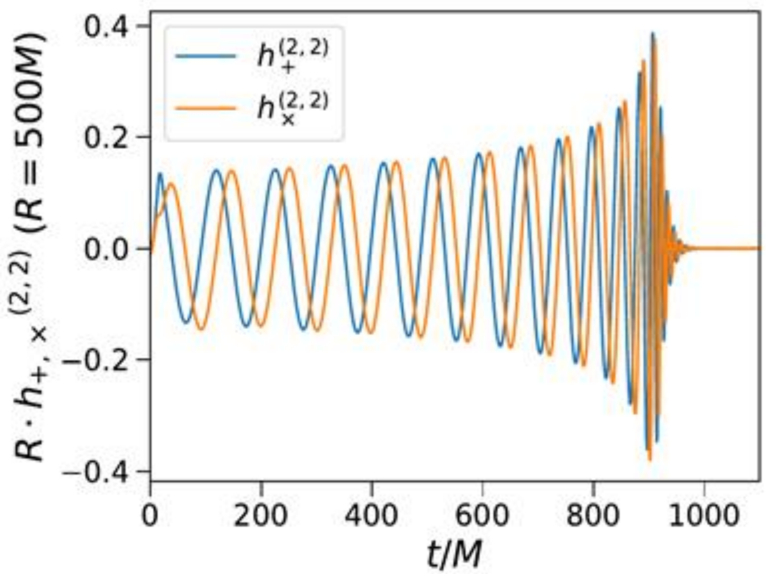

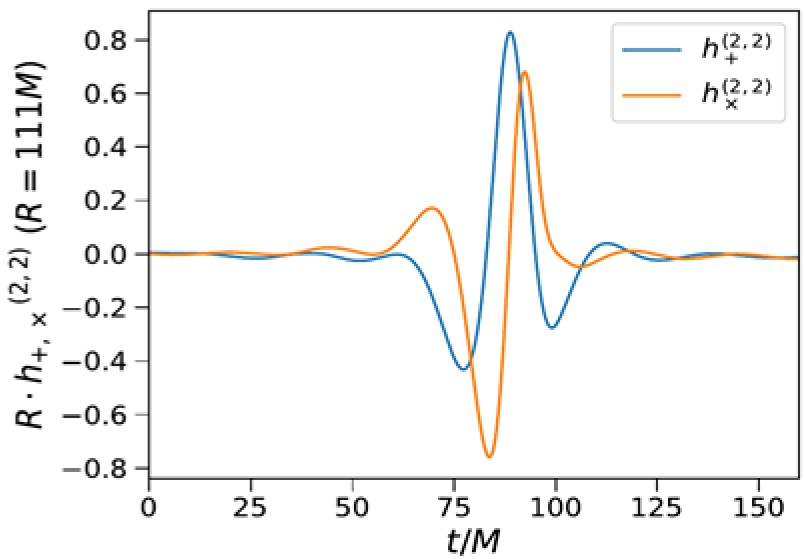

CHE (d/M=100, q=1, p/M=0.49, θ=4.01°)

CHE (d/M=100, q=1, p/M=0.49, θ=3.12°)

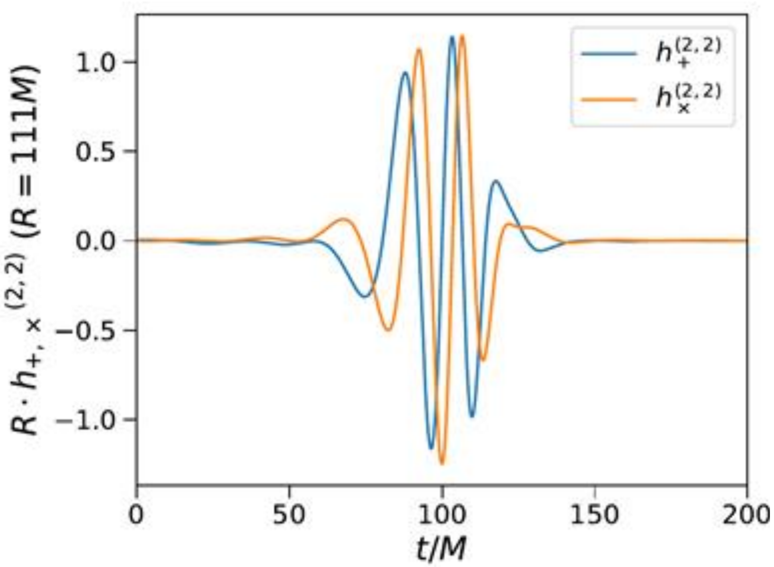

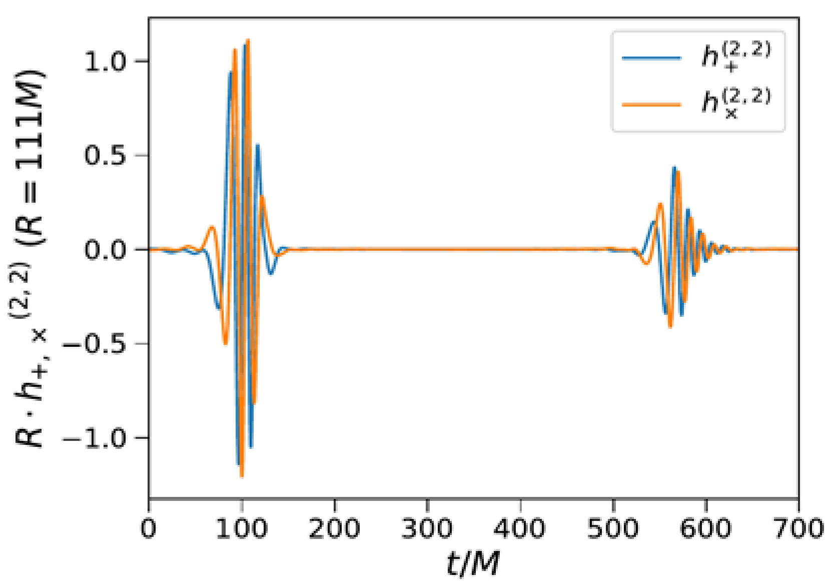

Dynamical capture (d/M=100, q=1, p/M=0.49, θ=3.11°)

Spin induction in dense clusters

Spin acquired at periastron, during GW emission.

Characterized by Kerr parameter **a**.

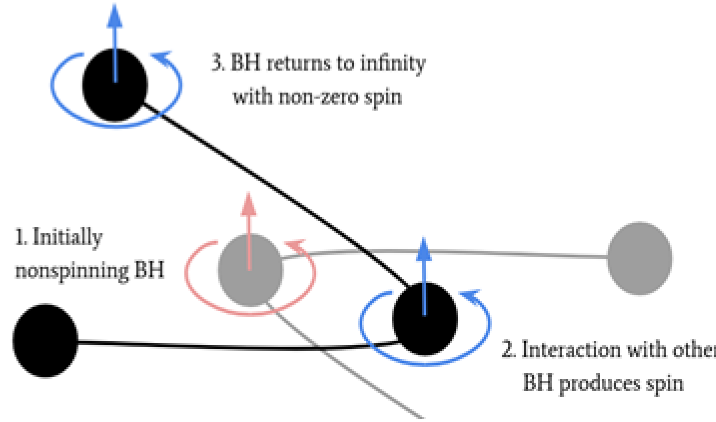

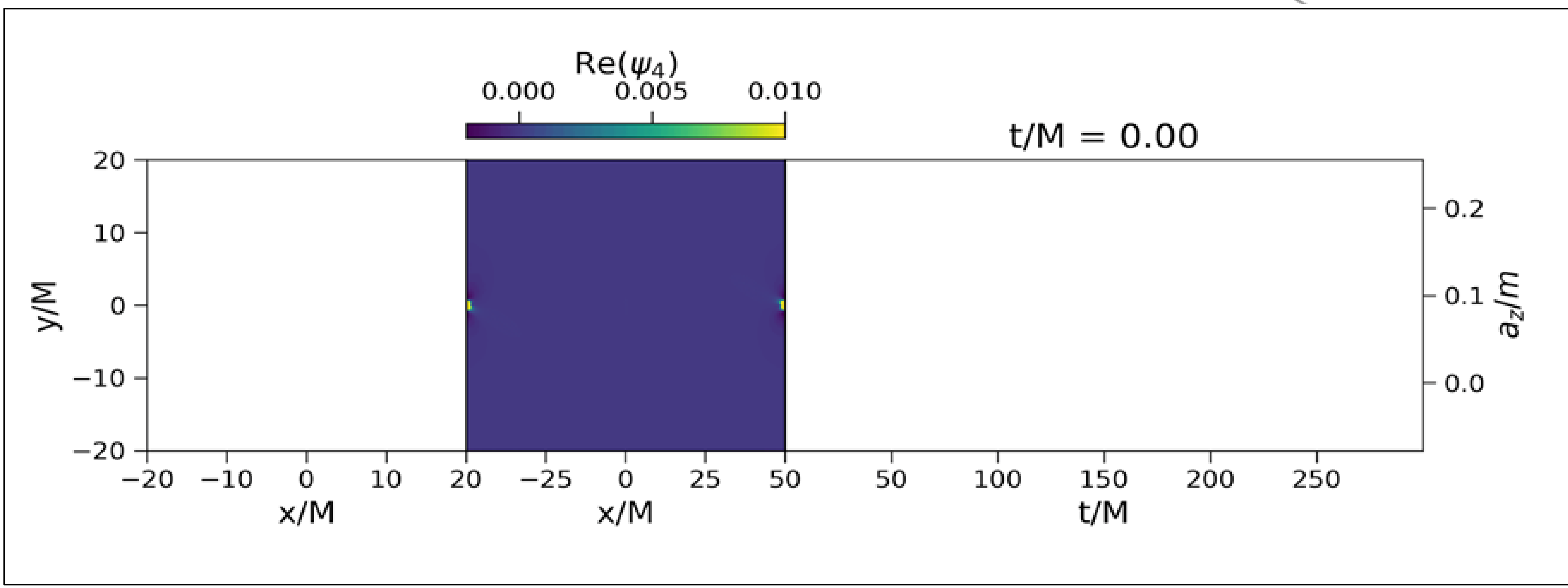

Spin induction in dense clusters

Highest spin is induced in most massive black hole. $q = m_2/m_1 \leq 1$.

Spin induction is enhanced for the massive black hole when $q \ll 1$.

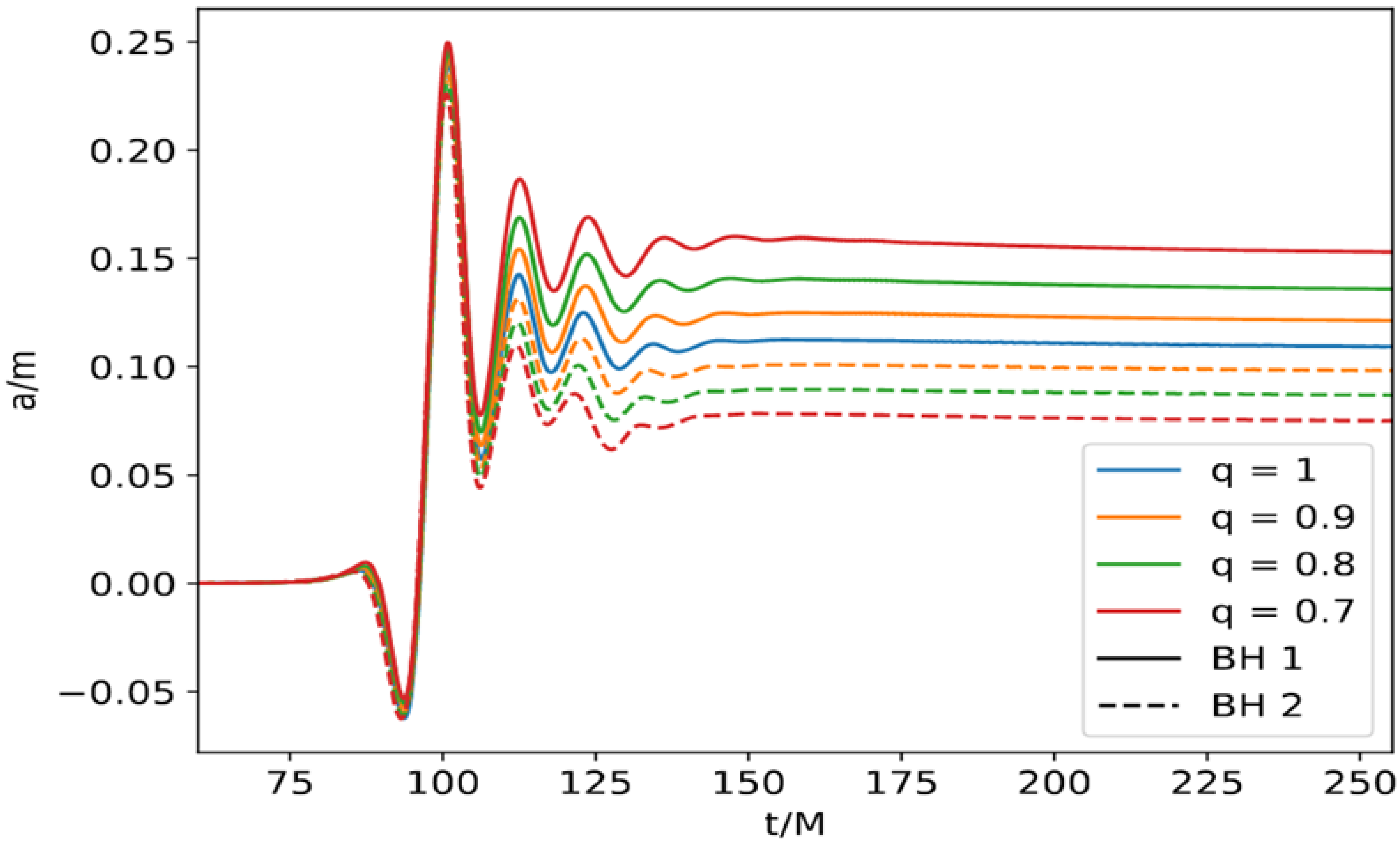

Observational Evidences

Observational evidence for primordial black holes

Carr, Clesse, JGB, Hawkins, Kühnel [2306.03903]

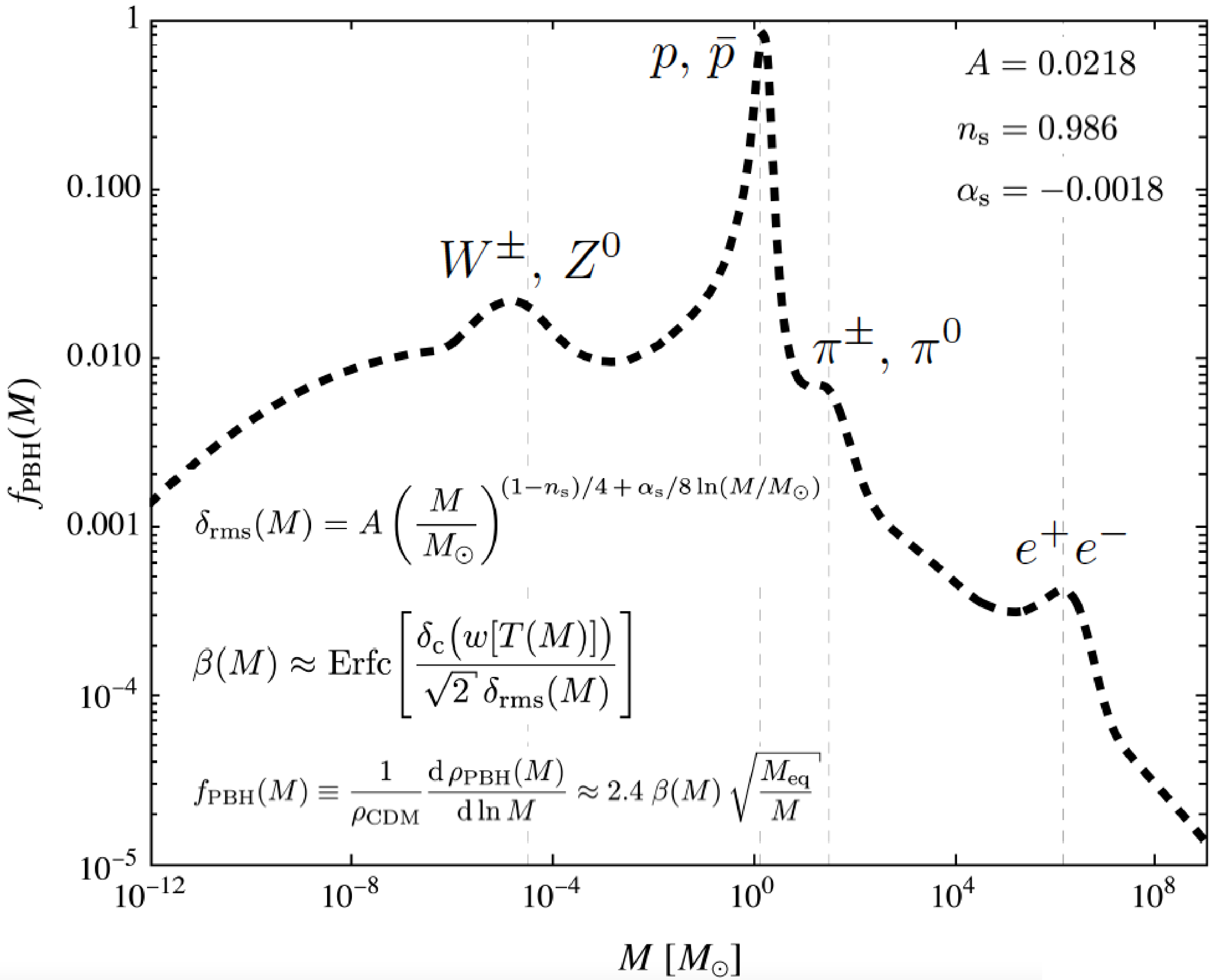

Observational evidence for primordial black holes

Carr, Clesse, JGB, Hawkins, Kühnel [2306.03903]

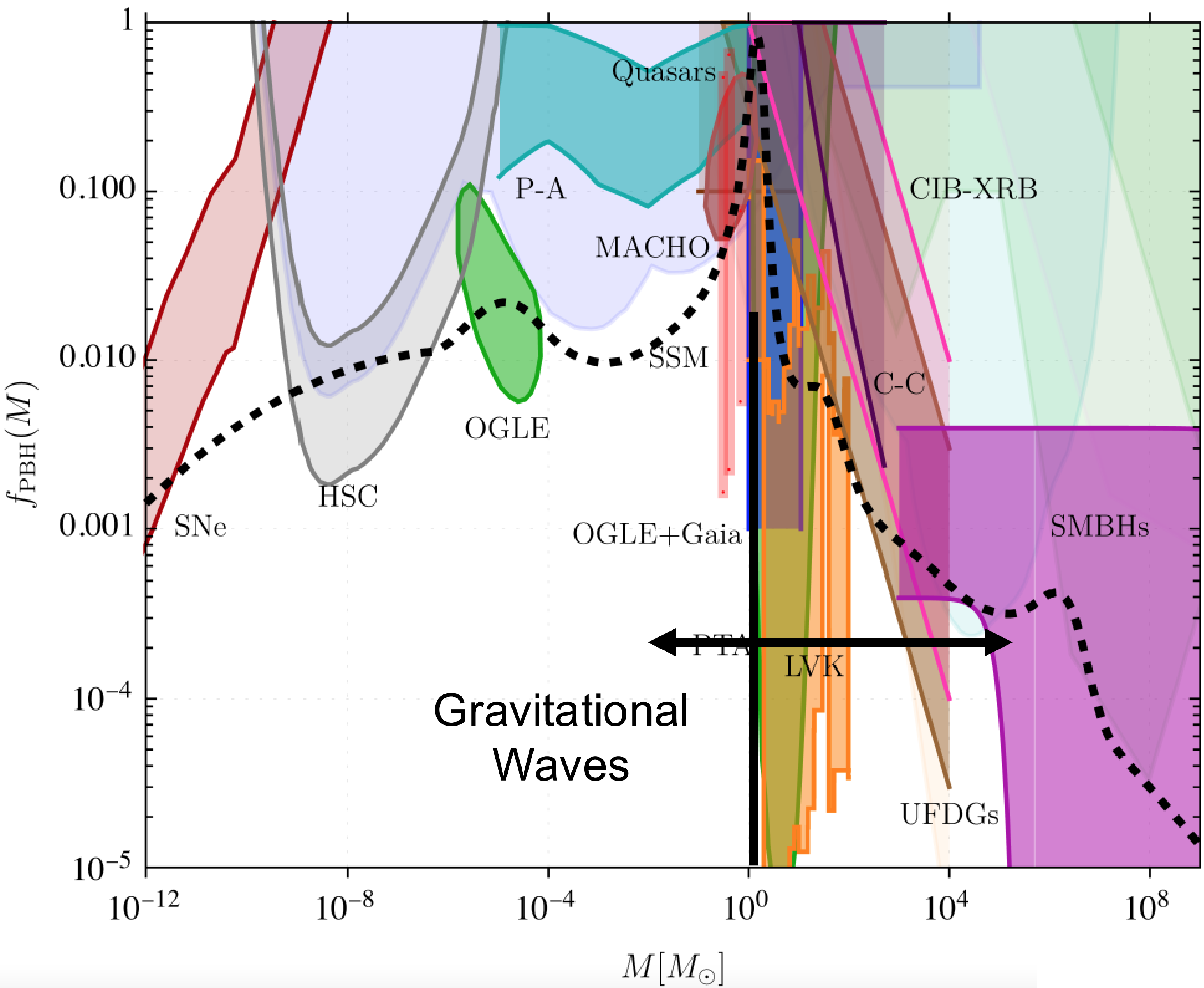

GWTC-1/4 LVK Coll. (2024)

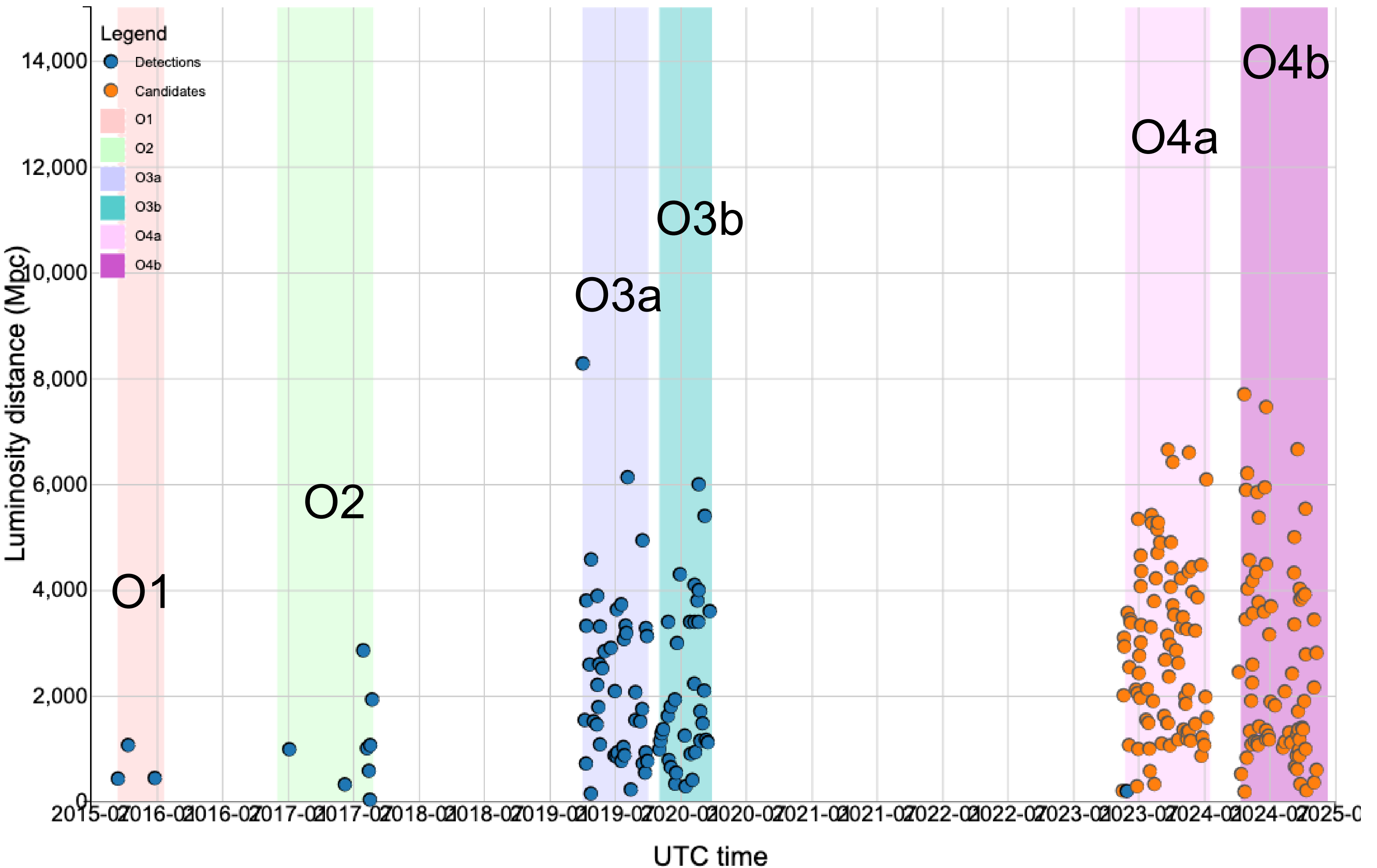

Primary and secondary masses

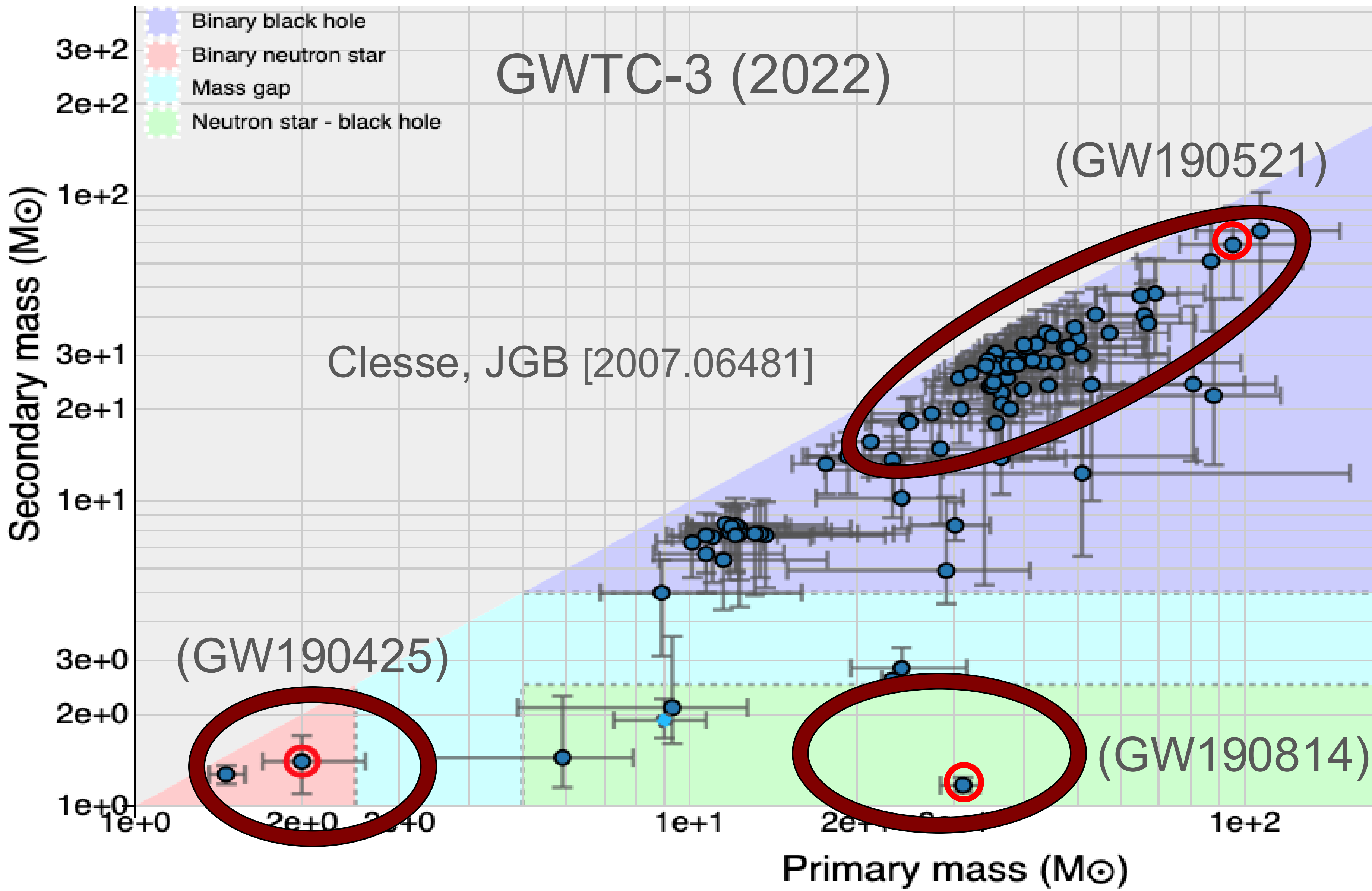

Are LIGO/Virgo BH Primordial?

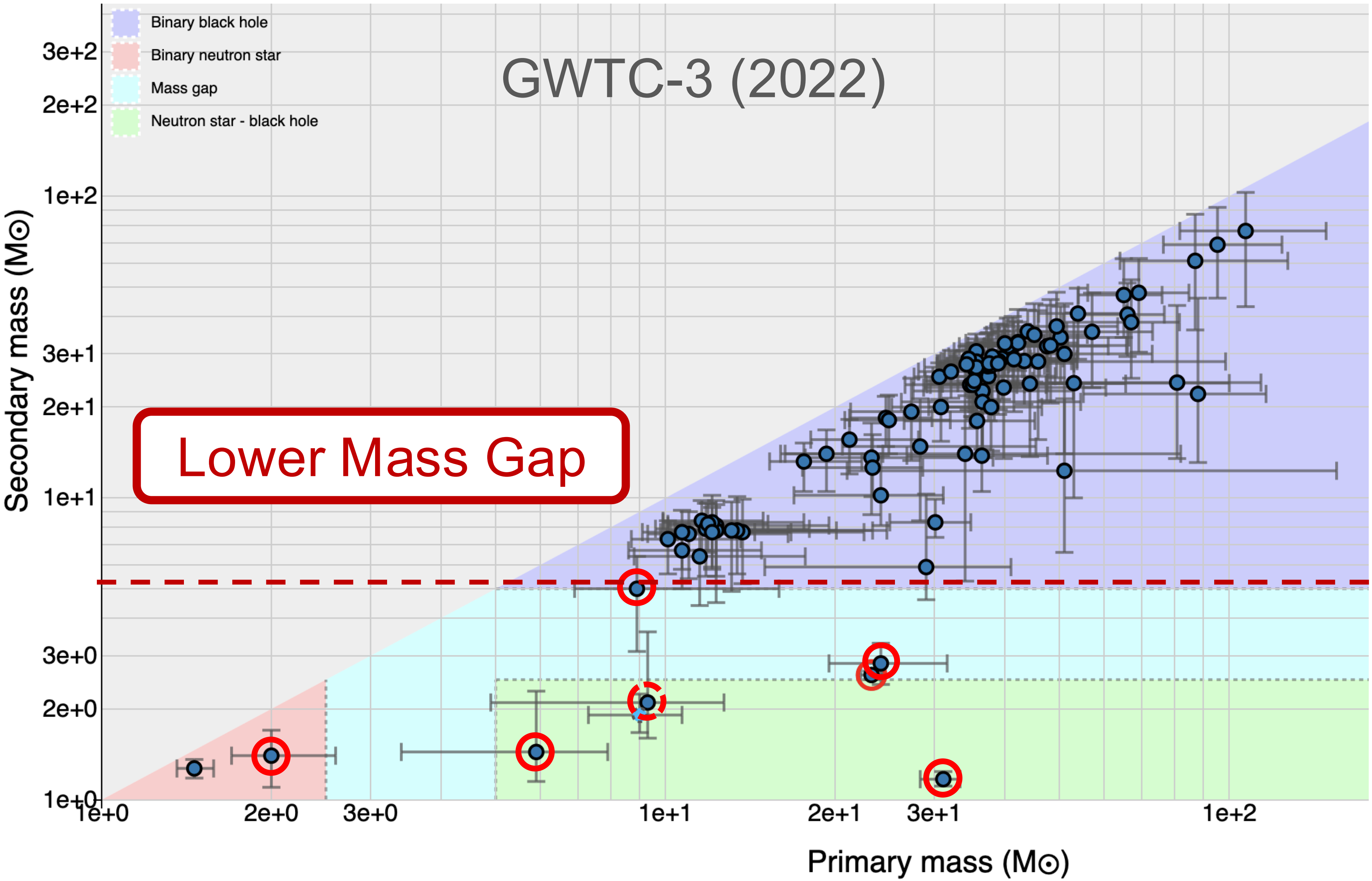

Are LIGO/Virgo BH Primordial?

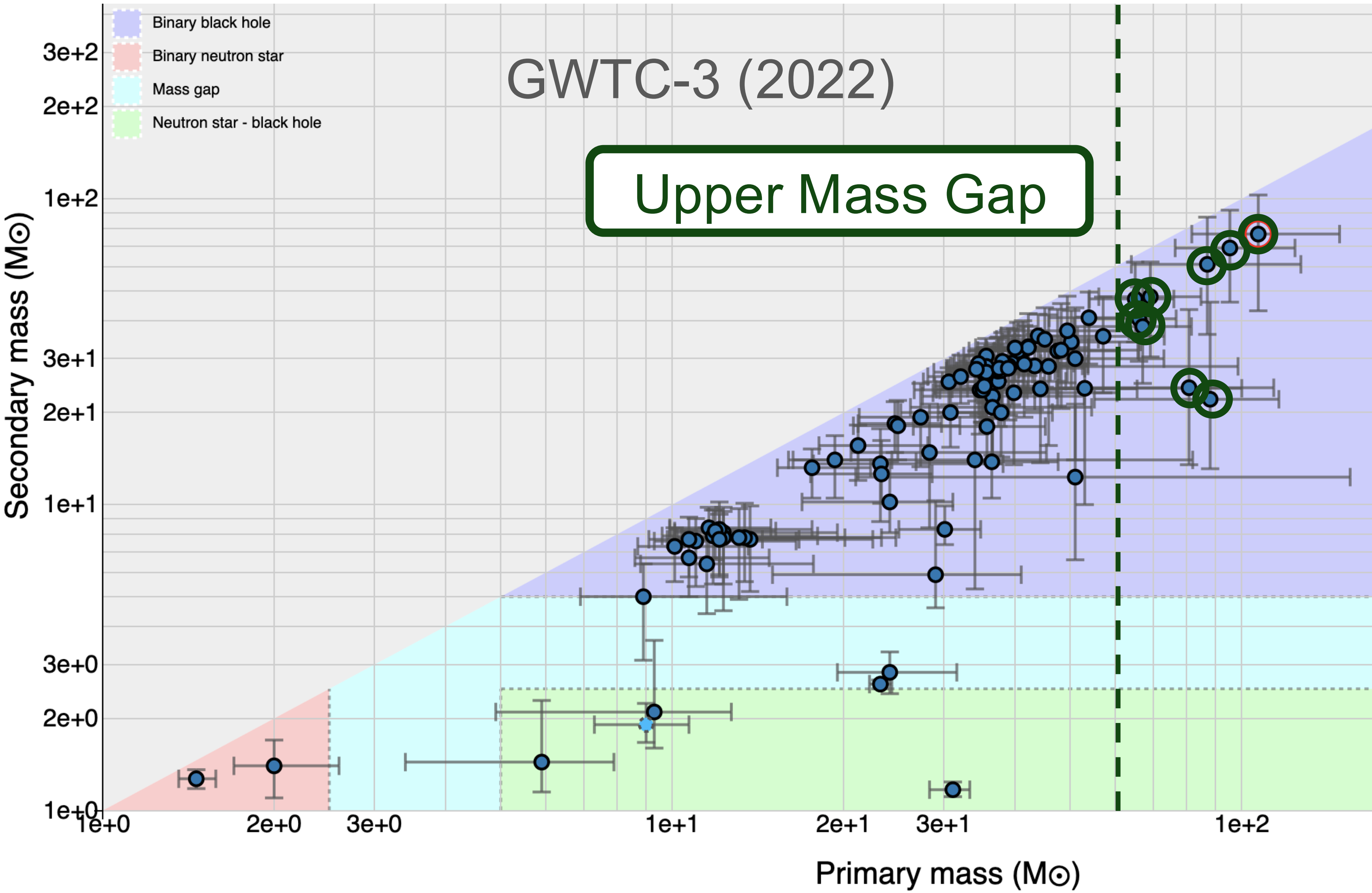

Are LIGO/Virgo BH Primordial?

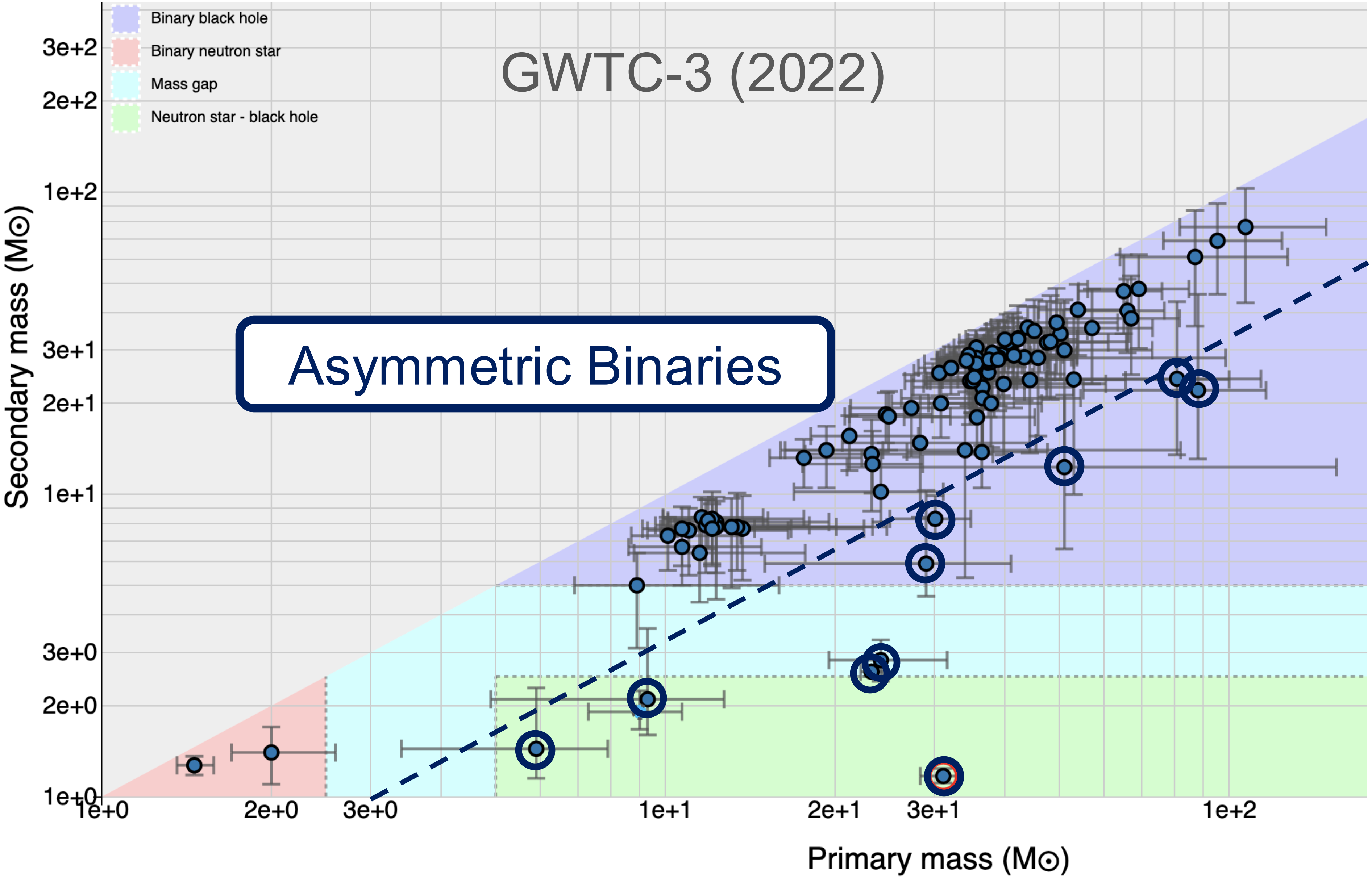

Are LIGO/Virgo BH Primordial?

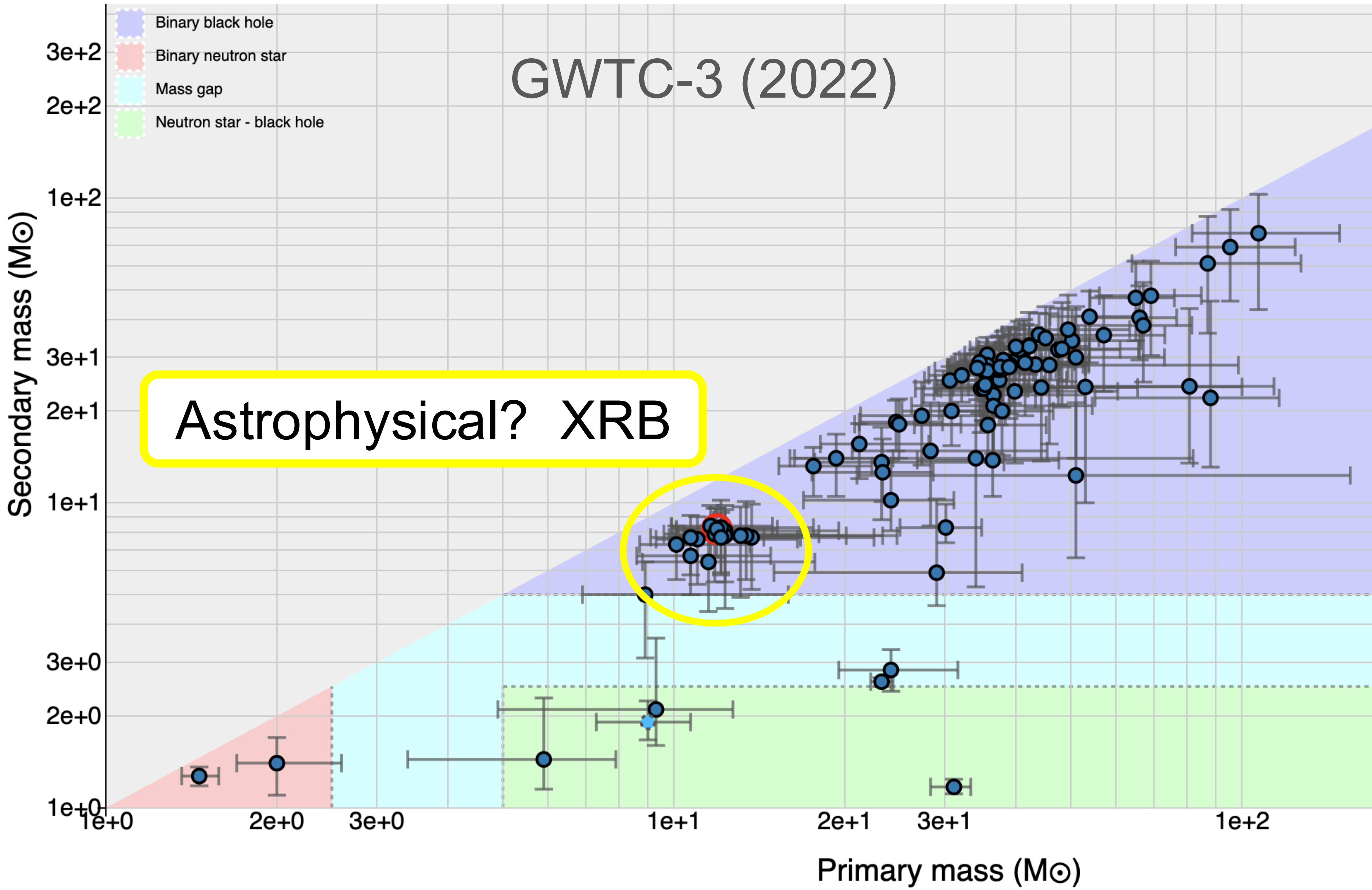

Are LIGO/Virgo BH Primordial?

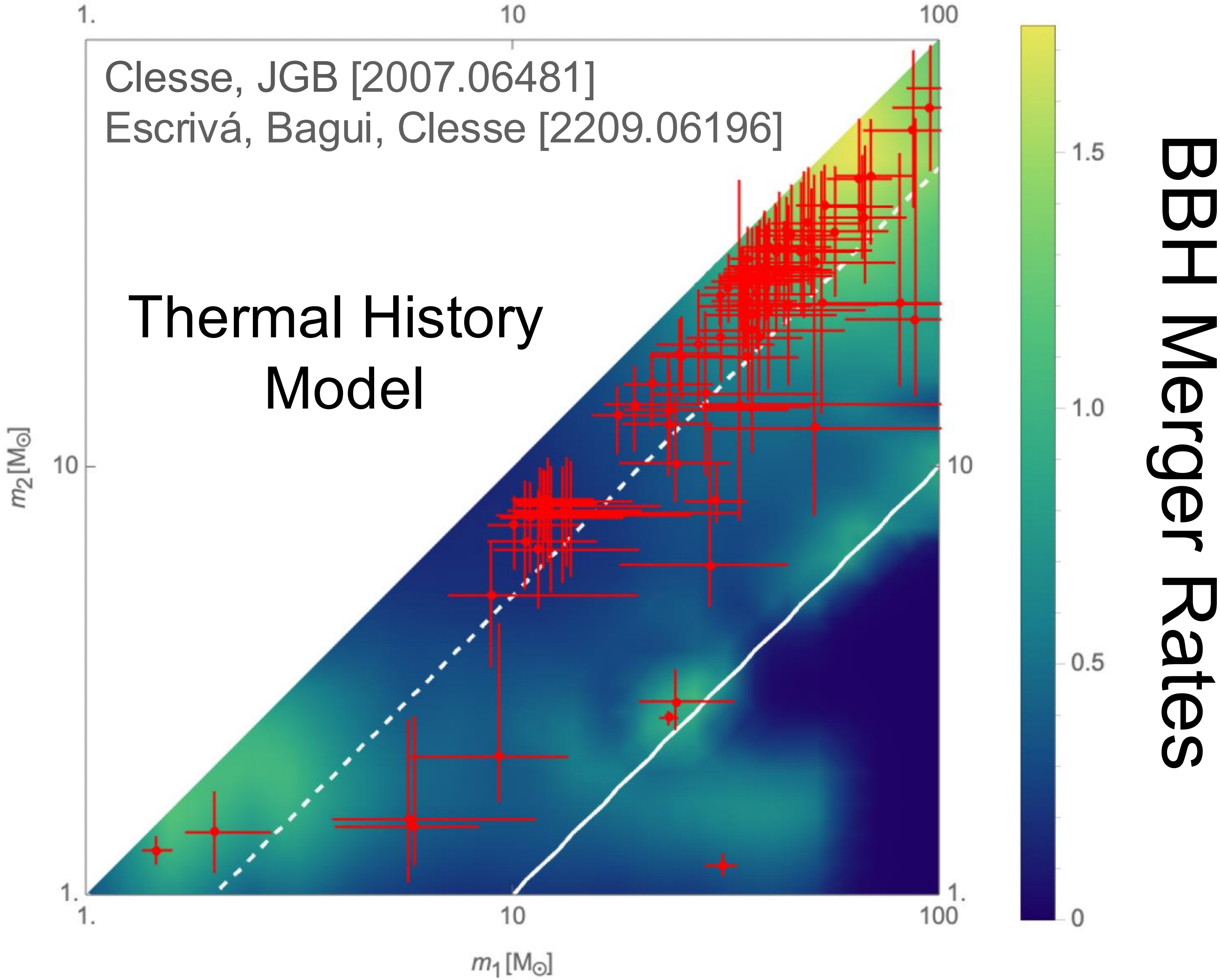

Effective and Final Spin

JGB – Phil.Trans.Roy.Soc.A 0091 (2019)

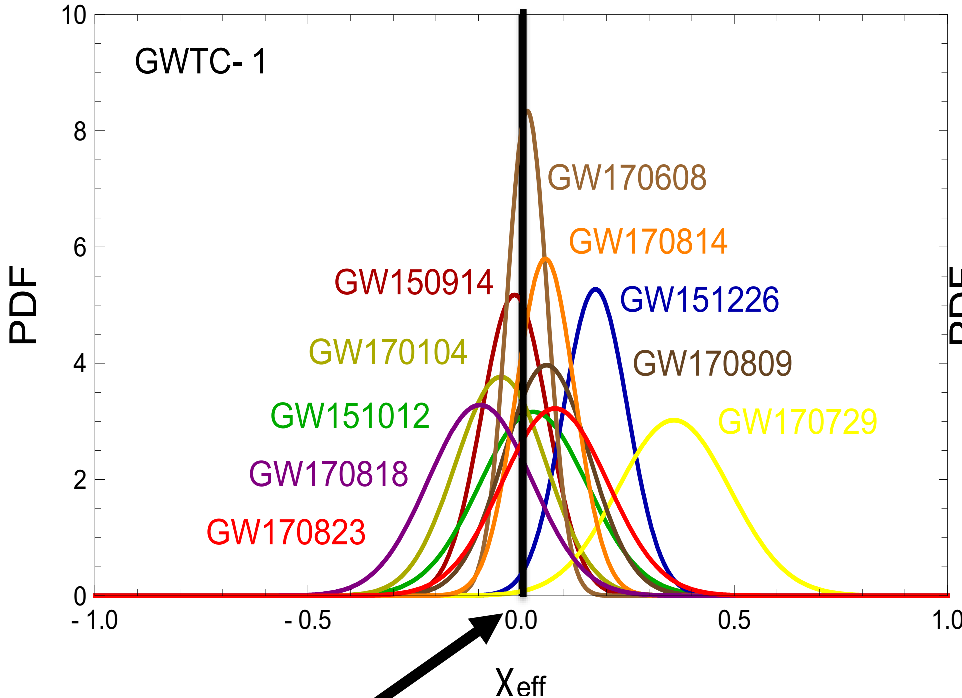

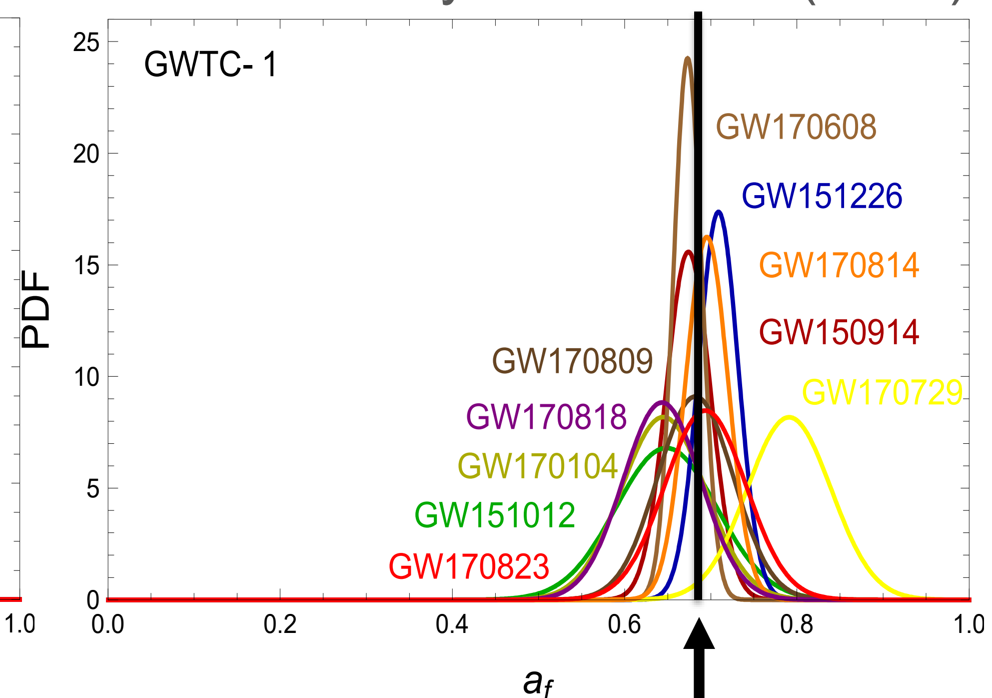

$$\chi_{\rm eff}(S_1 = S_2 = 0) = 0$$

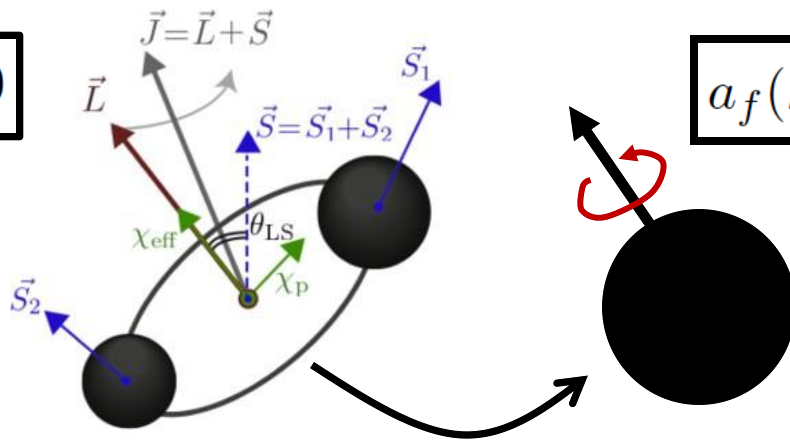

$$a_f(S_1 = S_2 = 0) = 0.686$$

Effective and Final Spin

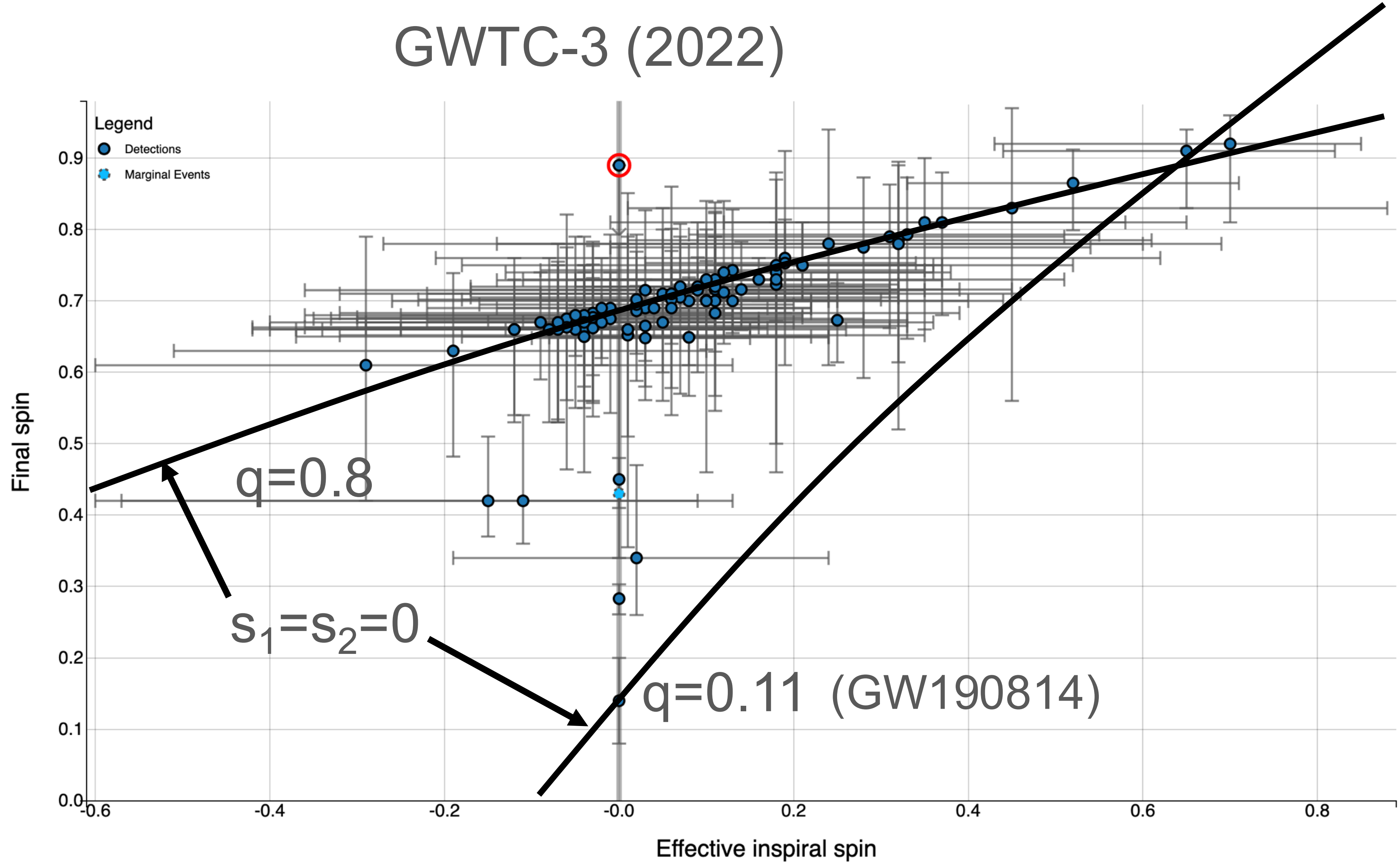

Effective and Final Spin

JGB, Nuño-Siles, Ruiz Morales [2010.13811].

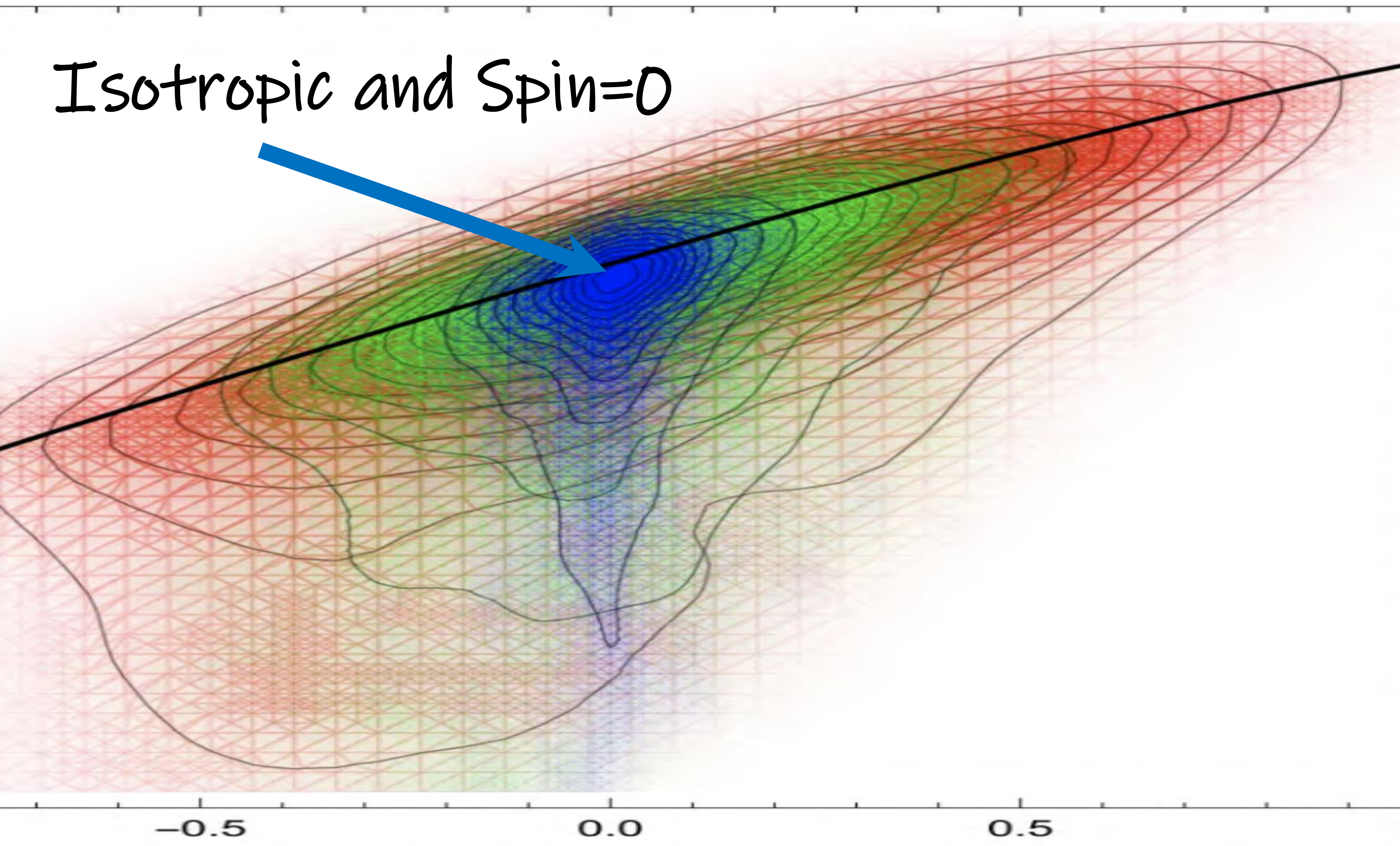

Spin distributions GWTC-3

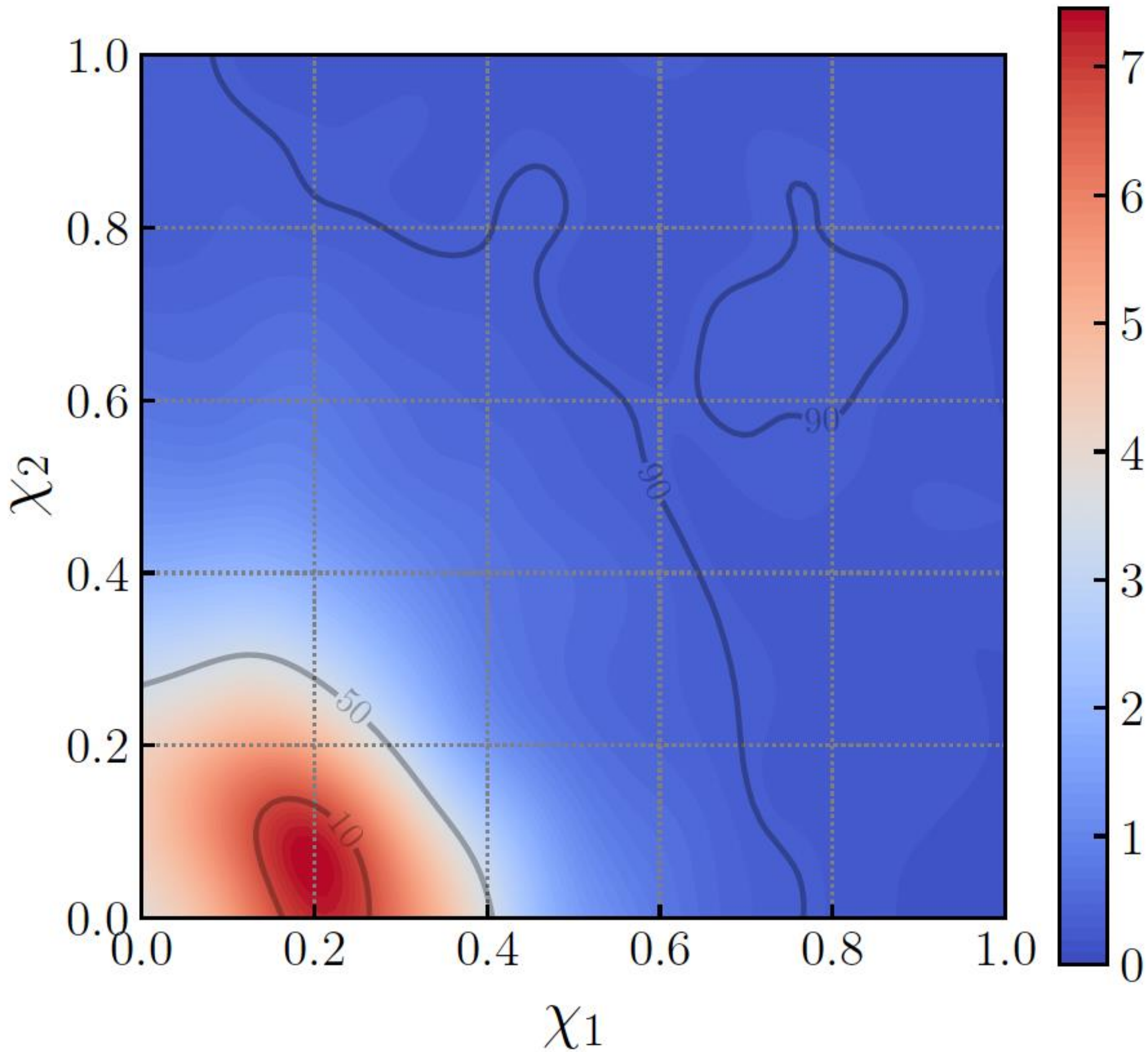

Hussain et al. [2411.02252]

Spin distributions GWTC-3

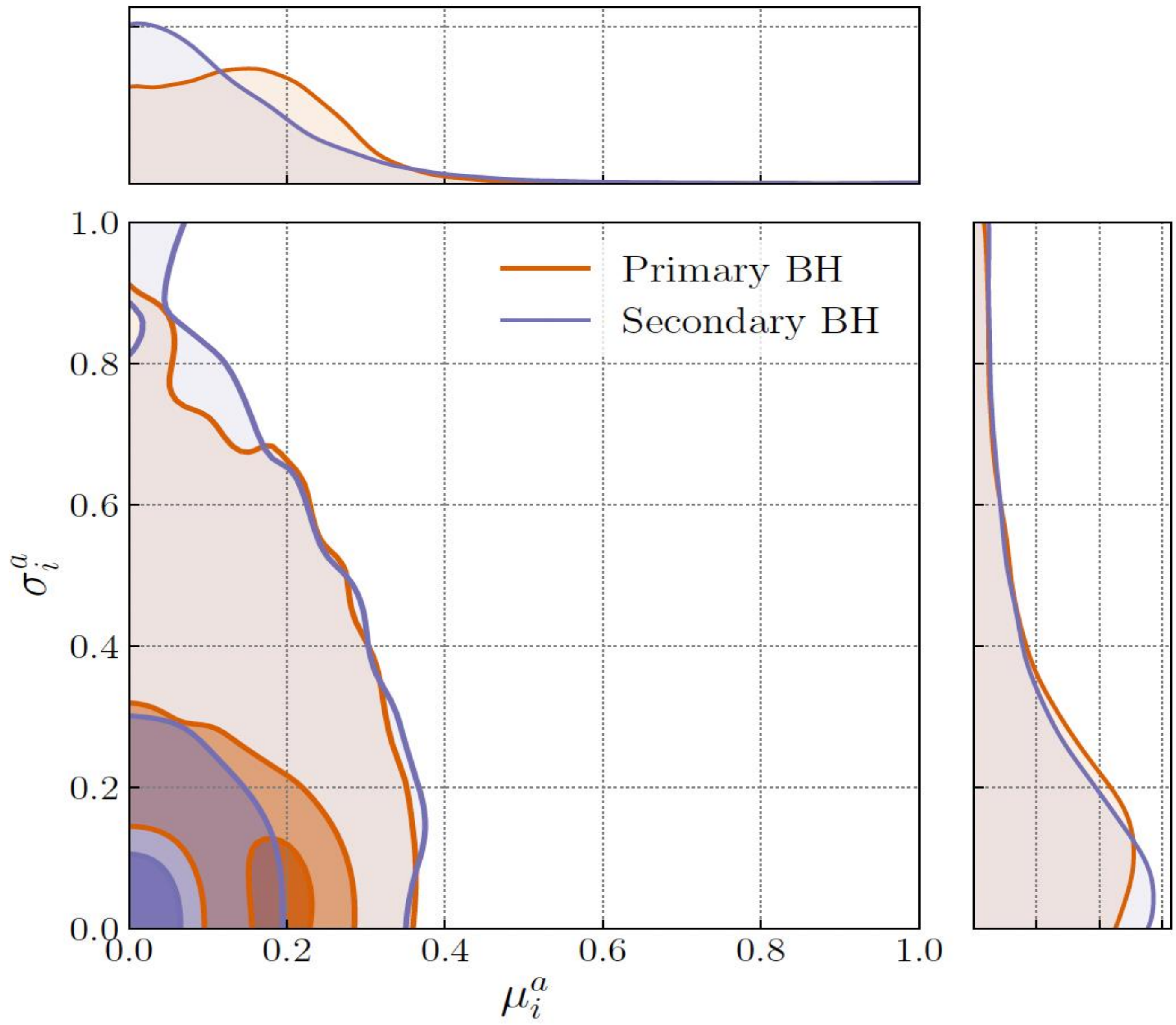

Hussain et al. [2411.02252]

Are there PBH in LIGO/Virgo?

SSM170401

Morras et al. [2301.11619]

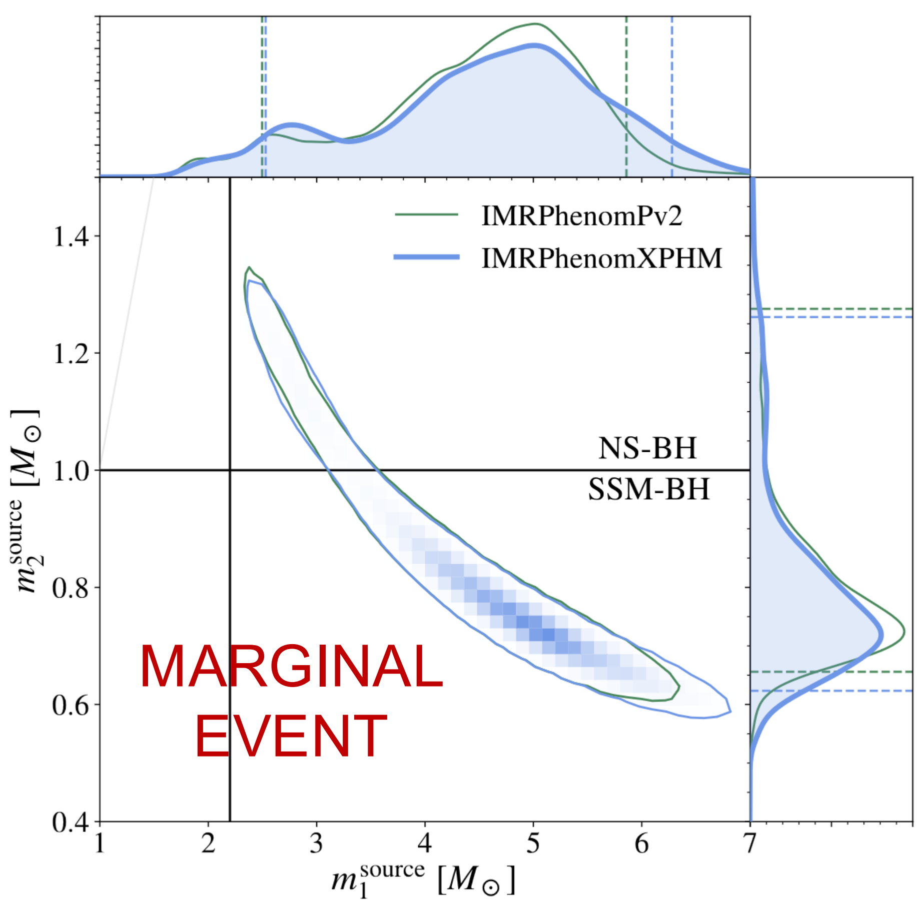

Parameter	IMRPhenomPv2	IMRPhenomXPHM
Signal to Noise Ratio	$7.98^{+0.62}_{-1.03}$	$7.94^{+0.70}_{-1.05}$
Primary mass ($M_\odot$)	$4.65^{+1.21}_{-2.15}$	$4.71^{+1.57}_{-2.18}$
Secondary mass ($M_\odot$)	$0.77^{+0.50}_{-0.12}$	$0.76^{+0.50}_{-0.14}$
Primary spin magnitude	$0.32^{+0.47}_{-0.26}$	$0.36^{+0.46}_{-0.30}$
Secondary spin magnitude	$0.48^{+0.46}_{-0.43}$	$0.47^{+0.46}_{-0.42}$
Total mass ($M_\odot$)	$5.42^{+1.10}_{-1.65}$	$5.47^{+1.43}_{-1.68}$
Mass ratio ($m_2/m_1 \leq 1$)	$0.17^{+0.34}_{-0.05}$	$0.16^{+0.34}_{-0.06}$
$\chi_{\rm eff}$ [51, 52]	$-0.06^{+0.17}_{-0.32}$	$-0.05^{+0.22}_{-0.35}$
$\chi_{\rm p}$ [53]	$0.28^{+0.34}_{-0.21}$	$0.33^{+0.33}_{-0.26}$
Luminosity Distance (Mpc)	119^{+82}_{-48}	124^{+82}_{-48}
Redshift	$0.028^{+0.018}_{-0.010}$	$0.028^{+0.017}_{-0.011}$
Ra (°)	-2^{+34}_{-35}	-1^{+34}_{-37}
Dec (°)	47^{+14}_{-26}	46^{+14}_{-29}
Final mass ($M_\odot$)	$5.34^{+1.11}_{-1.70}$	$5.40^{+1.45}_{-1.73}$
Final spin	$0.39^{+0.24}_{-0.07}$	$0.42^{+0.22}_{-0.10}$
$P(m_2 < 1\ M_\odot)$	85%	84%

Are there PBH in LIGO/Virgo?

SSM200308

Prunier et al. [2311.16085]

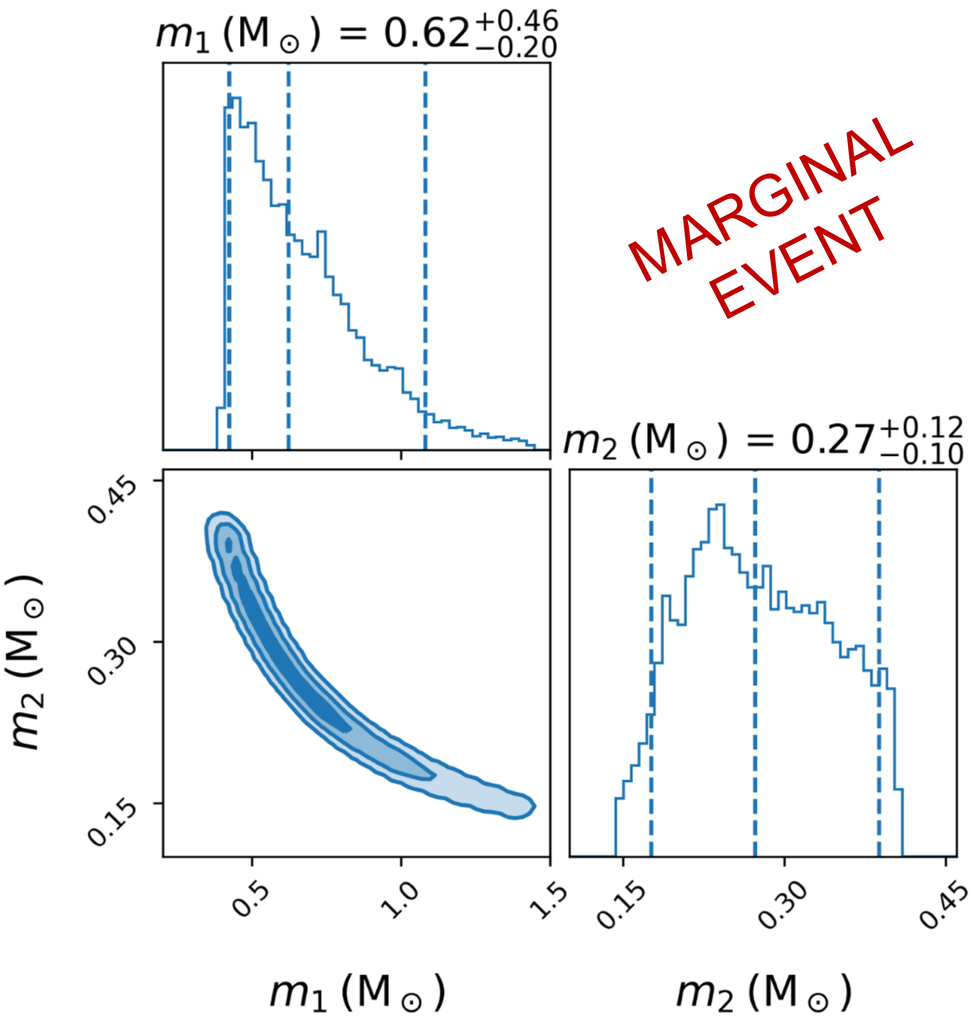

Parameter	
Matched Filter SNR	$8.02^{+0.49}_{-0.85}$
Primary mass ($M_\odot$)	$0.62^{+0.46}_{-0.20}$
Secondary mass ($M_\odot$)	$0.27^{+0.12}_{-0.10}$
Primary spin magnitude	$0.66^{+0.13}_{-0.25}$
Secondary spin magnitude	$0.44^{+0.33}_{-0.39}$
Total mass ($M_\odot$)	$0.88^{+0.35}_{-0.08}$
Detector-frame chirp mass ($M_\odot$)	$0.3527^{+0.0003}_{-0.0001}$
Mass ratio ($m_2/m_1 \leq 1$)	$0.44^{+0.48}_{-0.28}$
$\chi_{\rm eff}$ [27, 28]	$0.41^{+0.08}_{-0.04}$
$\chi_{\rm p}$ [29]	$0.37^{+0.24}_{-0.24}$
Luminosity Distance (Mpc)	90^{+43}_{-39}
Redshift	$0.02^{+0.01}_{-0.01}$
$P(m_1 < 1\ M_\odot)$	92%
$P(m_2 < 1\ M_\odot)$	100%

BBH sensitivity in future G3 GW

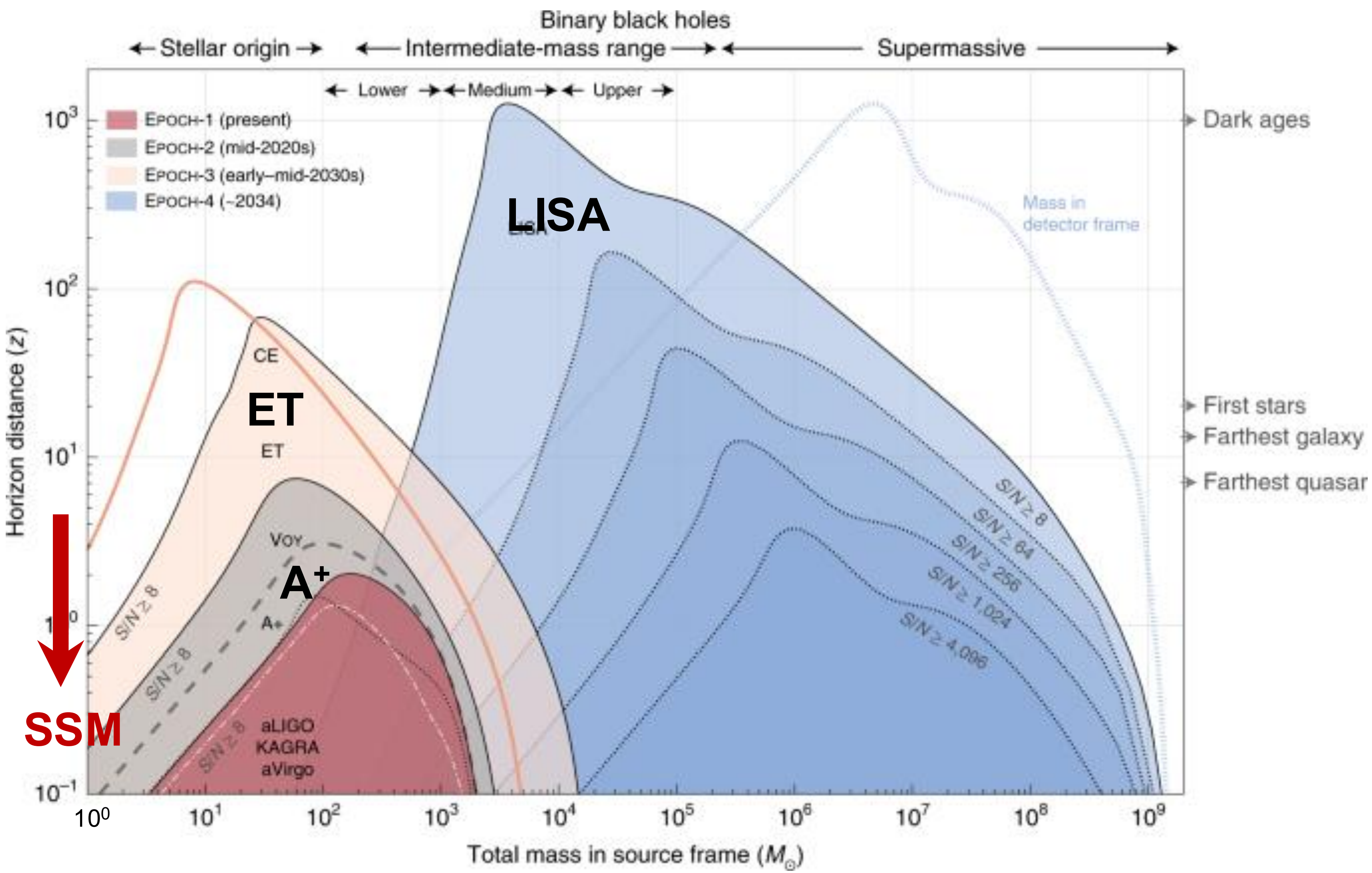

The future of GW (G3)

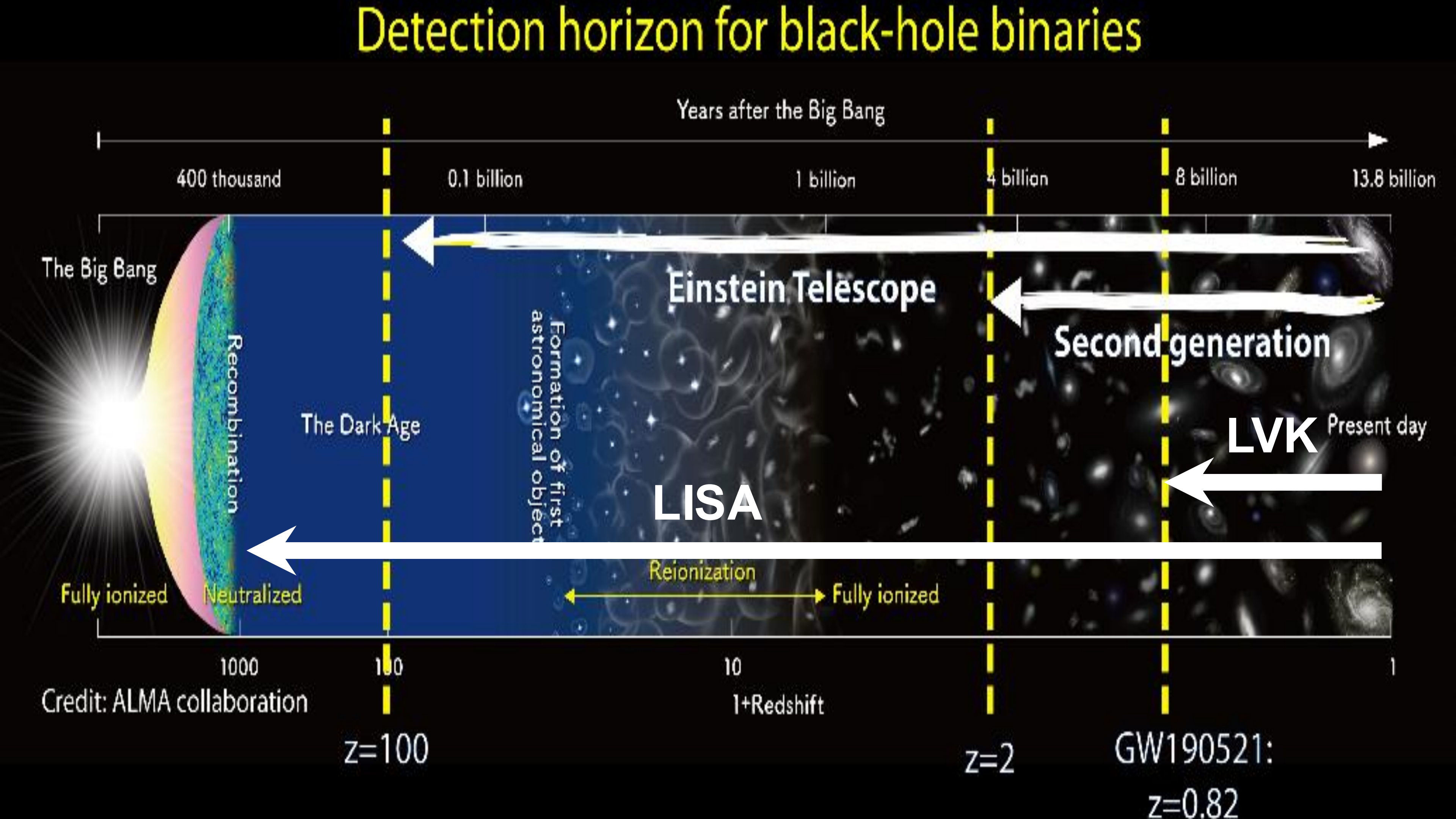

Conclusions

- Quantum diffusion inevitably generates PBH
- Thermal history predicts PBH with multimodal mass distribution $\sim 10^{-5}, 1, 100, 10^{6}\ M_\odot$ ($10^{-10}\ M_\odot$ also?)
- The predicted PBH spin and mass distribution has been measured by LIGO/Virgo + OGLE/Gaia around 1-100 $M_\odot$ (features: peak & plateau)
- Other peaks could be explored with microlensing of stars
- PBH scenario can explain various cosmic conundra (LSS)
- Paradigm shift in Structure Formation of the Universe
- Very rich phenomenology: multi-scale, multi-epoch, multi-probe => Future G3 detectors (ET, CE, LISA)